

**11 December 1999**

**THE PATCH-CLAMP TECHNIQUE: A THEORETICAL AND PRACTICAL  
INTRODUCTION USING SIMPLE ELECTRICAL EQUIVALENT CIRCUITS.**

**Dirk L. Ypey<sup>1</sup> & Louis J. DeFelice<sup>2</sup>**

**<sup>1</sup>Department of Physiology  
Leiden University Medical Center  
P.O. Box 9604  
2300 RC Leiden, The Netherlands**

voice 31-71-527 6815  
fax 31-71-527 6782  
email d.l.ypey@lumc.nl

**<sup>2</sup>Department of Pharmacology,  
Vanderbilt University Medical Center  
Nashville, TN 37232-6600, USA.**

voice 1 (615) 343 6278  
fax 1 (615) 343 1679  
email lou.defelice@mcmail.vanderbilt.edu

Neither the authors nor the Biophysical Society take responsibility for either personal damage or damage to equipment that may occur during the practical exercises suggested in this paper.

## INDEX

### 1. INTRODUCTION

- 1.1. What is patch clamping?
- 1.2. Five patch-clamp measurement configurations.
- 1.3. Why use electrical equivalent circuits?

Figure 1.1. Diagram of the five patch-clamp measurement configurations

Figure 1.2. A simple electrical circuit modeling the successive patch-clamp procedures for obtaining the whole-cell configuration

### 2. SIX BASIC ELECTRICAL EQUIVALENT CIRCUITS

- 2.1. Charging a capacitor: ERC-circuit I.
- 2.2. Charging a leaky capacitor: ERC-circuit II.
- 2.3. Clamping an ERC-model: ERC-circuit III.
- 2.4. Clamping an ERC cell membrane through a patch pipette: ERC-circuit IV.
- 2.5. Measuring and filtering the conductance response of an ERC membrane: ERC circuit V.
- 2.6. Switching conductors in an ERC membrane model: ERC-circuit VI.

Figure 2.1. Charging a capacitor: ERC-circuit I

Figure 2.2. Charging a leaky capacitor: ERC-circuit II

Figure 2.3. Clamping an ERC-model: ERC-circuit III

Figure 2.4. Clamping an ERC cell membrane through a patch pipette: ERC-circuit IV.

Figure 2.5. Electrical equivalent circuit (ERC-circuit V) of a Whole-Cell (WC) measurement configuration to illustrate filtering of WC-current steps: ERC-circuit V

Figure 2.6. Membrane potential and current changes during conductor switching in an ERC-membrane model in current clamp: ERC-circuit VI

### 3. MODEL CELL EXPERIMENTS

#### 3.1. Introduction

#### 3.2. Model cell and measurement set-up description

- 3.2.1. Equivalent circuit
- 3.2.2. Model hardware
- 3.2.3. Patch-clamp set-up

#### 3.3. Patch-clamp measurement procedures and configurations

- 3.3.1. Switching-on the patch-clamp: amplifier open input capacitance and resistance, and filtering
- 3.3.2. Connecting the pipette holder with pipette to the patch-clamp: extra stray capacity.
- 3.3.3. Immersing the pipette tip to measure pipette capacitance and resistance.

- 3.3.4. Giga-sealing the cell and canceling the fast capacity currents in the cell-attached-patch (CAP) configuration.
- 3.3.5. Making a whole-cell (WC): measuring series resistance and cell capacitance while canceling the slow capacity transients.
- 3.3.6. Pulling an outside-out patch (OOP) and checking the seal resistance.
- 3.3.7. Excision of an inside-out patch (IOP).
- 3.3.8. Making a permeabilized-patch WC (ppWC).

### 3.4. Some instructive model experiments

- 3.4.1. Checking intracellular voltage clamp during recording of single ion channel currents from cell-attached patches (CAP)
- 3.4.2. Checking whole-cell membrane potential and resistance
- 3.4.3. Checking the membrane potential change during WC voltage-clamp stimulation using an extra intracellular electrode
- 3.4.4. Checking whole-cell current filtering with a sudden conductance change

### 3.5. Conclusion

Table 3.1. Component abbreviations, used or recommended component values (nominal or estimated) in the model cell experiments and full names of the components

Fig. 3.1. Diagram of the electrical equivalent circuit of the model used to exercise patch-clamp procedures and measurements.

Fig. 3.2. Example of equivalent circuit wiring on the breadboard (or circuit board).

Figure 3.3. Voltage-clamp records obtained during patch-clamp procedures leading to the whole-cell (WC) configuration, all on one scale (lowest gain recording)

Fig. 3.4. Experimental procedures for preparing a conventional whole-cell experiment, including fast capacity current ( $I_{cf}$ ) and slow capacity current ( $I_{cs}$ ) cancellation during 10mV voltage step application.

Fig. 3.5. Slow capacity current ( $I_{cs}$ ) changes upon establishment of the outside-out-patch (OOP) measurement configuration.

Fig. 3.6. Fast capacity current ( $I_{cf}$ ) transients of the cell-attached-patch (CAP) and inside-out-patch (IOP) compared.

Figure 3.7. Single-channel current recordings from a cell-attached patch under perfect intracellular voltage clamp (square currents in frames a and b) and imperfect intracellular voltage clamp (decaying currents in frames c and d)

Fig. 3.8. Whole-Cell membrane potential changes upon sudden conductance changes and upon current-step stimulation.

Fig. 3.9. The membrane potential transient,  $V_m(t)$ , during the slow capacity current ( $I_{cs}$ ) transient upon voltage-clamp WC-stimulation and the lack of an effect of  $I_{cs}$  transient cancellation on  $V_m(t)$ .

Fig.3.10. Whole-cell current filtering by the  $R_{ser}C_m$  time constant.

## REFERENCES

## NOTES

## 1. INTRODUCTION

### 1.1. What is patch clamping?

When one hears the words "**patch-clamp**" or "patch-clamping" for the first time in the scientific context, in which this term is so often used (cell physiology and membrane electrophysiology), it sounds like magic or silly jargon. What kind of patch, clamp or activity is one talking about? Obviously, not clamping patches of material together as one might do in patchwork or quilting! "Patch" refers to a small piece of cell membrane and "clamp" has an electro-technical connotation. Patch-clamp means imposing on a membrane patch a defined voltage ("**voltage-clamp**") with the purpose to measure the resulting current for the calculation of the patch conductance. Clamping could also mean forcing a defined current through a membrane patch ("**current-clamp**") with the purpose to measure the voltage across the patch, but this application is rarely used for small patches of membrane. Thus, since the introduction of the patch-clamp technique by Neher and Sakmann in 1976, patch-clamp most often means "voltage-clamp of a membrane patch." Neher and Sakmann applied this technique to record for the first time the tiny (pico-Ampere, pA, pico =  $10^{-12}$ ) ion currents through single channels in cell membranes. Others had measured similar single-channel events in reconstituted lipid bilayers; however, the patch-clamp technique opened this capability to a wide variety of cells and consequently changed the course of electrophysiology. That was, at that time, an almost unbelievable achievement, later awarded the Nobel Prize [see the Nobel laureate lectures of Neher (1992) and Sakmann (1992)].

This accomplishment, and the quirky name of the technique, no doubt added to the magical sound of the term patch-clamp. Remarkably, the mechanical aspects of the technique are as simple as gently pushing a 1  $\mu\text{m}$ -diameter glass micropipette tip against a cell. The membrane patch, which closes off the mouth of the pipette, is then voltage-clamped through the pipette from the extracellular side, more or less in isolation from the rest of the cell membrane. For this reason the patch-clamp amplifiers of the first generation were called extracellular patch-clamps.

### 1.2. Five patch-clamp measurement configurations

Neher and Sakmann and their co-workers soon discovered a simple way to improve the patch-clamp recording technique. They used glass pipettes with super-clean ("fire-polished") tips in filtered solutions and by applied slight under-pressure in the pipette. This procedure caused tight sealing of the membrane against the pipette tip measured in terms of resistance: giga-Ohm sealing, giga =  $10^9$ ). This measurement configuration is called **cell-attached patch (CAP)** (see Fig. 1.1), which allowed the recording of single-channel currents from the sealed patch with the intact cell still attached. This giga-seal procedure allowed Neher and Sakmann and their co-workers to obtain three other measurement configurations, including one for intracellular voltage- and current-clamp: the membrane patch between the pipette solution and the cytoplasm is broken by a suction pulse while maintaining the tight seal (Hamill et al., 1981). In this so-called **whole-cell (WC)** configuration (Fig. 1.1), the applied pipette potential extends into the cell to voltage-clamp the plasma membrane. Alternatively, the amplifier could be used to inject current into the cell to current-clamp the cell membrane and to record voltage, for example to study action potentials of

small excitable cells, which was impossible until the development of the giga-seal. Another achievement of the WC-configuration was the possibility to perfuse the intracellular compartment with the defined pipette solution. Although the WC-clamp configuration is no longer a clamp of a small membrane patch, electrophysiologists continued to refer to the WC-clamp configuration as a variant of the patch-clamp technique, probably because the WC-clamp starts with giga-sealing a small membrane patch.

Two other variants are inherent to the patch-clamp technique, since they concern clamping a small area of membrane. The giga-seal cell-attached patch, sometimes called an "on-cell" patch, can be excised from the cell by suddenly pulling the pipette away from the cell. Often the cell survives this hole-punching procedure by resealing of the damaged membrane, so that the excision can be repeated on the same cell. The excised patch is called an **inside-out patch (IOP)** (Fig. 1.1), because the inside of the plasma membrane is now exposed to the external salt solution. This configuration allows one to expose the cytoplasmic side to defined solutions in order, for example, to test for intracellular factors that control membrane channel activity. Another type of excised patch can be obtained, but now from the WC-configuration rather than the cell-attached configuration. It is the **outside-out patch (OOP)**, which is excised from the WC configuration by slowly (not abruptly now!) pulling the pipette away from the WC (Fig. 1.1). This maneuver first defines a thin fiber that eventually breaks to form a vesicle at the tip of the pipette. The configuration obtained is indeed a micro-WC configuration, which allows one to study small populations of channels or single channels and to readily manipulate the "tiny cell" to different bathing solutions for rapid perfusion.

The connection of the current (I) or voltage (V) measuring amplifier to the pipette and the bath is shown in Fig. 1.1 for the OOP, but this connection applies to all other configurations as well. The measuring electrode is inserted in the pipette, while the reference electrode is in the bath. The resulting circuit is shown for the recording of a single OOP channel current, driven by an intrinsic voltage source in the channel and/or a voltage source in the amplifier. The fifth configuration is the **permeabilized-patch WC-configuration (ppWC)** (Fig. 1.1), in which the CAP is not actually ruptured for direct access to the inside of the cell, but made permeable by adding artificial ion channels (monovalent cation channel-forming antibiotics) via the pipette solution (Horn and Marty, 1988). Examples of such antibiotics are amphotericin and nystatin, both produced by microorganisms. The great advantage of this configuration is that it allows intracellular voltage- and current-clamp measurements on relatively intact cells, i.e. cells with a near normal cytoplasmic composition. This is in contrast to the perfused WC-configuration. The various patch-clamp configurations are beautifully described in Neher and Sakmann (1992).

It is the purpose of the present contribution to make the beginning student familiar with the electrophysiological procedures involved in experimenting with each of the five patch-clamp configurations. The required theoretical background will be provided and the explained theory will be exercised with patch-clamp experiments on a model cell designed for teaching and testing purposes.

### 1.3. Why use electrical equivalent circuits?

Patch clamping is an electrical technique, which requires some skill in electrical thinking and measuring. When a patch-clamper is going through the procedures to obtain one of the five measurement configurations, he or she is continuously monitoring voltage-step induced current responses or current-step induced voltage-responses to check whether the procedures work. While doing that, the experimenter is also continuously conceptualizing the measurement condition as a simple electrical circuit model consisting of resistors (R), capacitors (C), and batteries (E). Because these models are nearly equivalent to the real measurement condition in certain (but not all!) respects, these models are also called equivalent circuits.

Examples of this way of testing and proceeding are illustrated in Fig. 1.2a. The patch-clamp (pc) amplifier is here represented by a voltage source,  $E_{pc}$ , in series with a resistor,  $R_{pc}$ , both shunted by an input capacitance,  $C_{pc}$ . The measuring patch pipette can be represented by the pipette resistance,  $R_{pip}$ , and pipette capacitance,  $C_{pip}$ , as soon as the pipette enters the solution. Giga-sealing the patch pipette to the cell membrane can be represented by replacing the direct connection of the pipette with the grounded bath by the seal resistance  $R_{seal}$ . After forming the giga-seal, the pipette opening is closed off by the cell-attached patch (CAP) with its high resistance,  $R_{cap}$ . Breaking the CAP replaces  $R_{cap}$  for access resistance,  $R_{acc}$ , providing access to the inside of the whole-cell (WC) with its  $E_m:R_m:C_m$  membrane.

Fig. 1.2b shows that the three steps in the procedure for obtaining a WC-configuration can be simulated by a simple ERC-circuit with three switches (S). Closure of  $S_{pip}$  (double switch with  $S_{cpip}$  and  $S_{rpip}$ ) would represent entering the bath with the pipette, opening the switch  $S_{seal}$  symbolizes (abrupt) sealing, and closure of switch  $S_{acc}$  simulates WC-establishment by short circuiting  $R_{cap}$  with the access resistance  $R_{acc}$ . During actual experiments the experimenter can recognize entering the bath, giga-sealing the cell and making a WC by applying voltage steps in  $E_{pc}$  to the pipette and interpreting the current responses as if the circuit of Fig. 1.2b applies. This is the main value of equivalent circuits. The same is true for obtaining the other three patch-clamp configurations discussed above (IOP, OOP, ppWC). Thus, **thinking in terms of simple ERC-circuits is essential** for readily doing the tests and subsequent experiments. Therefore, students interested in learning patch clamping should begin to familiarize themselves with this way of thinking and measuring.

But how? Studying electronics (Horowitz and Hill, 1990) will help, but this may be an unwanted detour for those students ready to do the experiments. Many electronics courses and textbooks also discuss the properties of inductors, transistors and operational amplifiers, while these subjects are not of major importance for the beginning or even the advanced student in electrophysiology. In our opinion, mastering ERC-circuits should have the highest priority for obtaining measurement skills. A recently published book by one of us (DeFelice, 1997) is particularly devoted to providing the basics of bioelectricity to the beginning student and attempts to fill the gap between basic physical theory and more advanced membrane electrophysiology textbooks (Hille, 1992).

After the present introduction, we begin with the theory of the basic ERC-circuits relevant for patch clamping. Since patch clamping is a technique often used in multi-disciplinary teams of biomedical scientists, students from biology or medicine often want to learn the technique. As they frequently

do not have much background in physics or electronic technology, it may be helpful if such students have biological examples of the physics they are learning. Such examples are usually not provided in the general electronics courses. Here we take the opportunity to give such examples while explaining the theory. Fig. 1.2 already shows several important models and the above-mentioned book (DeFelice, 1997) should help provide the physical basics of ERC components and circuits. We stress, however, that whatever the importance of the theory, practical exercises are as important. Biophysics is an experimental science and trying to recognize ERC-circuit behavior in the electrical behavior of a real circuit or in a living cell is of great instructive value.

Manuals for practical classroom courses on the electronics of ERC-circuits for patch-clamp students are available (Ypey, 1997). However, the most attractive way to become introduced to patch-clamping is to exercise the theory in a real patch-clamp set-up on an equivalent circuit model of a cell showing all the relevant ERC-behavior of a living cell, i.e., with realistic E, R and C values. That is what we do in Chapter 3. It allows the student to combine learning the theory with becoming familiar with a practical set-up. It also forces the student to identify components of a patched cell with electric circuit components (E, R or C). Students ready to start patch clamping may use Chapter 3 as an instruction manual for how to test a set-up in preparation for actual experiments. Reading Chapter 3 before beginning experiments will serve the student more than merely reading the instruction manual of a patch-clamp amplifier, although that should not be forgotten!

To our knowledge, a **structured patch-clamp measurement exercise course** as presented here has not yet become available for general use and teaching. This is in contrast to the many computer programs available for teaching concepts of biophysical or physiological mechanisms (Note 1.3.1). Although these teaching models may be invaluable, in particular for patch-clampers, they do not provide practical measurement exercises. The latter are important because measurement conditions always present practical problems that must be solved before one is able to make sense of the observations.

There are, of course, **limitations** to the model exercises presented here. One is the lack of "wet" (i.e., physical-chemical) properties in the ERC-circuit cell model. Also there is no opportunity to encounter and solve electrode offset or junction potential problems, or to study the ionic dependence of membrane potentials. These topics must be dealt with separately. Another shortcoming of the ERC cell model one should notice is that it lacks Hodgkin-Huxley "excitability" conductance properties. That would be useful, but once able to make reliable measurements, the student will find that Hodgkin-Huxley teaching models for conceptual training (e.g., AXOVACS and MCHAN. See Note 1.3.1) are available for further exercises and experiments. A book of great practical use in all aspects of the patch-clamp technique is *The Axon Guide of Sherman-Gold* (1993).

A final comment on limitations: the ERC-circuit with a voltage source  $E_s$  in series with an internal source resistor  $R_s$  (thus two connection terminals) only applies to patch-clamp stimulation (voltage clamp or current clamp) because the patch-clamp is a true two-terminal input, single-electrode clamp. Although the approach in principle also applies to three-terminal, two-microelectrode voltage-clamp stimulation, this would require some rethinking and redrawing of the measurement configurations. A detailed justification for using ERC-circuit equivalents is given in Note 1.3.2.

## 2. SIX BASIC ELECTRICAL EQUIVALENT CIRCUITS

In the present chapter we discuss the properties of six simple electrical circuits representing six frequently encountered experimental conditions during patch clamping. For practical and didactic reasons, we discuss these successively as circuits of increasing complexity. Nevertheless, the different situations are rather similar and reduce to two types of basic circuits in many applications, one with one capacitor and the other with two. The simplest circuit, the first one, is most frequently employed during practical experiments. Here it is also used to introduce and explain the equations (Ohm's Law, Kirchoff's Law, and capacitor equation) that describe the behavior of all six circuits. The circuits are denoted as **ERC-circuits**, since they contain batteries (E), resistors (R) and capacitors (C). When introducing the circuits, we will indicate in which respect these circuits can serve as equivalents of practical patch-clamp configurations. The practical use of these circuits will become apparent in demonstrations on the model cell in Chapter 3. Where appropriate, we will discuss important properties of the circuits for real patch-clamp experiments.

Discussion of the six ERC-circuits will serve as preparation for the demonstrations. The theory of the six practical circuits is so important that one can hardly imagine doing patch-clamp experiments without understanding this theory. The circuits will also be used to explain the difference between voltage-clamp and current-clamp stimulation. Although these two stimulation techniques are methodologically very different, technically speaking they are only extremes of one and the same technique. It is very important that the student becomes fluent in switching from voltage-clamp to current-clamp thinking. Some electrophysiologists may rely too heavily on only voltage-clamp, even though voltage-clamp was designed primarily to understand the unclamped behavior of excitable cells. The ERC-circuit approach used here is an excellent way to integrate both ways of clamping in one framework. In a later stage of learning patch-clamp, this approach will help to understand and identify bad voltage-clamp recordings from excitable cells.

### 2.1. Charging a capacitor: ERC circuit I

Fig. 2.1a gives the most simple battery-resistor-capacitor (ERC) circuit (ERC-circuit I) one can conceive, because it consists of only one battery ( $E_s$ ), one resistor ( $R_s$ ) and one capacitor (C), all three components in series in a closed circuit. The index 's' (which stands for 'source') indicates that we consider the  $E_s:R_s$  combination as a source that provides the current to charge C. This source may be a voltage- or current-clamp instrument, and C may be the capacity of a patch pipette or of the membrane of a cell, as illustrated in Fig. 1.2. Before the pipette touches the bath,  $E_{pc}$ ,  $R_{pc}$ , and  $C_{pc}$  form the ERC-circuit I. After forming a giga-seal,  $E_{pc}$ ,  $R_{pc}$ , and  $C_{pc} + C_{pip}$  again form ERC-circuit I if  $R_{seal}$  and  $R_{cap}$  are very large. In the whole-cell  $E_{pc}$ ,  $R_{pc} + R_{pip} + R_{acc}$  and  $C_m$  may form ERC-circuit I, if  $R_m$  and  $R_{seal}$  are very large and  $C_{pc} + C_{pip}$  very small.

Here we want to understand how steps in the voltage  $E_s$ , as occur during patch-clamp experiments, charge the capacitor: **how rapidly is C charged, by which current, and to what voltage?** We consider step changes in  $E_s$  rather than other functions, such as sinusoidal or ramp functions, because step changes are widely used in electrophysiology for membrane stimulation. Electrophysiologists often study how membrane conductance changes when the voltage changes abruptly to a new, fixed value because this is simple to analyze. A quick way to do that is by applying a step change in potential.



We need three equations as mathematical tools to describe the behavior of circuits like Fig. 2.1 (for more theoretical background, see DeFelice, 1997). The first formula is **Ohm's law**,  $V = RI$ , which relates the voltage  $V$  (expressed in units of volts, with  $V$  as the symbol), across a resistor  $R$  (in units of ohms, with  $\Omega$  as the symbol) to the current  $I$  (in units of amperes, with  $A$  as the symbol) flowing through the resistor. You may think of  $R$  as proportionality constant between  $V$  and  $I$ .

It is **convention** in membrane electrophysiology to define intracellular **voltage** and membrane **current polarity** with respect to the ground (= arbitrary 'zero' voltage) on the external side of the membrane. Thus the ground symbols in Figures 2.1-5 indicate the external side of a membrane if the circuit is taken to represent stimulation of a cell with the  $E_s:R_s$  source. Voltage sources are then positive, if the positive side of the battery is facing the inside of the membrane. Membrane currents are positive when they flow from the inside to the outside, driven by a net positive voltage difference across the membrane.

In our derivations we will often choose positive voltage sources and consider a consistent path of current flow, but the resulting equations will describe voltages and currents for any voltage polarity.

For ERC-circuit I, Ohm's law implies

$$V_{rs} = E_s - V_c = R_s I_{rs} \quad (1a)$$

or

$$I_{rs} = (E_s - V_c) / R_s \quad (1b)$$

with  $V_{rs}$  the voltage across  $R_s$ ,  $E_s$  the source battery voltage,  $V_c$  the voltage (difference) across the capacitor  $C$  and  $I_{rs}$  the current through  $R_s$ . This equation also applies if  $V_c$  and  $I_{rs}$  change during charging of  $C$ . The way we write 'changing in time' mathematically is  $V(t)$ , which means that  $V$  is changing in time. Then  $V_c(t)$  and  $I_{rs}(t)$  should be substituted for  $V_c$  and  $I_{rs}$ , respectively.

The second equation is the **capacitor equation**,  $Q = CV$ , which relates the voltage  $V$  across a capacitor with capacity  $C$  (in units of farads, with  $F$  as the symbol) to the charge  $Q$  (in units of coulombs, with  $C$  as the symbol) accumulated on  $C$ . Thus  $C$  is proportionality constant in this equation between  $V$  and  $Q$ . In ERC-circuit I we refer to the voltage across  $C$  as  $V_c$  to contrast it with  $V_{rs}$ . The charge on  $C$  we call  $Q_c$ . The capacitor equation for circuit I then becomes

$$Q_c = CV_c \quad (2a)$$

or

$$V_c = Q_c / C \quad (2b)$$

This equation means that a given charge  $Q$  on a capacitor  $C$  causes a greater voltage difference across the capacitor when the capacitor is smaller. On the other hand, a large capacitor holds more charge at a given voltage than a small one.

In ERC-circuit I we want to describe the charging process of  $C$  upon a step-change of  $E_s$ , thus the changes in  $Q_c$  and  $V_c$ . We can easily change the capacitor equation from a (static) charge equation to a (dynamic) current equation, because the change in  $Q_c$  is exactly equal to the charging current  $I_c$

flowing into or out of C. Taken into consideration that a changing charge  $Q_c$  ( $dQ_c/dt$ ) causes a changing voltage  $V_c$  ( $dV_c/dt$ ), Eq. 2 can be rewritten as

$$I_c = dQ_c/dt = C \cdot dV_c/dt \quad (3)$$

This equation implies that a constant charging current  $I_c$  into capacitor C causes a linearly rising  $V_c$  ( $dV_c/dt$  constant) across the capacitor. Conversely, when there is a linearly rising  $V_c$ , there is a constant charging current.

When  $E_s$  in circuit I is stepped from zero V to a constant positive value, while the pre-step  $V_c = 0$ , a current will start to flow that is determined by Eq. 1, but the same current will change  $V_c$  according to Eq. 3. **Kirchoff's law** for currents entering ( $I_{in}$ ) and leaving ( $I_{out}$ ) a branching node in a circuit states that  $\text{Sum } I_{in} = \text{Sum } I_{out}$ . This implies for the simple branching node  $V_c$  in circuit I (only one entry and one exit) that:

$$I_{rs} = I_c, \quad (4)$$

and written in full with Eqs. 2 and 3 incorporated:

$$(E_s - V_c)/R_s = C \, dV_c/dt \quad (5a)$$

$$dV_c/dt = -(1/R_s \cdot C) \cdot (V_c - E_s) \quad (5b)$$

This is a simple, first-order linear **differential equation** relating the change in  $V_c$  ( $dV_c/dt$ ) to  $V_c$ , as is more clearly expressed by Eq. 5b. With  $V_c > E_s$ ,  $dV_c/dt$  is negative, and it is more negative at smaller  $R_s$  and C and at larger  $(V_c - E_s)$  values. For  $V_c < E_s$ ,  $dV_c/dt$  is positive, and even more positive at smaller  $R_s$  and C and at more negative  $(V_c - E_s)$  values. At  $V_c = E_s$  then  $dV_c/dt = 0$ , implying steady-state conditions. Therefore  $V_c$  moves toward  $E_s$  with lower and lower speed the closer it approaches  $E_s$ , both from more positive and from more negative values.

Usually, the steady-state value of  $V_c$  reached after changing  $E_s$  is directly determined from the differential equation by filling in the **steady-state** condition  $dV_c/dt = 0$ . For that case, Eq. 5 changes to:

$$V_c^* = E_s \quad (6)$$

with  $V_c^*$  the steady-state value of  $V_c$ . This solution is consistent with the above reasoning based on the properties of the differential equation.

Although the recipe of Eq. 5b is a perfect prescription for the change of  $V_c$  during the charging process of C, we would be happier with the **dynamics** of  $V_c$ , i.e. the exact **time course** of  $V_c(t)$  upon stepping  $E_s$  from one voltage to another. This time course  $V_c(t)$  is the solution of differential Eq. 5. The actual solution procedure is given in a separate note (Note 2.1). Here, we merely state the end result:

$$V_c(t) = E_s + (V_c(0) - E_s) e^{-t/\tau} \quad (7)$$

with

$$\tau = R_s C \quad (8)$$

This equation shows that C is charged up from its initial voltage  $V_c = V_c(0)$  to the steady-state value  $V_c^* = E_s$  (fill in  $t = 0$  and  $t = \text{very large}$ , respectively). The **time constant**  $\tau = R_s C$  determines how quickly  $V_c(t)$  moves toward  $E_s$ . The smaller  $\tau$ , i.e. the smaller  $R_s$  and  $C$ , the faster the  $V_c$  transient occurs. Therefore,  $\tau$  is generally used as a characteristic value indicating the charging time of the charging circuit. At  $t = \tau$ , the initial difference between  $V_c$  and  $E_s$ ,  $V_c(0) - E_s$ , has declined to the value  $(V_c(0) - E_s) / e$  (verify this result by filling in  $t = \tau$ ). At that exact time, about 60% of the total change of  $V_c$  has taken place. After  $t = 3\tau$ , about 95% of the full change has taken place.

Now that we know  $V_c(t)$  of the charging process, we can easily determine the **charging current** as a function of time by combining Eqs. 1b and 7:

$$I_{rs}(t) = [(V_c(0) - E_s) e^{-t/\tau}] / R_s \quad (9)$$

It is this charging current one sees upon voltage steps during a patch-clamp, voltage-clamp experiment on a very high resistance membrane patch or high resistance whole-cell. The voltage transient  $V_c(t)$  is never observed in a regular one-electrode patch-clamp, voltage-clamp experiment, but its time course can be deduced from the current transient. Fig. 2.1b shows the time courses of  $V_c$  (Eq. 7) and  $I_{rs}$  (Eq. 9) upon a step increase in  $E_s$ . The time constants of both transients are the same.

Eq. 9 shows that the charging current is maximal at  $t = 0$  and zero at very large  $t$  values ( $t \gg \tau$ ), consistent with the above differential equation. The peak current at  $t = 0$  is  $(E_s - V_c(0))/R_s$ , which is equal to  $E_s/R_s$  when  $V_c(0) = 0$ . When only the change in voltage ( $dE_s$ ) and current ( $dI_{rs}$ ) is considered, the  $dI_{rs}$  peak is equal to  $dE_s/R_s$ . This is a rule of thumb, which is used during every patch-clamp experiment after breaking the sealed membrane patch to obtain WC-conditions (see demonstration experiments below). This quick calculation serves to decide whether the voltage-clamp conditions of the newly obtained WC are good enough (low  $R_s$ ) to proceed with the experiment, to try to improve the conditions (lower  $R_s$ ), or to terminate the experiment and look for another cell. At the same time, one estimates  $\tau$  from the current transient in order to decide whether the rate of current decline, i.e. the rate of charging  $C$  of the cell is fast enough to faithfully record subsequent rapidly rising voltage-activated ionic currents. Thus, understanding the properties of simple basic ERC-circuit I is of extreme importance for successfully carrying out any WC patch-clamp experiment!

What does this all mean for obtaining **practical voltage-clamp or current-clamp conditions**? Good clamp conditions are conditions under which the clamped quantity is imposed by the clamping instrument, independent of the properties of the clamped object. Thus, at good voltage-clamp the  $E_s/R_s$  instrument clamps  $C$  to  $E_s$  in circuit I. At good current-clamp the  $E_s/R_s$  instrument injects a constant current  $E_s/R_s$  into  $C$ , with  $R_s$  in current-clamp  $\gg R_s$  in voltage-clamp. If the purpose of stimulation in ERC-circuit I is to voltage-clamp  $C$  to  $E_s$ , this stimulus condition results

in perfect steady-state voltage-clamp, since  $V_c$  becomes exactly equal to  $E_s$  (Eq. 6). Whether the voltage-clamp is fast enough to record rapidly activated currents upon the  $E_s$  step (which we don't show and do not discuss here), depends on the value of the time constant  $\tau_s$ . The smaller  $\tau_s$ , the better are the dynamic properties of the voltage-clamp, in this case only consisting of the  $E_s/R_s$  combination.

The current-clamp conditions in ERC-circuit I are worse. Only at the very beginning just after the step in  $E_s$  ( $t \ll \tau_s$ , with  $\tau_s$  much larger than in voltage-clamp), is  $I_{rs}$  determined by  $E_s$  (Fig. 2.1c). Soon after charging  $C$  by  $I_{rs}$ , the driving force ( $E_s - V_c$ ) declines, suppressing  $I_{rs}$  more and more, until  $I_{rs}$  has become zero. Thus, while it is impossible with ERC-circuit I to obtain good steady-state current-clamp conditions (at  $t \gg \tau_s$ ), it is impossible to obtain good voltage-clamp conditions just after the step change in  $E_s$  ( $t \ll \tau_s$ ).

## 2.2. Charging a leaky capacitor: ERC-circuit II

Although cell membranes may be very high resistant, they usually have some conductance (the inverse of resistance) in parallel with their capacitance. Thus, mostly we are dealing with capacitance ( $C$ ) shunted by resistance ( $R$ ). Such a parallel RC-combination is often called a **leaky capacitor**, as we do here. Fig. 2.2a shows a circuit with a leaky capacitor stimulated by the  $E_s/R_s$  source, as in Fig. 2.1a. Thus, the circuit of Fig. 2.2a, ERC-circuit II, is that of Fig. 2.1a with an added  $R$  across  $C$ .

The RC-part of this circuit looks like a patch pipette, with  $R = R_{pip}$  (pipette resistance) and  $C = C_{pip}$  (pipette capacitance) (see Fig. 1.2b for switches  $S_{pip}$  and  $S_{seal}$  closed) or a cell membrane, with  $R = R_m$  (membrane resistance) and  $C = C_m$  (membrane capacitance), but without a membrane potential (cf. Fig 1.2b for  $R_s = R_{pc} + R_{pip} + R_{acc}$ ,  $C_{pc} + C_{pip} = 0$ ,  $R_{seal} \gg R_m$  and  $E_m = 0$ ). The  $E_s/R_s$  combination may represent a voltage- or current-clamp used to measure  $R_{pip}$  and  $C_{pip}$  or  $R_m$  and  $C_m$ , respectively.

We investigate the behavior of the ERC-circuit II in the same way as we did for ERC-circuit I: **we want to know  $V_c(t)$  and  $I_{rs}(t)$  upon a step in  $E_s$** . The equations for  $I_{rs}$  and  $I_c$  are the same as for circuit I, but we have now one current more, the current  $I_r$  through the added  $R$ , which is, according to Ohm's law, equal to

$$I_r = V_c / R \quad (10)$$

Branching node  $V_c$  has one entry current ( $I_{rs}$ ) but two exit currents ( $I_c$  and  $I_r$ ). So, application of **Kirchoff's current law** results in

$$I_{rs} = I_c + I_r \quad (11)$$

By substitution of the equations for the three currents (Eqs. 1b, 3 and 10), one obtains again the **differential equation** describing the change in  $V_c$  ( $dV_c/dt$ ) upon  $E_s$  steps

$$(E_s - V_c)/R_s = C dV_c/dt + V_c/R \quad (12a)$$

or

$$dV_c/dt = (-1/\tau) \cdot (V_c - V_c^*) \quad (12b)$$

with

$$V_c^* = R E_s / (R_s + R) \quad (13)$$

and

$$\tau = R_{sp} C \quad (14)$$

with  $R_{sp}$  the parallel equivalent resistance of  $R_s$  and  $R$

$$R_{sp} = R_s R / (R_s + R) \quad (15)$$

Eq. 12a has been rewritten as Eq. 12b in order to obtain an expression which more clearly shows how  $dV_c/dt$  (written as a single term at the left side of  $=$ ) depends on  $V_c$  (present as a single term at the right side) with a proportionality constant to be multiplied with  $V_c$ . Try to do the algebra of this rewriting yourself!

The meaning of differential Eq. 12b can now be investigated in the same way as for Eq. 5b for ERC-circuit I:  $V_c$  moves toward  $V_c^*$ , both from  $V_c > V_c^*$  and from  $V_c < V_c^*$ , with a rate proportional to the absolute value of  $V_c - V_c^*$  and inversely proportional to  $\tau$ ,  $R_{sp}$  and  $C$ . At  $V_c = V_c^*$   $dV_c/dt = 0$ , then  $V_c^*$  (Eq. 13) is the value of  $V_c$  under **steady-state conditions**, as could have been found directly from Eq. 12a by filling in the steady-state condition  $dV_c/dt = 0$ . It depends on the relative value of  $R_s$  how close  $V_m^*$  is to  $E_s$ .

The **time behavior** of  $V_c$ , namely  $V_c(t)$ , can be found in the same way as for ERC-circuit I, i.e. by solving differential Eq. 12a. The result is given here directly:

$$V_c(t) = V_c^* + (V_c(0) - V_c^*) e^{-t/\tau} \quad (16)$$

with  $V_c^*$  given by Eq. 13 and  $\tau$  given by Eqs. 14 and 15. Thus, the  $V_c$  transient is a single-exponential, moving from  $V_c(0)$  to  $V_c^*$  with a time constant  $\tau$  determined by both  $R_s$  and  $R$ , but mainly by the smallest of the two resistors if they have a different value. One may be surprised that the time constant  $\tau$  is determined by the equivalent resistance  $R_{sp}$  of  $R_p$  and  $R$  in parallel, although the resistors are in series in the circuit. For the capacitor, they are apparently in parallel, because they are two parallel simultaneously charging/discharging pathways for the capacitor.

$V_c^*$  in **voltage-clamp** ( $R_s \ll R$ ) is unequal, though close to  $E_s$ , a condition different from that of  $V_c^*$  in ERC-circuit I. Thus, voltage-clamp of a leaky capacitor by the  $E_s/R_s$  source is never perfect. However, the equation for  $V_c^*$  (Eq. 13) shows that  $V_c^*$  can be very close to  $E_s$ , depending on the relative sizes of  $R$  and  $R_s$ . For  $R \gg R_s$ , voltage-clamp is very good, for example within 1% if  $R > 100R_s$ . Therefore, at very low  $R_s$ , both dynamic (small  $\tau$ ) and steady-state ( $V_c^*$  close to  $E_s$ ) voltage-clamp are good. The time course of  $V_c$  upon an  $E_s$  voltage-clamp step is graphically illustrated by Fig. 2.2b.

The **time course of the charging current**  $I_{rs}$ ,  $I_{rs}(t)$ , now follows by substituting Eq. 16 in Eq. 1b. We have done something similar with ERC-circuit I, but the result is now different because of the presence of  $R$ :

$$I_{rs}(t) = [E_s - V_c(t)] / R_s \quad (17a)$$

or

$$I_{rs}(t) = [E_s - (V_c^* + (V_c(0) - V_c^*) e^{-t/\tau_{sp}})] / R_s \quad (17b)$$

with

$$I_{rs}(0) = [E_s - V_c(0)] / R_s \quad (17c)$$

and

$$I_{rs}^* = [E_s - V_c^*] / R_s = E_s / (R_s + R) \quad (17d)$$

The difference between Eq. 17 and the current equation of ERC-circuit I (Eq. 9) is that R allows a steady-state current to flow, namely  $I_{rs}^*$ .

Eqs. 13-17 allow us to further **define good voltage- and current-clamp conditions**. Eq. 13 implies that a leaky capacitor is very well voltage-clamped to the applied,  $E_s$ , if  $R_s \ll R$ . For that condition, Eq. 17 implies that the steady-state current in the circuit,  $I_{rs}^*$ , is then almost completely determined by R (or by conductance G, in Siemens,  $S = 1/\text{Ohm}$ ) and that slow changes in R (or G) will be well reflected by  $I_{rs}$  changes. "Slow" means with transient times  $\gg \tau_{sp}$ , with  $\tau_{sp} \sim R_s C$  ( $R_s \ll R$ ). Voltage-clamp records are illustrated in Fig. 2.2b.

Good **current-clamp** conditions are guaranteed for the condition  $R_s \gg R$ , since then  $I_{rs}$  will be independent of R (cf. Eq. 17d).

$V_m^*$  will then be

$$V_m^* = R I_{cc} \quad (18)$$

with the current-clamp current  $I_{cc}$

$$I_{cc} = E_s / R_s \quad (19)$$

Although  $I_{rs}(0)$  will still overshoot  $I_{rs}^*$  a little bit under this condition, the shape of the increase in current upon a step increase in  $E_s$  will be nearly stepwise. The time constant of  $V_c(t)$  is now  $\tau_{sp} \sim R_s C$ , which is much larger than under voltage-clamp with  $\tau_{sp} \sim R C$ . This is illustrated in Fig. 2.2c. Notice that the  $V_c$  value in current-clamp always remains a small fraction of the applied  $E_s$ !

### 2.3. Clamping an ERC model: ERC-circuit III

Cell membranes are leaky capacitors, which are charged because they accumulate charge on the capacitor through the "leaks" that generate a membrane potential. By voltage- or current-clamp stimulation one can change the charge on the capacitor. So far, we have neglected the presence of an **intrinsic voltage source in the leaky capacitor** stimulated by the external  $E_s/R_s$  source (ERC-circuit II). Fig. 2.3a shows ERC-circuit III, which is circuit II with the voltage source E placed as an extra component in the R branch, in series with R. Here we study the properties of this circuit, which is equal to the WC-circuit drawn in Fig.1.2 for  $R_s = R_{pc} + R_{pip} + R_{acc}$  and  $C_{pc} = C_{pip} = 0$ .

The behavior of ERC-circuit III upon steps in  $E_s$  can be derived in the same way as for ERC-circuit II. The only equation that is different is that for  $I_r$ , which is

$$I_r = (V_c - E) / R \quad (20)$$

This difference affects the differential equation resulting from the application of **Kirchoff's current law** to the currents in node Vc

$$I_{rs} = I_c + I_r \quad (21a)$$

which becomes, after substituting the equations for I<sub>rs</sub> (Eq. 1b), I<sub>c</sub> (Eq. 3) and I<sub>r</sub> (Eq. 20),

$$(E_s - V_c)/R_s = C \, dV_c/dt + (V_c - E)/R \quad (22b)$$

The student herself may now derive all the other equations describing both the steady-state and dynamic behavior of ERC-circuit III upon steps in E<sub>s</sub> by following the procedures explained under ERC-circuits 1 and 2. We provide them here without much further explanation of the derivations.

The rewritten **differential equation** is

$$dV_c/dt = -(1/\tau) \cdot (V_c - V_c^*) \quad (22c)$$

with

$$V_c^* = (R_s E + R E_s) / (R_s + R) \quad (23)$$

and

$$\tau = R_{sp} C \quad (24)$$

with

$$R_{sp} = (R_s R) / (R_s + R) \quad (25)$$

The **steady-state behavior** of V<sub>c</sub>, V<sub>c</sub><sup>\*</sup>, is given by Eq. 23. E is now present in the equation to contribute to V<sub>c</sub>. The relative values of R<sub>s</sub> and R determine whether V<sub>c</sub> is more at the E<sub>s</sub> side (R<sub>s</sub> << R for voltage-clamp by E<sub>s</sub>) or at the E side (R<sub>s</sub> >> R for current-clamp by the E<sub>s</sub>/R<sub>s</sub> source).

The **time behavior** of V<sub>c</sub> upon steps in E<sub>s</sub> is described by

$$V_c(t) = V_c^* + (V_c(0) - V_c^*) e^{-t/\tau} \quad (26a)$$

with V<sub>c</sub><sup>\*</sup> given by Eq. 23. Note that Eq. 26a is identical to Eq. 16. The difference is in the actual value of V<sub>c</sub><sup>\*</sup> (Eq. 23) because of the presence of E. Upon **voltage-clamp** steps in E<sub>s</sub> from E<sub>s</sub> = 0 (R<sub>s</sub> << R), V<sub>c</sub> moves with a single-exponential time course (τ ~ τ = R<sub>s</sub>C) from a value close to the pre-step E<sub>s</sub> = 0 value to one close to the E<sub>s</sub> step value (Fig. 2.3b). Upon **current-clamp** steps in E<sub>s</sub> from E<sub>s</sub> = 0 (R<sub>s</sub> >> R), V<sub>c</sub> moves relatively slowly (compared to under voltage-clamp) with a single-exponential time course (τ ~ τ = R.C) from a value close to E to a value close to E plus a voltage drop across R due to the current-clamp current I<sub>cc</sub> = E<sub>s</sub>/R<sub>s</sub> (Fig. 2.3c). In equation

$$V_c(t) = E + R I_{cc} (1 - e^{-t/\tau}) \quad (26b)$$

The equation for the **current behavior** of I<sub>rs</sub>(t) upon steps in E<sub>s</sub> is obtained again by substituting Eq. 26a in Eq. 1b, which results in the next equation (the same expression as Eq. 17a):

$$I_{rs}(t) = [E_s - V_c(t)] / R_s \quad (27a)$$

or

$$I_{rs}(t) = [E_s - (V_c^* + (V_c(0) - V_c^*) e^{-t/\tau_{sp}})] / R_s \quad (27b)$$

with

$$I_{rs}(0) = [E_s - V_c(0)] / R_s \quad (27c)$$

and

$$I_{rs}^* = [E_s - V_c^*] / R_s = (E_s - E) / (R_s + R) \quad (27d)$$

Thus,  $E$  shows up in the expressions for the steady-state voltages and currents, whether they apply to voltage-clamp or current-clamp. In **voltage-clamp**,  $E$  does not contribute much to the clamped potential, but it does clearly contribute to the current, because  $E_s$  and  $E$  values in practical situations are of the same order of magnitude, while  $R_s \ll R$  (cf. Eq. 27d). In **current-clamp** ( $R_s \gg R$ )  $E$  dominates  $V_c$ , but significant current to bring  $V_c$  away from  $E$  can only be applied if  $E_s \gg E$ . This is demonstrated by Eq. 23 after rewriting for the current-clamp (CC) condition  $R_s \gg R$ :

$$V_c^* = E + R I_{cc} \quad (28)$$

with

$$I_{cc} = E_s / R_s \quad (29)$$

Voltage-clamp and current-clamp records are illustrated in Fig. 2.3b and 2.3c, respectively. In principle they have the same shape, but the overshoot under current-clamp is hardly noticeable.

Instead of starting with the simpler circuits II and I, we could have started with ERC-circuit III for the derivation of all the equations describing the behavior of the circuit upon stimulation with voltage or current steps. We could have shown, then, that the equations for the simpler circuits II and I easily follow from those of the more complete ERC-circuit III. Assuming  $E = 0$  yields the equations of circuit II, and assuming  $E = 0$  and  $R = \text{infinity}$  yields those of circuit I. The beginning student is better off with the above procedure, because the concepts and derivations are better introduced and explained there. The advanced student could, however, certainly follow the inverse sequence from circuit III to I.

The **general conclusion** from ERC-circuits I to III is that **voltage-clamp and current-clamp stimulation are extremes of the same stimulation technique** with an  $E_s/R_s$ -containing instrument. But membrane electrophysiologists know how different both techniques are in methodological respect and how important it is to have them both at your disposal. Good voltage-clamp allows complete voltage control over membrane conductance behavior, since the various ionic conductances in the membranes of living cells are voltage and time dependent but not current dependent. Thus, when applying constant current under current-clamp, the membrane voltage is changed. This may further amplify the changing voltage by opening up ionic channels affecting the membrane potential in the same direction and may result in an impulsive change in membrane potential called excitability. It was for the purpose of studying the mechanisms of excitability that voltage-clamp techniques were developed. Voltage-clamp instrumentation involves modern operational amplifier technology rather than a simple controllable  $E_s$  battery with a good low-resistance  $R_s$  component. Conceptually, however, the  $E_s/R_s$  combination serves as a good electrical equivalent of the clamp instrument because it summarizes what the technology has achieved: providing an ideal controllable voltage source with a relatively low output resistance  $R_s$  for the purpose of measuring very small currents (nA to pA).



## 2.4. Clamping an ERC cell membrane through a patch pipette: ERC-circuit IV

A cell membrane cannot directly be voltage- or current-clamped, as suggested by the discussions of ERC-models I-III. One always needs access electrodes between the clamping source and the clamped membrane. The **access pathway** directly connected to the cell is a patch pipette with its narrow, high resistance tip and its pipette capacitance of the thin glass wall between the pipette solution and the extracellular bathing solution. The reference electrode usually does not add much access resistance or parallel capacitance to the circuit, because it is directly immersed in the bathing solution surrounding the cell (cf. Fig. 1.2). ERC-circuit IV in Fig. 2.4a gives a better representation of this condition than the previous circuits. It is identical to the circuit drawn in Fig. 1.2 for the WC-configuration (with  $R_{\text{seal}} \gg R_m$ ).  $C_p$  and  $R_p$  may be seen as representing the pipette capacitance and the pipette plus access resistance, respectively, and  $C_m$ ,  $R_m$ , and  $E_m$  represent the ERC-circuit of the cell. Usually, in voltage-clamp  $R_s \ll R_p \ll R_m$  and  $C_p < C_m$ . If  $E_s$  is a step function,  $R_s$  acts as an access resistance for charging  $C_p$ . Subsequently,  $R_p$  acts as an access resistance to charge up  $C_m$ . Because there are two capacitors coupled by a resistor, there is a **two-phase charging process** in the measurement circuit, which occurs during each voltage-step in a patch-clamp experiment. This will be analyzed now using ERC-circuit IV.

After the discussion of ERC-circuits I to III, we don't need to explain the equations for currents through resistors (Ohm's law) or currents into capacitors (capacitor equation). We can instead directly apply **Kirchoff's current law** to the two nodes  $V_p$  and  $V_m$ .

For node  $V_p$  (see Fig. 2.4) we write

$$I_{rs} = I_{cp} + I_{rp} \quad (30)$$

or

$$(E_s - V_p) / R_s = C_p dV_p / dt + (V_p - V_m) / R_p \quad (31a)$$

or

$$R_s R_p C_p dV_p / dt = -(R_s + R_p) V_p + R_p E_s + R_s V_m \quad (31b)$$

Eqs. 31a is a first order differential equation, but its solution is undetermined because it includes  $V_m$  as another variable obeying another first order differential equation (see below). Given that  $V_m$  is undetermined, the steady-state solution of Eq. 31 (for  $dV_p/dt = 0$ ) is

$$V_p^* = (R_p E_s + R_s V_m^*) / (R_p + R_s) \quad (32)$$

Although this equation does not provide a unique solution of  $V_p^*$ , because  $V_m^*$  is undetermined ( $V_m^*$  depends on  $E_m$  and  $R_m$ , which are not included in this equation, see below!), it provides a measure of  $V_p^*/V_m^*$  value pairs consistent with steady-state conditions. We need to incorporate  $E_m$  and  $R_m$  in the equation to find a unique value of  $V_p^*$  (see Eq. 36).

For node  $V_m$  (see Fig. 2.4a) Kirchoff's current law allows us to write

$$I_{rp} = I_{cm} + I_{rm} \quad (33)$$

or

$$(V_p - V_m) / R_p = C_m dV_m/dt + (V_m - E_m) / R_m \quad (34a)$$

or

$$R_p R_m C_m dV_m/dt = -(R_p + R_m) V_m + R_p E_m + R_m V_p \quad (34b)$$

Eq. 34b is also a first order differential equation. It is coupled to differential Eq. 31 through  $I_{rp}$ . Together these equations form a set of **two coupled linear first order differential equations**. The steady-state solution ( $dV_m/dt = 0$ ) for  $V_m$ , again with no unique solution, is

$$V_m^* = (R_p E_m + R_m V_p^*) / (R_p + R_m) \quad (35)$$

Eqs. 32 and 35 form a set of two **steady-state equations** with two unknowns. We can solve them by substitution, both for  $V_p^*$  and for  $V_m^*$ . The result is

$$V_p^* = [(R_p + R_m) E_s + R_s E_m] / (R_s + R_p + R_m) \quad (36)$$

and

$$V_m^* = [R_m E_s + (R_s + R_p) E_m] / (R_s + R_p + R_m) \quad (37)$$

These equations imply that  $V_m^* \sim V_p^* \sim E_s$  under good **voltage-clamp** conditions, with  $R_m \gg R_p \gg R_s$ , as wanted. However,  $V_p^*$  is closer to  $E_s$  than it is to  $V_m^*$ , because of loss of voltage across  $R_p$ . During practical experiments  $R_p$  (and an extra access resistance associated with  $R_p$ , see Chapter 3) may become a problem if  $R_m$  is not much larger than  $R_p$ . Then the cell will escape voltage-control and an excitable cell may fire a distorted action potential upon voltage-steps, seen as an action current instead of a voltage-controlled current.

$R_p$  may also complicate **current-clamp** recordings, since  $V_p^*$  is usually measured instead of  $V_m^*$ , although the interest is in  $V_m^*$ . For the condition  $R_s \gg R_m R_p$  (current-clamp), Eq. 36 becomes

$$V_p^* = E_m + (R_m + R_p) I_{cc} \quad (38)$$

with

$$I_{cc} = E_s / R_s \quad (39)$$

Thus, only for  $R_p \ll R_m$  the change in  $V_p^*$  upon current-clamp stimulation is largely due to  $R_m$ .

The **voltage time courses**  $V_p(t)$  and  $V_m(t)$  for  $E_s$  steps are more difficult to determine, because this requires solving two coupled differential equations. This can be done by writing first two separate second order differential equations by substitution of one into the other, and vice versa, as when solving any two equations with two unknowns. Both second order equations can be written in a general form

$$K_p \cdot d^2 V_p/dt^2 + L_p dV_p/dt + M_p V_p = N_p \quad (40)$$

and

$$K_m \cdot d^2 V_m/dt^2 + L_m dV_m/dt + M_m V_m = N_m \quad (41)$$

with  $K$ ,  $L$ ,  $M$  and  $N$  being constants defined in Note 2.4.1.

The solutions of these two equations have a general form (Hirsch and Smale, 1974; see Ince et al., 1986 for a similar problem).

$$V_p(t) = A_p e^{-t/T_{p1}} + B_p e^{-t/T_{p2}} + D_p \quad (42)$$

and

$$V_m(t) = A_m e^{-t/T_{m1}} + B_m e^{-t/T_{m2}} + D_m \quad (43)$$

with A, B and D being constants. Thus, these solutions have the shape of the sum of two exponential functions, with T1 and T2 being complex functions of  $\tau_p = R_s C_p$ ,  $\tau_m = R_p C_m$  as well as other parameters.

Instead of analyzing the explicit expressions of Eqs. 42 and 43, here we follow a practical approach by numerically calculating (see Note 1.3.1) the functions  $V_p(t)$  and  $V_m(t)$  for the equivalent circuit of Fig.2.4a under good **voltage-clamp** conditions ( $R_s \ll R_p \ll R_m$ ). The forms of these functions are sketched in Fig. 2.4b.  $C_p$  is charged in two phases, an initial rapid phase and a second slow phase.  $C_m$  is charged with a sigmoidal time course in which the onset corresponds to the rapid charging of  $C_p$  and the later phase corresponds to the slow charging of  $C_p$ . The initial fast charge is close to the time constant  $\tau_p = R_s C_p$  and the long charge is close to the time constant  $\tau_m = R_p C_m$ . Thus, the time constants T1 and T2 in the equations  $V_p(t)$  and  $V_m(t)$  correspond to approximately to  $\tau_p$  and  $\tau_m$ , respectively. This seems reasonable because at extreme differences between  $R_s$ ,  $R_p$ , and  $R_m$ , as occur during good voltage-clamp, charging of  $C_p$  and  $C_m$  is virtually independent. In the calculated **current-clamp** responses to  $E_s$  steps, the presence of a significant  $R_p$  can be seen as an initial shoulder in the  $V_p(t)$  response and as a small delay in the  $V_m(t)$  response (see Fig. 2.4c). The calculated **charging currents,  $I_{rs}(t)$** , are also given in Fig. 2.4b,c. The voltage-clamp currents (lower record of figure b) clearly show successive  $C_p$  and  $C_m$  charging.  $I_{rs}(t)$  was calculated from the equation (cf. Eq. 1b) :

$$I_{rs}(t) = (E_s - V_{cp}(t)) / R_s \quad (44)$$

The explicit form of this expression is not derived here.

For **voltage-clamp** conditions, the above equation describes what every patch-clamper knows well as a two-phase (fast and slow) capacitance charging current in response to voltage steps (see Fig. 2.4b), on which they spend so much time, cell after cell, to measure and cancel. The fast current transient mainly reflects  $C_p$  charging, while the slow transient mainly reflects  $C_m$  charging, as discussed above for the voltage changes  $V_p(t)$  and  $V_m(t)$ .

Under **current-clamp** conditions ( $R_s \gg R_p R_m$ ), Eq. 44 describes the current leaving the clamp instrument, but not exactly the current entering the membrane, because the initial fast current component mainly serves to charge  $C_p$ . The actual current of interest,  $I_{rp}(t)$ , is described by

$$I_{rp}(t) = [(V_p(t) - V_m(t)) / R_p] \quad (45)$$

but it is impossible to catch this current in one-electrode patch-clamp experiments, in which one can only record current  $I_{rs}$  (in voltage-clamp) or  $V_p$  (in current-clamp). Fortunately, the difference between  $I_{rs}$  and  $I_{rp}$  is of no concern if  $R_s \gg R_m \gg R_p$  and  $C_p < C_m$ . In that case the current steps

are practically square both for  $I_{rs}$  and  $I_{rp}$ . There should nevertheless be a very small two-component overshoot in the applied current  $I_{rs}$ , but this is hardly visible in records (cf. Fig. 2.4c).

Eqs. 36, 37, and 42-44 are probably the most important and practical equations of this course, because they describe the patch-clamp stimulation technique in a way that includes both voltage- and current-clamp stimulation under ideal and non-ideal clamp-conditions. Although many problems can be understood through these equations, practical problems can, of course, be more complex than modeled by the ERC-circuits discussed so far. For example, a cell may be coupled to another cell, so that the stimulated object is no longer a single ERC-compartment. In that case the ERC-circuit representing the stimulated object should be extended with another resistively coupled ERC-compartment. If the equivalent circuit becomes complex, it may be useful to employ a computer model to simulate the measurement configuration or to make an electrical equivalent model as we did in Chapter 3 for demonstrating the ERC-circuit theory of this chapter.

Finally, it is of interest to mention that ERC-circuit IV is identical to a **model of two electrically coupled cells**. The  $E_sR_sC_p$ -circuit would represent cell 1 and the  $E_mR_mC_m$ -circuit cell 2, with  $R_p$  being the coupling resistance of a gap junction. This model can be used to study the effect of  $E_s$  changes in cell 1 on  $V_m$  of cell 2, as well as the role of the membrane resistances ( $R_s$ ,  $R_m$ ), the coupling resistance ( $R_p$ ), and membrane capacitors ( $C_p$ ,  $C_m$ ) in this interaction. Thus, ERC-models may be of great use, not only for practical patch clamping but also in more general problems of cell physiology. We will see this demonstrated again below (chapter 2.6).

## **2.5. Measuring and filtering the conductance response of an ERC-membrane in voltage clamp: ERC-circuit V**

Thus far we have discussed ERC-circuits of patch-clamp conditions from the point of view of the stimulation technique, whether it was voltage-clamp or current-clamp. We have only looked at the passive response of the clamped circuit.

The active response of a membrane of a living cell to an evoked change in potential often is a change in membrane resistance. Patch-clampers (usually voltage-clampers) speak of conductance changes rather than of resistance changes as the focus is on the membrane instead of on the stimulation technique. This is because conductance changes under voltage-clamp are directly reflected in current changes, which makes interpreting the observations easier. We follow this view, although the conductance changes can easily be translated back to resistance changes.

Microscopic conductance changes upon membrane potential changes are essentially abrupt, since they are changes resulting from abrupt opening or closing of ion channels in the membrane (Hille, 1992). Although macroscopic conductance changes seem more gradual, with an apparent smooth time course, they are in fact the summed-average result of a collective opening or closing process of individual ion channels, each with its stochastic, abrupt opening or closing behaviour (DeFelice, 1997). Here, and in the subsequent section, we consider membrane current and potential behaviour resulting from such abrupt conductance changes in a cell. It is because of this abrupt opening and closing channel behaviour that we can use the same equivalent-circuit theory to describe the membrane potential and channel current changes resulting from channel activity as employed above for the explanation of the experimental procedures of the patch-clamp technique. Using this

approach, we demonstrate that a whole-cell **membrane current** induced by abrupt conductance activation (one large channel or a simultaneous activation of a large group of small channels) is **always filtered by the RC-properties of the whole-cell measurement configuration**, and that additional filtering occurs in the voltage-clamp amplifier.

Figure 2.5 illustrates the circuit to be discussed. The cell (right side of circuit) consists of a Gk-branch, parallel to a membrane capacity Cm. The Gk-branch contains an Ek, Rk (or Gk) and a switch, Sk, to activate or deactivate Gk. Thus if Sk is off, the membrane has zero conductance. The voltage-clamp consists of a voltage source Es in series with a source resistance, Rs. The source resistance is shunted by a source capacitance, Cs. The V-clamp is coupled to the whole-cell by a pipet with pipette resistance, Rp, and pipette capacitance, Cp, to ground. Component values are such that Rk >> Rp >> Rs and Cm >> Cp. New in this circuit is the presence of a third capacity, Cs, connected across Rs (besides Cm and Cp). Cs is naturally associated with Rs (a “stray” capacitance), or it can be added for filtering purposes. Because Es is in series with Cs, Cs cannot simply be seen as a parallel capacity of Cp, certainly not for current flow due to Es-steps. The way in which Cs causes current filtering of the fast capacity current Ics we explain in chapter 3.3.2 and Note 3.3.2. Here we focus on the role of Cs in the filtering of current resulting from membrane conductance activation.

If we assume that Vm = Es = 0 mV and that Cs = Cp = 0 pF, and Gk is suddenly switched on by Sk, it is easily shown with the theory explained above (Ohm’s and Kirchoff’s laws and the capacitor equation) that Cm is charged to a steady Vm value Vm\*

$$V_m^* = (R_p + R_s) E_k / (R_p + R_s + R_k) \quad (46)$$

with a time course

$$V_m(t) = V_m^* + (V_m(0) - V_m^*) e^{-t/\tau_{pm}} \quad (47)$$

with

$$\tau_{pm} = R_{pm} C_m \sim \tau_p = R_p C_m \quad (48)$$

because

$$R_{pm} = (R_p + R_s)R_m / (R_p + R_s) + R_m \sim R_p R_m / R_p + R_m \sim R_p.$$

Vm\* is much smaller than Ek (Vm\*~0mV), because in this WC-measurement configuration Vm is clamped to Es=0mV.

The current flowing into Rp and into the V-clamp is Irp ~ Vm(t)/Rp, thus this current does not flow abruptly upon the abrupt activation of Gk, but instead it gradually builds up with an exponential time course with time constant ~ p. **Rp and Cm cause signal filtering of whole-cell currents, inherent to the measurement configuration.** To make this filtering effect less worse, one should make Rp as small as possible and pick small cells to obtain small Cm values. This RpCm-filtering effect is illustrated in the model cell experiment of chapter 3.4.4. Once steady Irs is measured in a real experiment, Gk can be calculated if Ek is known, or it can be measured separately.

Often one just tries to record WC-currents at the best possible WC-conditions (minimal  $p = R_p C_m$ ) in order to be able to decide later in the experiment to filter out disturbing high frequency signals (e.g. noise) using filters inside the amplifier. The role of  $C_s$  is essential in understanding this filtering, as we explain now for a simplified version of the circuit of Fig. 2.5.

If we assume that  $C_m = C_p = 0$  pF (to offer a perfect current step upon  $G_k$  activation to the amplifier) and also that  $E_s = 0$ mV (to get the simplest possible equation) we can derive that the steady voltage  $V_s^*$  is equal to

$$V_s^* = R_s E_k / (R_s + R_p + R_k) \quad (49)$$

Notice that  $V_s \ll V_m$  or  $E_k$  at all times, because the cell is voltage-clamped to  $E_s$  and  $E_s = 0$  in this case.

The time course of  $V_s$  is described by

$$V_s(t) = V_s^* + [V_s(0) - V_s^*] e^{t/\tau} \quad (50)$$

With

$$\tau = R_s / (R_p + R_k) C_s \sim R_s C_s \quad (51)$$

This means that steep current steps injected into the amplifier (circuit point  $V_s$ ) are reshaped to an exponential voltage change in  $V_s$  with time constant  $\tau$  and that the voltage-clamp current  $I_{rs}$  calculated from  $V_m(t)$ , and  $I_{rs}(t) = V_m(t)/R_s$  has the same exponential time course. Thus, if  $C_s$  can be chosen large enough, the internal amplifier  $R_s C_s$ -filter can filter out high frequency signals that passed through the  $R_p C_m$ -filter. Usually  $C_s \gg C_p$ , which justifies assuming  $C_p=0$  in the derivations.

The same idea must hold if  $R_p$ , and if  $C_m$  and  $E_s$  do not have zero values. This can be checked by deriving an equation for  $I_{rs}(t)$  for the complete circuit of Fig.2.5. The basic differential equation describing the circuit must be a 3<sup>rd</sup> order differential equation because of the presence of three capacities and the equations shown above must be solutions for the simple cases considered.

The present explanation of filtering by the amplifier is based on the simple equivalent  $E_s R_s C_s$ -circuit of the amplifier shown at the left side of Fig. 2.5. Although this circuit is too simple to precisely describe practical filtering of a patch-clamp, it illustrates a basic filtering mechanism as a property of a simple RC-circuit, which can only serve as a first and rough didactic approximation of the filtering process in the amplifier. The relationship between RC-filtering (in the time domain) and frequency filtering (in the frequency domain) is explained in Note 2.5.

## 2.6. Switching conductors in an ERC-membrane model in current clamp: ERC-circuit VI

We finally discuss membrane potential and membrane current resulting from abrupt conductance changes in a cell in the case that the cell membrane or a membrane patch has only three channels. It is because of this abrupt opening and closing behavior that we can use the same equivalent-circuit theory to describe the membrane potential and channel current changes resulting from channel

activity as employed above for the explanation of the experimental procedures of the patch-clamp technique. It should be realized, however, that this theory only describes the voltage and current changes between the channel opening and closing events.

Let us consider the **parallel conductance** (or resistance!) **circuit** of Fig. 2.6a. Three conductance pathways (G1-3) parallel to a membrane capacitance (Cm) are drawn. Each conductance branch contains, besides the conductor G, a voltage source E and a switch S. Closure of the switch causes abrupt opening of the channel (or insertion of a conductance) – and opening does just the opposite. To avoid confusion we let “switch-on” mean “switching-on the channel” (or conductance). Likewise, switch-off will mean “off” for both switch and channel (or conductance).

First we examine the parallel conductance circuit with all three switches on, without a voltage-clamp or current-clamp connected. The question to be answered is this: **which membrane potential, Vm, does the circuit produce upon switching on and off any of the conductances and which currents are flowing** in the various branches?

**Kirchoff's current law** allows us to write, as before, for an arbitrary external current Irs from a clamping device (Fig. 2.6a)

$$I_{rs} = I_{r1} + I_{r2} + I_{r3} + I_{cm} \quad (52)$$

By applying Ohm's law (now  $I = G V$ , since  $G = 1/R$ ) to the currents through the branches, and by using the capacitor equation for the capacitance current, Eq. 1 can be rewritten for  $I_{rs} = 0$  (no external clamping device) as

$$G_1 (V_m - E_1) + G_2 (V_m - E_2) + G_3 (V_m - E_3) + C_m dV_m/dt = 0 \quad (53a)$$

Other forms of this equation can be found below (Eqs. 53b and 53c). This **differential equation** is similar to the one derived for circuit III (Fig. 2.3a), but it contains one more term for the extra branch. Thus, it is as if the  $E_s/R_s$  source is now included in the membrane! Hence it is no surprise that the approach for describing the parallel conductance circuit properties of a membrane is the same as that for the ERC-circuit of the patch-clamp measurement condition.

The **steady-state** membrane potential  $V_{m123}^*$  (measurable with a good zero-current-clamp!) of our parallel 3-conductance circuit is found by assuming  $dV_m/dt = 0$ :

$$V_{m123}^* = (G_1.E_1 + G_2.E_2 + G_3.E_3) / (G_1 + G_2 + G_3) \quad (54a)$$

or, when written in terms of resistances ( $G = 1/R$ ),

$$V_{m123}^* = (R_2.R_3.E_1 + R_1.R_3.E_2 + R_1.R_2.E_3) / (R_1 + R_2 + R_3) \quad (54b)$$

$V_{m123}^*$  is the steady-state  $V_m$  when all three channels are on. If channel 3 suddenly closes ( $G_3 = 0$ , substitute in Eq. 53a),  $V_{m123}^*$  changes to

$$V_{m12}^* = (G_1.E_1 + G_2.E_2) / (G_1 + G_2) \quad (55a)$$

or

$$V_{m12}^* = (R_2.E_1 + R_2.E_1) / (R_1 + R_2) \quad (55b)$$

$V_{m13}^*$  can be derived from Eq. 54a by substituting  $G_2 = 0$  and  $V_{m23}^*$  is found by substituting  $G_1 = 0$ . These equations have the same shape and structure as the one for  $V_{m12}^*$ . Obviously,  $V_m^*$  for any of the three possible one-conductance ERC-circuits is found by substituting zero for the two other conductances in Eq. 54a, e.g. for  $G_2 = G_3 = 0$   $V_{m1}^* = E_1$ . The **time behavior** of the present three-conductance ERC-circuit upon channel opening is still quite simple, because the presence of only one capacitor,  $C_m$ , in parallel insures that all transients are single-exponentials. The time constants of the transients depend on which channels are open.

Eq. 53a can be rewritten to obtain an expression to easier find the time behavior  $V_{m123}^*(t)$  of the 3-conductance ERC-circuit:

$$dV_m/dt = -(G_1 + G_2 + G_3)/C_m \cdot [V_m - (G_1.E_1 + G_2.E_2 + G_3.E_3)/(G_1 + G_2 + G_3)] \quad (53b)$$

or

$$dV_m/dt = -1/\tau_{123} \cdot [V_m - V_{m123}^*] \quad (53c)$$

with

$$\tau_{123} = R_{123} C_m \quad (56)$$

with

$$R_{123} = 1 / (G_1 + G_2 + G_3) = R_1 R_2 R_3 / (R_1 R_2 + R_1 R_3 + R_2 R_3) \quad (57)$$

and with  $V_{m123}^*$  given by Eq. 54b. The solution of Eq. 53c is

$$V_{m123}(t) = V_{m123}^* + (V_m(0) - V_{m123}^*) e^{-t/\tau_{123}} \quad (58)$$

Thus, the time constant of the exponential transient is equal to the equivalent resistance of the parallel resistors times  $C_m$ . The more parallel resistors, the faster the transient, with the smallest resistance (largest conductance) having the largest influence.

In a similar way it can be shown that

$$V_{m12}(t) = V_{m12}^* + (V_m(0) - V_{m12}^*) e^{-t/\tau_{12}} \quad (59a)$$

and

$$V_{m13}(t) = V_{m13}^* + (V_m(0) - V_{m13}^*) e^{-t/\tau_{13}} \quad (59b)$$

and

$$V_{m23}(t) = V_{m23}^* + (V_m(0) - V_{m23}^*) e^{-t/\tau_{23}} \quad (59c)$$

Here the time constants are the products of the equivalent resistance values of the two parallel conductances times  $C_m$  in exactly the same way as derived for ERC-circuit III, in which the  $E_s/R_s$  branch of the patch-clamp was parallel to the  $E/R$  branch of the membrane to be clamped. Obviously, when only channel remains open, the exponential transient with time constant  $\tau_i$  is given by

$$V_{mi}(t) = E_i + (V_m(0) - E_i) e^{-t/\tau_i} \quad (60)$$



Thus, for the description of  $V_m(t)$ , one must simply choose the right equation, the one with 3, 2 or 1 (and this is random!) conductances.  $V_m(0)$  in all those cases is  $V_m$  just before the channel opened or closed. If all channels close, the  $V_m$  value just before closing the last channel will persist until one of the other channels opens again. Fig. 2.6b shows a calculated  $V_m$  during opening and closing of channels of the circuit in a certain sequence.

Finally, we examine the **time course of the channel currents** during channel activity. The equation for this time course is derived in the same way as for the voltage-clamp current in ERC-circuit III. The polarity of the currents through all the branches will then be consistent with convention: outward current positive and inward current negative. The current,  $I_{gi}(t)$ , through channel  $i$  of conductance branch  $i$  is then given by

$$I_{gi}(t) = G_i (V_{m123}(t) - E_i) \quad (61)$$

if all three channels are open. If two channels are open, or only one, the applied  $V_m(t)$  should be included. Examples of channel currents in response to channel openings and closings are illustrated in Fig. 2.6b (lower records).

## 2.7. Conclusion

A few final remarks may place the simple equivalent ERC-circuit approach of the present chapter in a broader perspective. This approach helps to understand how and what one is measuring during patch-clamping, but the **ERC-circuit theory used here only describes voltage and current changes upon abrupt changes of the components of the ERC-circuit**. Abrupt E-changes apply to the patch-clamp technique with its voltage- and current-clamp jumps. Abrupt R-changes apply to channel openings and closures and relatively sudden conductance changes. Sudden C-changes seem less relevant, but are nevertheless easily described with the same equivalent circuit theory. Fusion of two cells or vesicles with different membrane potentials would be an example of interest.

The simple **ERC-circuit approach does not apply to the kinetics** of voltage dependent channel or conductance activation, which is widely studied in membrane electrophysiology. This field of study requires additional concepts, bridging the microscopic mechanisms of single channel activation and macroscopic electric phenomena like excitability. Students interested in this subject are referred to other texts (Hille, 1993; DeFelice, 1997) or are referred to the instructive teaching models now widely available (see Note 1.3.1).

The ERC-models discussed above bring up an interesting thought: if one of the three conductances of Fig.2.6 would be much larger than the other two, the voltage source of that conductance branch would in effect voltage-clamp the other conductances in the membrane. So, **natural voltage-clamp conditions** may actually occur in the membrane of a living cell. An example of indigenous voltage-clamp is the condition that the resting membrane potential of a cell is close to the potassium Nernst potential. In that case the membrane is “voltage-clamped” by its  $K^+$  conductance.

**Natural current-clamp** might occur if a high-resistance conductance with a relatively large-voltage source (e.g.  $\sim 100\text{mV}$ ) would send its current into a low-resistance neighboring branch with a small-voltage source (say a few mV). Only in that case the receiving conductance branch would receive

current without significantly contributing to that current. Electrogenic ion pumps are probably better internal current-clamp components of the membrane than ion channels, because they may produce relatively large electrogenic voltage sources with relatively large source resistances (Läuger, 1991).

A recommended next step after this chapter is to exercise your grasp of the equivalent circuit theory by testing it in a real patch-clamp set-up with a model cell displaying ERC-circuit properties like those shown above. How to proceed is explained in the next chapter. Or one could also directly go to actual patch-clamp experiments, but we have learned from experience that it is still difficult in the beginning to recognize ERC-circuit phenomena in living cells. Instant recognition during experiments may be important for quick decisions about how to continue successful protocols if technical problems arise. However, spending some extra time now on a model cell saves time in the long run, because the observations are not obscured then by accidental experimental complications.

### 3. MODEL CELL EXPERIMENTS.

#### 3.1. Introduction

The following demonstrations and exercises will be presented more or less in the sequence of a real patch-clamp experiment, from switching on the equipment to, for example, pulling an outside-out patch, through all the intermediate phases, such as pipette testing, giga-sealing and whole-cell formation. Fortunately, this sequence is in line with the sequence of the ERC-circuits discussed in the previous chapter. We will often refer to those ERC-circuits, including the derived equations. No new equations need to be derived. The descriptions will be as if we were giving a demonstration, but with suggestions to the reader for doing her own extra experiments. If you do the experiments, make sure that you start each session with a standard amplifier and model (see below). Otherwise, you may get lost in abnormal amplifier behavior (e.g. oscillations), or the amplifier may look dead (in saturation), or you may misinterpret the model cell responses. Prevent touching the (+) input of the patch-clamp amplifier as much as possible, since your body is a capacitor (probably isolated from ground by non-conducting shoes) and may be charged to quite a few volts with respect to ground. This body capacitance shares its charge and voltage with the small input capacitance of the patch-clamp, and large voltages may damage the input. Therefore use insulated forceps to contact the circuit or ground yourself first before touching the circuit so that you will not carry large harmful voltages.

The importance of the demonstrations and experiments is that they provide **exercises in recognizing simple electric circuit behavior in complex experimental conditions**. Without such exercises it might take months, or even years, to develop that skill.

#### 3.2. Model cell and measurement set-up description

##### 3.2.1. Equivalent circuit

Fig. 3.1 shows the electrical equivalent circuit of the model cell used to illustrate the electrophysiological properties of the various patch-clamp measurement configurations in a real patch-clamp set-up. It is an **ERC-circuit model**, i.e. it only consists of voltage sources (E), resistors (R) and capacitors (C). **Switches** (S1-12) are used at various points in the circuit to switch the circuit from one configuration to another or to represent opening and closing of ion channels and abrupt activation of ion conductances. It is very similar to the ERC-model in Fig. 1.2b but more detailed. For example, it includes specific resistors or conductors in the CAP and WC and also allows the establishment of the IOP, OOP and ppWC configuration. E, R and C components and values as well as switches are listed in Table 3.1. Component values are in the physiological range. Switches are drawn in the standard initial positions, from where changes are defined.

The circuit left of the patch-clamp connection switch S<sub>pc</sub> (# 2) is the **ERC-circuit equivalent of the patch-clamp amplifier**. Switch S<sub>vc</sub> (# 1) is used to switch between the two measurement modes, voltage-clamp (vc) and current-clamp (cc). The circuit includes an ideal volt (V) meter and an ideal current (I) meter (with  $I = V_{vc}/R_{vc}$  representing the current to voltage conversion). E<sub>pc</sub> corresponds to E<sub>s</sub>, and R<sub>vc</sub> and R<sub>cc</sub> represent the two extremes ( $R_{cc} \gg R_{vc}$ ) of R<sub>s</sub> values in the ERC-circuits of the previous chapter. C<sub>pc</sub> is the input capacity of the patch-clamp. Switch S<sub>pc</sub>

connects the pipette-holder (with pipette) to the patch-clamp and introduces the extra capacity  $C_{pip}$  to the amplifier input. Practical information on patch-clamp amplifier settings is given below. Simultaneous closing of switches  $S_{cpip}$  (# 3) and  $S_{rpip}$  (# 4) represents **entering the bath solution with the pipette**, thus connecting pipette capacitance  $C_{pip}$  and pipette resistance  $R_{pip}$  to the patch-clamp input. Closing only  $S_{cpip}$  simulates testing a clogged pipette with immeasurably high  $R_{pip}$ . Opening switch  $S_{seal}$  (# 5) after closing switches 2, 3, and 4 symbolizes **giga-sealing** of the pipette tip to the cell and the **formation of a cell-attached patch (CAP)** with resistance  $R_{cap}$  and capacitance  $C_{cap}$ . Closure of channel switch  $S_{capch}$  (# 6) in the CAP activates a CAP-channel by inserting in the CAP the CAP-channel resistance  $R_{capch}$ , shunting the resistance of the CAP membrane,  $R_{mcap}$ .  $R_{cap}$  is the equivalent of  $R_{mcap}$  and  $R_{capch}$  in parallel. The CAP-membrane and CAP-channel have not been given intrinsic voltage sources (CAP-membrane potential and channel reversal potential), assuming that the pipette solution has an ionic composition, which is essentially the same as the cytoplasm.

Breaking the CAP for **establishing the whole-cell (WC)** configuration is simulated by closing access switch  $S_{acc}$  (# 7), which short-circuits  $R_{cap}$  by inserting the much lower access resistance  $R_{acc}$  as an extra resistance in series with  $R_{pip}$ . Switching inside-out-patch (IOP) switch  $S_{iop}$  (# 8) to the left, from its WC-position to the IOP-position while  $S_{acc}$  is open, imitates **excision of an IOP** from the cell by abruptly pulling up the pipette in the CAP-configuration. With  $S_{acc}$  closed,  $S_{iop}$  in the WC-position and outside-out-patch switch  $S_{oop}$  (# 9) closed we are in the conventional WC-configuration, from where we can **enter the OOP-configuration** by opening switch  $S_{oop}$ . Conductance switches  $S_{gl}$  (# 10),  $S_{gk}$  (# 11) and  $S_{gna}$  (# 12) can be used to suddenly activate or deactivate the three WC membrane conductances  $G_l$  (leak conductance),  $G_k$  ( $K^+$  conductance) and  $G_{na}$  ( $Na^+$  conductance), respectively. Total membrane conductance  $G_m = G_m' + G_{oop}$ , with  $G_m'$  being the sum of the active conductances  $G_l$ ,  $G_k$ , and  $G_{na}$ , thus excluding  $G_{oop}$  and  $G_{cap}$ . WC membrane capacitance is  $C_m = C_m' + C_{oop}$ , thus excluding  $C_{cap}$ . **Formation of the permeabilized-patch WC (ppWC)** configuration simulated by inserting successively decreasing  $R_{acc}$  values

The grounded side of the circuit is the extracellular side of the cell membrane. The patch-clamp potential,  $E_{pc}$ , the pipette potential,  $V_{pip}$ , the membrane potential,  $V_m$ , and the reversal potentials,  $E_{oop}$ ,  $E_l$ ,  $E_k$ , and  $E_{na}$  are measured (or defined) with respect to this extracellular ground potential.  $V_{rvc}$  is the voltage across the resistor  $R_{vc}$ .

### 3.2.2. Model hardware

The present information on the hardware components and patch-clamp set-up that we used is only important for those students who want to do the model exercises themselves in their own time on an available patch-clamp set-up. The other students can directly proceed to the demonstrations (chapter 3.3.).

The **model circuit** was not constructed by soldering together ERC components and mechanical switches. That turned out to be unsatisfactory, because of unwanted stray capacities in the switches, sensitivity to hand-movement artifacts during manipulations on the circuit, and limited flexibility for changes of the circuit. Furthermore, switches showed “bouncing” of the contacts causing undefined switching. We preferred to employ commercially available circuit boards (“bread

boards") generally used for prototype circuit building and for teaching. A small board of 8x6cm (see Fig. 3.2) was ideal to build up the entire circuit and to place it on the stage of the microscope instead of a cell chamber with bathing solution and cells. It was fixed in place with magnetic strips adhering to a grounded metal plate on the microscope stage. This plate in fact corresponds to the grounded bath solution around the cells in a cell chamber. Working in this way and using the regular equipment of a set-up gives the "feel" of doing a real patch-clamp experiment. One also benefits from the grounded environment around the model circuit, screening off the model cell from 60 (or 50) Hz interference.

A **breadboard** is a plastic board with groups of rows of internally interconnected holes for insertion of the leads of the components (Fig. 3.2). Connected holes quickly join components together (instead of soldering) and unconnected rows of holes can be bridged by components, thus easily creating ERC-circuits of a pipette, a membrane patch, and a whole-cell membrane as well as the switches between these circuits and the components. The switches were just simple solid (insulated) wires (Sseal, Siop, Soop), or component leads, inserted into or pulled out of the holes by hand or by using a forceps with insulated tips. In certain cases, when switching had to occur quickly and be well timed, magnetic switches (reed contacts) were used. Moving a small magnet on a rod along the contact operated magnetic switches. In order to protect the input of the amplifier during manipulation, we insulated the leads of components by putting shrink isolation tubing around them. This tubing shrinks tightly around the leads when heated, for example, by holding a solder gun close to the tubing.

Small-size 3.4-volt lithium cells in a voltage-dividing resistor circuit were employed to obtain physiological reversal potentials for insertion in the parallel conductance branches of the cell membrane. Resistor values of 1-100 M $\Omega$  and capacitors of 1-100pF can usually be obtained in a departmental electronic workshop or can be bought in a commercial shop for electronic components. Higher resistor values probably need special ordering. Axon Instruments Inc. (Foster City, CA 94404, USA) offers a low-price selection of Giga Ohm values. Low stray capacity (< 0.5pF) is an important specification of good high resistance components, in particular for the cell-attached-patch resistors and the seal resistance. The small capacity Ccap was not an added component, but was the actual stray capacitance naturally associated with the circuit connections in the board and with the resistors coupled together in the CAP-section of the model.

### 3.2.3. Patch-clamp set-up

Each **patch-clamp set-up** requires specific instruction. Therefore, we only briefly describe the patch-clamp set-up we used for the demonstration measurements presented here. The heart of the set-up is the cell chamber on the stage of the microscope with the small patch-clamp preamplifier box (probe or head-stage) above the cells. The head-stage is held and manipulated by a micromanipulator and has a connector for connecting the pipette-holder. In our exercises the circuit board with **the cell model takes the place of the cell chamber**, and a 5-cm wire serves as a pipette-holder connecting the (+) input to the pipette resistor, Rpip, and pipette capacity, Cpip (Fig. 3.2). The grounded reference (-) input of the head-stage (the probe) is connected to the external side of the model membrane. The patch-clamp used is the **L/M-PC amplifier** of List-Medical (D-6100 Darmstadt, Germany). As all commercial patch-clamps, it can either be used in the voltage-clamp or current-clamp mode. It also has the standard facility to cancel fast (pipette) and slow (whole-cell)

capacitance currents and to measure the capacities ( $C_{pip}$  and  $C_m$ ) and series resistances ( $R_{vc}$  and  $R_{pip} + R_{access}$ ) causing these voltage-step induced transients. The amplifier is equipped with electronic low-(frequency)-pass filters to remove high-frequency components from the signal at different cut-off frequencies (1-80KHz).

It is important that all switches and dials of the main patch-clamp unit in the rack are in **standard initial positions** before starting any experiment: Amplifier mode should be on voltage-clamp;  $V_{pip}$  offset and  $V_{hold}$  potentiometer dials should be on zero; series compensation should be off; capacity cancellation dials should be on zero, and the cancellation switch(es) should be off; filter setting should be on 10 kHz (80 kHz in the initial experiments, see Fig. 3.3), and step steepness on  $2\mu s$  rise time (no rounded voltage steps). Finally, the gain and stimulus scaling should be standard or as required by the software used.

The application of **voltage- and current-clamp protocols** to the model cell and the simultaneous storage of the evoked responses can be controlled by a personal computer using **pClamp/Clampex** software (MS-DOS or Windows) of Axon Instruments (Foster City, CA 94404, USA). The monitor of the PC run by pClamp can in principle be used as an oscilloscope screen to monitor the stimulus steps and the current or voltage responses, but we found it useful to use a separate oscilloscope and simple block pulse generator for extra tests. Emphasis in this demonstration is on the direct interpretation of the records, so we will not use sophisticated data analysis procedures. Note that pClamp is not necessary for these experiments; all that is required is a function generator and an oscilloscope.

### 3.3. Patch-clamp measurement procedures and configurations

#### 3.3.1. Switching-on the patch-clamp: amplifier open input capacitance and resistance, and filtering

When you observe a patch-clamp experiment for the first time, you may see the patch-clamper turning on her equipment and bringing the switches and dials of her patch-clamp and other instruments to standard settings. Then she may start **voltage-clamp step stimulation** while watching the oscilloscope for the display of signals. The voltage steps clearly evoke sharply peaked, needle-like current responses ( $\sim 30\mu s$  **spikes** at 10KHz low pass filtering;  $\sim 5\mu s$  spikes at 80KHz filtering, see Fig. 3.3a). But, what is being clamped here? There is no pipette or cell connected to the input. The input is open. It is only exposed to the air! Is the air being voltage clamped? In a sense, yes.

That there is no steady current during the application of steady voltage is no surprise, since air has no conductance (infinitely large resistance). But then where do the spikes come from? Although air has no conductance, it separates the conducting input terminals. And one of these, the (-) input (the reference electrode) is connected to ground, i.e. to a great conducting mass surrounding the set-up, and therefore in some proximity to the (+) input (the measuring terminal). Thus, air functions as a dielectric, creating capacitance which is called here **stray capacitance** ( $C_{str}$ ), because it is unintended and distributed over the conducting mass around the (+) input terminal, inside and outside the head-stage in an unforeseeable way, but clearly measurable. It is this capacitance, also indicated as  $C_{pc}$  (C of the patch-clamp), which is charged by the voltage-clamp step through the internal resistance  $R_{vc}$  of the amplifier (Fig. 3.1). And the resulting short-duration charging

currents, spike-like on an ms-time base, are visible on the oscilloscope. Note that this is an example of ERC-circuit (Fig. 2.1)! The appearance of the spikes on the oscilloscope indicates to the experimenter that the patch-clamp amplifier and connected equipment are working and that she may go on to the next step in her experiment.

But first we measure this stray capacity  $C_{pc}$ . The patch-clamp instrument is equipped with a capacity measurement option based on precise **cancellation of a capacitance current transient** by adding to the transient at the input (from within the amplifier) an identical (single-exponential) current transient of opposite polarity. At precise cancellation the adjustment dials can be read off in terms of canceling capacitance  $C_f$  ( $f$  of fast transient) and canceling time constant  $\tau_f$  or resistance  $R_f$  (or conductance  $G_f$ ).  $R_f$  can be derived from  $\tau_f$  and  $C_f$  or  $\tau_f$  can be derived from  $R_f$  and  $C_f$  using  $\tau_f = R_f C_f$ , as explained at ERC-circuit 1. With this cancellation measurement, which can be carried out at any filter setting though easier at the higher settings, we find for our patch-clamp that  $C_f = C_{pc} = 1.0 \text{ pF}$  at  $\tau_f \sim 2 \text{ } \mu\text{s}$ . This capacitance may look very small, but is nevertheless well measurable. The time constant  $\tau_f$  could not precisely be determined from the dial, but the estimated  $C_f$  and  $\tau_f$  values allow us to calculate an estimated series resistance  $R_{vc} = R_f$  from  $\tau_f = R_{vc} C_{pc}$  (cf. ERC-circuit I). Then,  $R_{vc}$  seems to be  $\sim 2.5 \text{ M}\Omega$ . This is too large for reliable voltage-clamp measurements of  $R_{pip} \sim 1 \text{ M}\Omega$ , as we will see below. What could be the reason of this high estimated  $R_{vc}$  value? It may be an inaccurate reading of the  $\tau_f$  canceling dial. This dial is not well calibrated, because measuring  $\tau_f$  is not an important goal during patch-clamp experiments.

Let us try to obtain  $R_{vc}$  from direct, **current peak measurements**. At ERC-circuit 1 it was explained that  $R_{vc} = dE_{vc}/dI_{peak}$ . Therefore we measure  $dI_{peak}$  at 10KHz (standard) filtering for  $E_{vc}$  steps of 10mV and use this equation. We find  $R_{vc} = 10\text{mV}/0.5\text{nA} = 20 \text{ M}\Omega$ . Even much higher than the value obtained by the canceling procedure! What could be the reason here for the overestimation of  $R_{vc}$ ? One possible answer is the internal filtering in the patch-clamp amplifier, which lowers  $dI_{peak}$ .

We briefly discussed signal **filtering** in terms of ERC-circuits in the previous chapter. The relationship between RC-filtering and frequency filtering is further explained in Note 2.5. Filtering is here simply defined as an electronic procedure to selectively suppress fast wave (high frequency), medium or slow wave (low frequency) components of a recorded signal such as a voltage-clamp current signal. A patch-clamp usually has various filter settings allowing to remove the higher frequency components from the record. Standard filter setting is here at a cut-off of  $>10\text{KHz}$  frequencies and best setting is at  $>80\text{KHz}$  cut-off. This means that the  $5\text{-}\mu\text{s}$  ( $2 \text{ } \tau_f$ ) duration transient is drastically filtered by a frequency setting that is too low to faithfully record the fast capacitance peak transient. This results in a drastic reduction of the peak amplitude of the fast capacitance current transient and in a much slower time course of the remaining signal.

This is a reason to record the fast transient at the best possible frequency setting: 80KHz (as in Fig. 3.3). This high frequency filter requires recording at a better time resolution than the analog-to-digital conversion (ADC) card for pClamp controlled data storage may provide. Therefore, the readings are done from the oscilloscope. We find shorter ( $\sim 5\mu\text{s}$ ) and much higher peak transients ( $\sim 2.6\text{nA}$  on the scope,  $\sim 2\text{nA}$  in pClamp records, see Fig. 3.3a) and, consequently a much better  $R_{vc}$  value ( $\sim 4\text{M}\Omega$ ), but still worse than the amplifier rating. Understandably, we cannot reliably measure

a 5- $\mu$ s transient with an 80KHz filter. Furthermore, the steepness of the voltage step (2 $\mu$ s) also limits  $I_{peak}$  of the presumed 5- $\mu$ s transient. Thus we may think that measured  $I_{peak}$  values are too low and, consequently, calculated  $R_{vc}$  values too high. As we cannot do better now, we find another way to estimate  $R_{vc}$  below.

We summarize the results and **conclusions** as follows:

- \* Although the charging current transients upon voltage steps are heavily filtered by the amplifier, current cancellation is perfectly possible with fast ( $\sim 2.5\mu$ s) single-exponential current transients of opposite polarity.
- \* Thus, ERC-circuit I applies to the open input properties of the patch-clamp amplifier, and, in principle, it is possible to measure input capacity and resistance by cancellation.
- \* Series resistance ( $R_{vc}$ ) estimation from current peak measurements provides  $R_{vc}$  values that are too high because of signal filtering inside the amplifier.

### 3.3.2. Connecting the pipette-holder with pipette to the patch-clamp: extra stray capacity

We expect that connecting the pipette-holder (with inserted pipette) to the input would affect these spikes by making them wider, but not higher, as we predicted from the properties of ERC-circuit I. This is because the mass and surface of the input wiring is increased, and probably also the proximity to ground. If the charging source voltage-step  $E_{vc}$  and the charging internal source resistor  $R_{vc}$  remain the same and  $C_{str}$  increases, then the charging time constant would increase but not the peak height of the charging current. This can be checked by **connecting a pipette-holder (with inserted pipette) equivalent** to the (+) input by closing switch  $S_{pc}$  (see Fig. 3.1), namely, a 5cm wire, a soldered resistor,  $R_{pip}=2.2M$ , and a capacitor  $C_{pip}=4.7pF$  (not grounded). All other switches of the circuit are in the initial standard setting; filter still at  $>80KHz$  cut-off). Maybe to your surprise, it is the peak of the spike that is increased rather than the spike duration (cf. Fig. 3.3a,b). The added capacitance, measured by cancellation at  $f\sim 2.5\mu$ s (for best canceling), is  $\sim 1.0pF$ .

What is the cause of the **increase in peak height instead of peak width** when increasing  $C$ ? The answer, which again lies in the internal filtering of the amplifier, will also solve the above problem about why the  $R_{vc}$  values calculated from the peaks of the fast capacitance transients are too high. We only briefly touch this problem here, because it is not of great importance for actual patch-clamp experiments on living cells. A detailed explanation is given in Note 3.3.2. Students may skip the following brief explanation in italic text without having problems with the rest of this chapter. Students with technical background may enjoy this explanation.

*The calculation of  $R_{vc}$  from the operational amplifier circuit in the patch-clamp amplifier assumes that this (equivalent) internal voltage-clamp resistor has no parallel capacity  $C_{vc}$ . However, the equivalent resistor  $R_{vc}$  is derived from the feedback resistor  $R_{fb}$  in the current-to-voltage converter in the patch-clamp amplifier (cf. Note 1.3.2), and this  $R_{fb}$  usually has a stray capacitance  $C_{fb}$ , from which we obtain a parallel equivalent capacitance  $C_{vc}$  with  $R_{vc}.C_{vc} = R_{fb}.C_{fb}$  (see Note 3.3.2). This  $C_{vc}$  is rather large compared to  $C_{pc} + C_{pip}$  and therefore provides an (almost instantaneous) extra charging current that bypasses  $R_{vc}$  to charge  $C_{pc} + C_{pip}$  to a value determined by the voltage division of  $E_{vc}$  over  $C_{vc}$  and  $C_{pc} + C_{pip}$ . This extra charging*



*current is not measured by the patch-clamp, because it only measures current through  $R_{vc}$ . The subsequent slower charging "fast" capacitance current through  $R_{vc}$  is, however, measured by the patch-clamp, and it charges the external capacitance  $C_{pc} + C_{pip}$  from the initial voltage fraction of  $E_{vc}$  to the final voltage  $E_{vc}$  with a time constant  $R_{vc} \cdot (C_{vc} + C_{pc} + C_{pip})$ , where  $C_{vc} \gg (C_{pc} + C_{pip})$ . Therefore, the peak values of the fast capacitance current transients are smaller than expected, but the time constants of these transients are slower than expected. It may now be clear that doubling an external relatively small  $C$  from, e.g.,  $C_p$  to  $C_p + C_{pip}$ , will double the current peak but not the time constant. Finally, the amplifier is constructed in such a way that  $C_{vc}$  decreases with increased high frequency filter settings. Thus, both the peak and the time constant of the fast capacitance current transient reflect filter setting (including  $C_{vc}$ ) rather than the properties of ERC-circuit I consisting only of  $E_{vc}$ ;  $R_{vc}$  and external stray capacity (no  $C_{vc}$ !).*

Assuming this rather difficult to understand filtering effect of  $C_{vc}$ , we further explore the effect of externally added stray capacity on the fast capacitance current ( $I_{cf}$ ) transient by inserting a longer (10-20cm) wire (unconnected to the reference input terminal) in the (+) input. Indeed, we do see now an even further increased  $C_{str}$  (measured by cancellation). We can also observe an increase in  $C_{str}$  when the wire is brought closer to surrounding grounded objects. Wires of the type used by us introduce approximately  **$C_{str} \sim 0.1\text{pF per } 2\text{ cm wire length}$** . The same wire in the reference input does not have effect, unless the wire is used to bring ground closer to the (+) input. Apparently, the surface enlargement of the already large ground mass does not contribute to  $C_{str}$ .  $C_{str}$  can be increased drastically by holding the (insulated!) input connection wire (pipette-holder) between your fingers and grounding yourself, because this action brings ground very close (but not in touch!) to the (+) input terminal!

These simple tests illustrate not only the drastic effects of stray capacity, but also indicate an obvious way to obtain better estimations of  $R_{vc}$ . This is done by measuring capacitance peak height at higher and higher  $C$ 's intentionally applied across the patch-clamp input, and by calculating the  $R_{vc}$  values from  $dE_{vc}/dI_{peak}$  until calculated  $R_{vc}$  becomes constant. In this way one can find that  **$R_{vc} < 100\text{Kohm}$** , quite acceptable for a patch-clamp which should be able to measure  $R_{pip}$  values  $>1\text{M}$  .

During these measurements with increasing  $C$ 's one only observes slower capacitance transients with increasing  $C$ 's for the higher  $C$ 's (equal to or  $>C_{vc}$ ), because the time constant of the transients is  $R_{vc} \cdot (C_{vc} + C_{external})$ , as explained above. But the shapes of these transients, in particular at small applied  $C$ 's, are not pure single exponentials but show "**oscillatory ringing**", i.e. over- and under-shoot behavior upon voltage-step stimulation. This response to abrupt stimulation stems from the properties of the filters of the amplifier and makes it difficult to recognize the single-exponential nature of the fast capacitance transients. The fact that these fast capacitance transients are very well cancelable by single-exponential transients of opposite polarity at the input means that the  $E_{vc}/R_{vc}/C_{pc}$  ERC-circuit of the patch-clamp still holds and that the non-exponential shape of these fast transients are **response deformations resulting from amplifier (filter) properties**. However, these deformations do affect capacitance peak current measurements. Thus, calculated  $R_{vc}$  values are not precise but can be improved by using less steep voltage steps causing less ringing. (Try it, this option is present on the patch-clamp). Nevertheless, the drastic increase in  $dI_{peak}$  with increasing applied  $C$  shows that calculated  $R_{vc}$  values are orders of magnitude smaller

than measured at the intrinsic  $C_{pc} = 1\text{pF}$ . For precise  $R_{vc}$  measurements we would need another approach (not discussed here).

Sooner or later you may switch the patch-clamp to **current-clamp** while measuring in the air. Do it now to discover that the voltage is probably not stable at 0 V but soon increases to large (out of range) positive or negative values, even though there is no voltage source connected to the input or intentional current injected into the input. The reason of the building input voltage is a tiny **offset current** produced by the amplifier input and injected into the stray capacity at the input from inside. Thus, the accumulating charge on  $C_{str}$  causes the increasing potential, as explained at ERC-circuit I and illustrated in Fig. 2.1c. Switching the amplifier back to zero voltage-clamp can easily discharge the input again.

The  $CC_{zero}$  screw on the front plate of the L/M-PC patch-clamp can compensate the input offset current. It will be very difficult to zero the input potential at an open input, but you can show that bringing offset compensation out of balance in the positive or negative direction determines the polarity and the speed of input voltage development. This **input offset current compensation** procedure is of great importance for voltage measurements from high-resistance voltage sources, as we will see later.

We draw the following **conclusions** from these experiments:

- \* Stray capacity, amplifier filtering, and input offset current further complicated our open-input patch-clamp measurements to identify ERC-circuit I in this measurement condition.
- \* The tests on stray capacity showed that two factors are of importance to reduce  $C_{str}$ , one is the size of the leads to the (+) input, the second is the proximity of these leads to ground surfaces. This is, for example, important in the design of pipette-holders (Buisman et al, 1990), which should not add more than 0.5pF to the input capacitance of the patch-clamp.
- \* Adding capacity to the patch-clamp amplifier input was a useful method to estimate the value of  $R_{vc}$  and the series resistance in charging  $C_{str}$ , according to equivalent ERC-circuit I.
- \* Amplifier filtering deformed the capacitance current responses to steep voltage steps, but this deformation did not affect the capacity measurements by cancellation.
- \* Input offset current errors in voltage measurements are important to consider when measuring from high-resistance voltage sources.

### 3.3.3. Immersing the pipette to measure pipette capacitance and resistance

We proceed with the patch-clamp experiment by "immersing the pipette tip in the bathing solution" (by closing switch  $Sc_{pip}$  in Fig. 3.1) during **voltage-clamp stimulation** to find out that "the pipette tip is not well filled with pipette solution and is clogged by an air bubble in the outer tip" ( $S_{r_{pip}}$  is not yet closed, see Fig. 3.3c). This allows us to observe the effect of **inserting only  $C_{pip}$**  in the circuit without masking the charging current  $I_{c_{pip}}$  by the current through the pipette resistance  $R_{pip}$ . We see again an increased spike peak (cf. Fig. 3b and 3c) rather than increased spike duration.  $C_{pip}$  measurement by cancellation yields  $C_{pip} = 5\text{pF}$  (nominal value 4.7pF) as an added capacitance to  $C_{pc} + C_{pip_{hold}}$  (~2pF). Cancellation this increased  $C_f$  value requires an increased  $I_f$  value, as expected from  $I_f = R.C$ .

$C_{pip}$  is the capacitance between the pipette solution and the bath solution across the thin glass wall separating the two conductors. We are clamping the glass wall of the non-conducting pipette! In practice one can check that this immersed glass wall is the origin of  $C_{pip}$  by immersing the pipette deeper into the solution. It will increase  $C_{pip}$ .

Now it is time to "unclog the pipette by removing the air bubble by suction or blowing". If that is unsuccessful, we "take a pipette that is filled better." Both actions correspond to **inserting  $R_{pip}$**  by closing switch  $S_{rpip}$  in addition to switch  $S_{cpip}$  (switch #4 in Fig. 3.1). The voltage-clamp step now causes steady (DC) current to flow during the pulse after the initial  $I_{cf}$  spike (Fig. 3.3d). The applied voltage divided by the measured steady current yields a resistance of  $2.2M\ \Omega$ , which is the right value. Thus, the voltage-clamp is good enough to reliably measure  $R_{pip} \sim 2M\ \Omega$ , which implies that  $R_{vc} \ll 2M\ \Omega$ .

The spiky, cancelable, and overshoot current response to the voltage step indicates that the immersed pipette has the properties of ERC circuit II, even though this spike is strongly affected by amplifier filtering, as explained above for the role of  $C_v$  in this filtering. Therefore, this spike can only be seen clearly when the amplifier is set at sufficiently high (80KHz) low-pass filtering, because the spike is a high frequency signal. At lower high frequency cutoffs (e.g. 10KHz) the spike may become lower than the steady current response of a pipette, in particular when  $R_{pip} < 2M\ \Omega$ . Fig. 3.4a is a record example, where the spike just overshoots the steady pipette current at 10KHz filtering. When using PC controlled analogue-to-digital conversion (ADC) one may miss such fast transients when choosing too low sample frequencies.

**Current-clamping** the un-clogged pipette will not give the current-offset problem seen above for the open input. The tiny offset current may flow, but would only build up a tiny voltage on  $C_{pc} + C_{piphold} + C_{pip}$ , until the current through  $R_{pip}$  equals the offset current. That will be at a potential equal to  $I_{offset} \times R_{pip}$ , as explained at ERC-circuit 2. If  $I_{offset} \sim 1pA$ , then  $C_{pip}$  will be charged to  $2\mu V$  ( $1pA \times 2Mohm$ ), which is small enough to be neglected. A  $10G\ \Omega$  resistance would, however, be polarized by 10 mV and an open input would change its potential by 1 Volt in 1 s (rate of change 1V/s, see equation 2.3). Thus, offset currents are particularly disturbing when measuring voltages from high resistance voltage sources.

The general **conclusions** from these experiments are:

- \* Pipette capacity can simply be measured by cancellation when a pipette is clogged (non-conducting) in the outer tip.
- \* Fast capacitance pipette currents overshooting steady pipette currents upon step stimulation of a (non-clogged) patch pipette can only be seen at minimal signal filtering. Thus, ERC-circuit 2 applies during  $R_{pip}$  and  $C_{pip}$  measurements.
- \* The input resistance  $R_{vc}$  of the amplifier is small enough to carry out good measurements of  $R_{pip} > 1M\ \Omega$ .
- \* Stray capacity of the pipette-holder and pipette capacity should be minimized when patch-clamp measurements require high frequency resolution. This can be done by using short leads, small size pipette holders and short patch pipettes with thickened glass tips (covered with Sylgard, a silicone coating), containing little filling solution and not deeply immersed in the bathing solution.

### 3.3.4. Giga-seals and canceling the fast capacity currents in the cell-attached-patch (CAP) configuration

Once the experimenter knows that his equipment functions properly and that his patch pipette has the right resistance (usually 1-3M  $\Omega$ ), i.e. not clogged or broken, he checks the pipette for offset potential in zero current-clamp or for offset current in zero voltage-clamp. He does this in order to compensate this offset with the use of the  $V_{pip}$  offset potentiometer on the patch-clamp. This will not be necessary for our model pipette, since it does not include a voltage source. The present model, however, provides the opportunity to check whether the zero voltage settings ( $V_{hold}$  and  $V_{pip}$  offset) of the amplifier are all right and whether there are other hidden voltage sources in the instruments to be compensated.

After the necessary checks and adjustments a cell is selected for a seal attempt. The pipette is gently pushed against the cell and slight suction is applied to initiate giga-sealing. Sealing may occur slowly (minutes) or very quickly (seconds). The obtained measurement configuration is the **cell-attached patch (CAP)**, so widely used for single-channel current recording. In practice, the appearance of spontaneous single channel activity is often the best proof of the establishment of a CAP.

In the present cell model sealing occurs abruptly, when switch  $S_{seal}$  (switch 5 in Fig. 3.1) is opened. This action represents the exchange of the short-circuit connection of the pipette to ground for the giga-seal resistance  $R_{seal}$  (20G  $\Omega$ ). It is illustrated in Fig. 3.3d-e (for <80KHz low pass (or >80KHz high cut-off) filtered records), where the open pipette response before sealing is indicated in panel d and the remaining fast capacitor current on- and off-spikes after sealing in panel e. These **giga-seal spikes** are practically the same as the spikes measured for the clogged pipette. In fact, after giga-sealing the pipette is clogged again, but now by a CAP with a very small capacitance  $C_{cap}$  and a very high resistance  $R_{cap}=R_{mcap}=20G$ , shunted by  $R_{seal}=20G$ . Thus, the apparent seal resistance  $R_{capseal}=10G$  (measurable at higher gains and voltage steps), since the **series resistance of the attached cell** with  $R_m < 1G$  may be (practically) neglected. The **membrane capacity  $C_m$  of the attached cell** may also be neglected, since the two capacities in series ( $C_{cap}$  and  $C_m$ ) are equivalent to a capacitance

$$C_{cpm} = C_{cap}C_m / (C_{cap} + C_m) \sim C_{cap}, \text{ for } C_m \gg C_{cap}.$$

Thus, for resistance and capacitance measurements on the CAP, it is as if the CAP is directly coupled to ground at its intracellular side.

The **membrane potential of the attached cell** may not, however, be neglected. It is imposing its voltage on the CAP through the voltage-clamp circuit (as it would also do without the voltage-clamp!) and the voltage-clamp may add its voltage to that membrane potential. That is all what the voltage-clamp can do, change the existing membrane potential across the CAP. In certain applications it is a disadvantage that  $V_m$  is unknown or is not constant.

At zero voltage-clamp and in the absence of voltage sources in the CAP,  $V_m$  is the driving force for current through the CAP, sending current through the CAP and into the voltage-clamp, because the

currents will not choose the high resistance path to ground through  $R_{\text{seal}}$ . This current, if significant, is seen in the voltage-clamp as a **small holding current**.

Under favorable conditions (high  $R_{\text{seal}}$ , no intrinsic  $E_{\text{cap}}$ ) we can see part of  $V_m$  in zero **current-clamp recordings from a CAP**. In our model we expect to measure about  $0.5V_m$ , since  $V_m$  is voltage-divided over  $R_{\text{cap}} (=R_{\text{mcap}})$  and  $R_{\text{seal}}$ . This can be confirmed after mineralizing  $I_{\text{offset}}$  from the amplifier first, which is now very important because of the high resistance of the CAP and the seal.

We return now to the capacitance measurements (by  $I_{\text{cf}}$  canceling) to check whether the charging capacity in the fast capacity current transients is still  $C_{\text{pc}} + C_{\text{pip}} + C_{\text{pip}} + C_{\text{pip}}$ , as in the current transients charging the clogged pipette in the bath. This turns out to be roughly the case when using fast transient cancellation alone, as before. However, the canceling is not perfect and the values are not exactly the same. It looks as if one has to force fast transient cancellation with compromised  $C_f$  and  $f$  settings. It is as if sealing has added a small and slower capacitance transient to the step response. The reason for this could be that connection of  $R_{\text{pip}}$  to the circuit adds  $R_{\text{pip}}$  as an extra series resistance to the stray capacitance (e.g.  $C_{\text{cap}}$ ) of the circuit.

Fast capacity current cancellation is useful for  $C_{\text{pip}}$  measurement, but another use of this option is not less important: the **removal of the large sharp current spikes** from the voltage step responses. This is of particular importance for the responses to the larger voltage steps, as they can saturate the amplifier and spoil its high frequency performance. Clipping of signals because of amplifier saturation can be evoked by increasing the voltage step size under the conditions of the experiment of Fig. 3.3.

### 3.3.5. Whole-cell (WC) recording: measuring series resistance and cell capacitance while canceling the slow capacity transients

In many cases the CAP is only a transient stage toward reaching the final goal, the **whole-cell (WC)** configuration. As explained in chapter 1.2, WC-conditions are obtained by breaking the CAP while maintaining the giga-seal to the attached cell. If this is done during voltage-clamp stimulation with voltage steps, one can easily conclude from the responses whether a WC is obtained and whether the quality of the WC is good enough to proceed with the planned experiment. This procedure will be demonstrated now.

With the model cell (Figs. 3.1 & 3.2) one can simulate WC-formation by closing switch  $S_{\text{acc}}$  (no 7). This action causes shunting of  $R_{\text{mcap}}$  by  $R_{\text{acc}}$ , as illustrated by the experiment of record f in Fig. 3.3, where  $R_{\text{acc}} = 2.2\text{M}\Omega$ . Record f shows that WC-formation causes the sudden appearance of an extra, slow capacitor current transient upon voltage-step stimulation. This slow transient is much smaller in amplitude ( $\sim 2\text{nA}$ ) than the fast capacitor transient ( $\sim 12\text{nA}$ , at  $80\text{kHz}$  filtering) and its time constant  $\tau_s$  ( $\sim 0.25\text{ms}$ )  $\gg$   $\tau_f$  ( $\sim 2.5\mu\text{s}$ ). The observed amplitude and time constant are consistent with the slow component properties of ERC-circuit 4 (Fig. 2.4), with  $R_{\text{p}} = 4.4\text{M}\Omega$  (the series resistance  $R_{\text{ser}} = R_{\text{pip}} + R_{\text{acc}}$ ) and  $C_{\text{m}} = 50\text{pF}$  in the present case.

The predicted amplitude is  $10\text{mV}/4.4\text{M}\Omega = 2.2\text{nA}$  and the predicted  $\tau = 4.4\text{M}\Omega \times 50\text{pF} = 0.22\text{ms}$ . The steady-state change in current of  $10\text{mV}/1\text{G}\Omega = 10\text{pA}$  cannot be seen on the current scale of Fig.3.3.

The experienced patch-clamper routinely estimates  $R_{\text{ser}} = R_{\text{pip}} + R_{\text{acc}}$  from the peak height of the slow capacitance transient on the oscilloscope or PC screen and  $C_s = C_m$  from the time constant  $\tau_s$ . She will then know whether  $R_{\text{ser}}$  is low enough to continue the experiment on the whole-cell (WC) obtained, or try to get better access to the WC (lower  $R_{\text{acc}}$ ) by extra suction. In the recent Windows versions of the Axon Instruments patch-clamp acquisition software (pClamp7 and 8)  $R_{\text{ser}}$ ,  $C_s$  and  $\tau_s$  are calculated on-line from the records. When  $R_{\text{ser}}$  is satisfactory, the experimenter starts to cancel the slow capacitor transient in order to obtain flat control records for easier recognition of voltage-activated currents evoked by larger voltage steps.

The **canceling procedure** is illustrated in Fig. 3.4 for the same cell as in Fig. 3.3, but at an increased current resolution, which is closer to regular experimental practice. High frequency cut-off filtering is now at 10KHz. The current through the pipette in the bath is as expected for a  $2.2\text{M}\Omega$  pipette resistance (frame a). After giga-sealing the fast capacity current transient ( $I_{\text{cf}}$ ) remains (frame b). This transient must be cancelled (frame c) to prevent amplifier saturation at higher current gains and voltage steps and to better be able to recognize the shape of the slow capacitance current transient ( $I_{\text{cs}}$ ) of the whole-cell. WC-transients  $I_{\text{cs}}$  are illustrated in frame d, where the curve labeled  $R_{\text{acc}} = 47\text{M}\Omega$  exemplifies a "bad" WC, in which CAP perforation is incomplete so that  $R_{\text{acc}}$  remains high ("small CAP hole").  $I_{\text{cs}}$  improves if  $R_{\text{acc}} = 10\text{M}\Omega$  is taken, but it is best (high and fast) if  $R_{\text{acc}} = 2.2\text{M}\Omega$ . Remember that it is  $R_{\text{ser}}$  that matters for the shape of  $I_{\text{cs}}$ , and that  $R_{\text{ser}} = R_{\text{pip}} + R_{\text{acc}} = 2.2\text{M}\Omega + R_{\text{acc}}$ . The lower  $R_{\text{ser}}$ , the higher and the faster is  $I_{\text{cs}}$ , thus the sooner the cell membrane is charged to the clamped potential (10mV here). In practice, similar successive  $I_{\text{cs}}$  transients as in Fig. 3.4d may be obtained during successive attempts (repeated suction pulses) to get better and better WC-conditions on the same cell. They may occur in reverse order if WC-conditions deteriorate due to closure of the hole in the CAP-membrane (resealing of the ruptured CAP-membrane).  $R_{\text{ser}} = 2R_{\text{pip}}$  is usually considered the best obtainable WC-condition.

Notice also that breaking into the cell causes a small holding current because of the appearance of the membrane potential ( $= E_{\text{l}} = \sim -60\text{mV}$ , measurable in current-clamp after careful zeroing input offset current) and conductance ( $= G_{\text{l}} = 1/R_{\text{l}}$ ) in the circuit. This would produce  $\sim 60\text{mV} / 1\text{G}\Omega = 60\text{pA}$  outward (positive) current at the holding potential of 0mV. The 10mV voltage step would add another 10pA, but the resolution in Fig.3.4 is too poor to precisely measure these current changes.

Frames e and f show how the records look like during the  **$I_{\text{cs}}$  cancellation** procedure. In frame e  $C_s$  is increased from 0 to 70pF at exactly the right  $R_s = 4.3\text{M}\Omega$  value, close to the expected value of  $R_{\text{pip}} + R_{\text{acc}} = 4.4\text{M}\Omega$  (nominal value). At 51 pF the response is exactly flat, at smaller  $C_s$  the response is positive, while the responses are negative at too large  $C_s$  values (e.g. 70pF). But all transients are mono-phasic, whether they are positive or negative.

In frame f,  $R_{\text{ser}}$  is adjusted at exactly the right  $C_s$ .  $R_{\text{ser}}$  is decreased from  $>100\text{M}\Omega$  to 10, 4.3 and  $3.3\text{M}\Omega$ . At  $4.3\text{M}\Omega$  cancellation is perfect (flat record). Both at higher and lower  $R_{\text{ser}}$  the current

transients are biphasic. At higher  $R_{ser}$  (10M  $\Omega$ ), the biphasic transient is positive-negative. At lower  $R_{ser}$  (3.3M  $\Omega$ )  $I_{cs}$  is negative-positive. From these examples one may derive a quick procedure for  $I_{cs}$  cancellation for obtaining flat current records despite the abrupt steps in voltage. Quick action is required, since cancellation time is at the expense of experiment time.

First, quickly adjust  $C_s$  to a value estimated in the physiological range. Second, dial  $R_s$  to a value at which there is neither an initial overshoot nor an initial undershoot. Third, adjust  $C_s$  to flat or almost flat records. In the latter case  $R_{ser}$  and  $C_s$  may need fine-tuning according to the same procedure.

The **biphasic nature of the records** in frame f can easily be understood from the nature of the cancellation procedure.  $I_{cs}$  has, under ideal conditions, a single exponential shape, in which the peak current is equal to  $V/R_{ser}$  and the time constant of the decay is equal to  $R_{ser}C_m$ . When the cancellation procedure is carried out, the amplifier produces from the voltage step an exponential current transient of opposite polarity to  $I_{cs}$  at the input of the amplifier. The peak of this opposite transient is determined by the value on the dial that cancels  $R_{ser}$ , while the dial that cancels  $C_s$  determines the time constant of the decay of the cancelled transient according to  $R_{ser}C_s$ . If the canceling  $R_{ser}$  is smaller than the real  $R_{ser}$  but at approximately the right canceling  $C_s$ , the canceled transient is larger in peak size and shorter in duration than the real  $I_{cs}$ . Thus, the addition of the negative canceling transient to the positive real transient results in an initial negative peak. Furthermore, because of the shorter canceling transient, canceling occurs only in the first part of  $I_{cs}$ , thus the second part of  $I_{cs}$  is not cancelled and remains positive. In this way the negative-positive  $I_{cs}$  transient arises at  $R_{ser} = 3.3M \Omega$  in Fig. 3.4f. In a similar way the positive-negative capacity transients at canceled  $R_{ser}$  values that are too large can be explained. Insight in the origin of the shape of the partially cancelled transients helps in following a quick and rational procedure for capacity transient cancellation. This also applies to  $I_{cf}$  canceling, though the condition may look a bit more difficult, because the extremely fast  $I_{cf}$  transients ( $\mu s$  time constants) are usually distorted even by the best amplifier filter settings. Reconstruction of the various incompletely cancelled  $I_{cs}$  shapes is best illustrated by drawing by hand the summation of various  $I_{cs}$  transients and various canceling exponential transients of opposite polarity.

The  $R_{ser}$  value read from the canceling dial is an important indicator of the quality of voltage-clamp conditions (the lower  $R_{ser}$ , the better, see chapter 2), while the  $C_s = C_m$  value that is determined is important for normalizing the current records to cell size (reflected in  $C_m$ ). Since  $R_{ser}$  may change during an experiment,  $R_{ser}$  should be checked by  $I_{cs}$  cancellation regularly in the course of an experiment. **The first indication of  $R_{ser}$  changes after perfect  $I_{cs}$  canceling is the appearance of biphasic  $I_{cs}$  transients** in the records, positive/negative if  $R_{ser}$  improves (i.e., decreases) and negative/positive if  $R_{ser}$  increases, as can be understood now from the above explanations.

It is important to emphasize here that  $I_{cs}$  cancellation is only a safety against amplifier saturation and a cosmetic procedure, because it does not improve the voltage-clamp conditions. The flat base line may give better records for current recognition. However, if you would record the membrane potential with an independent electrode during a voltage-clamp step after  $I_{cs}$  cancellation, you would observe that the membrane potential still follows the applied voltage step with an exponential transient with time constant  $R_{ser}C_m$  (see the model experiment of Fig. 3.9). As a rule, only after  $\sim 3X$  the time constant is the membrane potential actually clamped to the applied potential. For this

reason, experimenters may sometimes choose not to fully cancel  $I_{cs}$ , keeping a small  $I_{cs}$  visible to remind themselves of the actual duration of the membrane potential transient in the cell. Thus, it remains important to make  $R_{ser}$  as small as possible.

### 3.3.6. Pulling an outside-out patch (OOP) and checking the seal resistance

As explained in chapter 1.2, the **outside-out patch (OOP)** is obtained by gently pulling a vesicle from the WC. Thus, the OOP is a micro-WC with only one or a few channels. An exception is when a large vesicle is drawn or channel density is very high in the OOP. The OOP allows the patch-clamper to study single-channel activation kinetics and co-operative channel behavior. With the present equivalent-circuit cell model we demonstrate a few OOP properties of methodological interest.

Fig. 3.5 shows how the slow capacity current ( $I_{cs}$ ) changes upon establishing the OOP measurement configuration.  $I_{cwc}$  in frame a shows a non-cancelled  $I_{cs}$  in the WC configuration ( $I_{cf}$  is cancelled!). It is from the same cell as in Fig. 3.4. After perfect  $I_{cwc}$  transient cancellation at  $R_{ser} = 4.3M\ \Omega$  and  $C_s = 51pF$ , the record is flat (see arrow). Pulling a successful OOP by opening switch  $S_{oop}$  (switch 9 in Fig. 3.1) suddenly causes the **appearance of a large inverted exponential transient** of a similar size as that of  $I_{cwc}$ . An OOP attempt is unsuccessful if the seal is lost during pulling up of the pipette. In that case, the 10mV voltage step causes a very large off-screen current response and the holding current may already jump off-screen at small offsets or holding potentials. This does not happen here, because  $R_{seal} = 20G\ \Omega$  is kept constant. Here, we observe a small change in holding current, since the membrane potential ( $E_l \sim -60mV$ ) is no longer in series with  $R_l = 1G\ \Omega$ , but with the much larger  $R_{oop} = 20G\ \Omega$ .

The inverted transient is, in fact, an overcompensated  $I_{coop}$  response revealing the major part of the  $I_{cwc}$  canceling transient causing the flat record in frame a. This over cancelled  $I_{coop}$  is not exactly equal to an inverted  $I_{cwc}$ , because there is a remaining  $I_{coop}$  made visible in frame b by removing transient cancellation with the switch on the amplifier. Without  $I_{cs}$  cancellation one would see a change from  $I_{cwc}$  (Fig. 3.5, frame a) to  $I_{coop}$  (frame b) upon OOP-formation.  $I_{coop}$  could be perfectly cancelled at the same series resistance  $R_{ser} = 4.3M\ \Omega$  as for canceling  $I_{cwc}$ , but with a much smaller capacitance  $C_s = 6.1pF$ . Although this  $C_s$  value is larger than the nominal value of  $C_{oop} = 3.3pF$ , it is quite acceptable, because the nominal value is imprecise and the circuit easily adds a few pF stray capacitance to this nominal value. The important observation is that  $R_{ser}$  has the same value as that for  $I_{cwc}$  cancellation. This implies that  $I_{cwc}$  and  $I_{coop}$  should have the same peak current (see theory of ERC-circuits I-IV). Frame b shows that  $I_{coop}$  has a smaller peak than  $I_{cwc}$ . This is due to the use of the 10KHz-filter, which affects the very short  $I_{coop}$  more than the larger duration  $I_{cwc}$ . Changing the filter to 80KHz indeed increased the  $I_{coop}$  peak to that of  $I_{cwc}$ .

A few current-clamp observations are instructive. After careful zeroing current offset with the CCzero screw,  $V_m$  of the WC ( $V_{mwc}$ ) was measured to be  $-57.8mV$ . For  $V_{moop}$  one would expect approximately  $V_{mwc}/2$ , because of **voltage division of  $E_l \sim -57.8mV$  over  $R_{oop}$  and  $R_{seal}$** .  $V_{moop}$  was found to have the expected value of  $-28.9mV$ .

The general **conclusion** from these observations is that one easily recognizes the formation of a good OOP from an  $I_{cs}$  cancelled WC by the sudden appearance of an inverted  $I_{cwc}$  and the



maintenance of high resistance conditions ( $R_{\text{seal}}$  not affected). Pulling an OOP can sometimes even serve as a test to see whether a high apparent WC conductance is due to a high membrane conductance or to a bad seal (low  $R_{\text{seal}}$ ). In current clamp, voltage division of the membrane potential over the various resistors of the circuit was as expected, provided the input offset-current was well zeroed.

### 3.3.7. Excision of an inside-out patch (IOP)

An inside-out patch (IOP) is obtained by excision of a CAP from the attached cell by a sudden pull-up of the sealed patch pipette. In the above discussion of the CAP configuration we argued that the RC-properties of the CAP and the attached cell membrane hardly contribute to the response of a giga-sealed CAP to voltage-step test pulses. The measured spikes (Fig. 3.3e), though heavily filtered, were mainly reflecting  $C_{\text{pip}}$  charging through  $R_{\text{vc}}$ . Thus, one would expect that these **spiky test responses of a CAP would not change upon excision of an IOP**. This turns out to be the case in the model experiment of Fig. 3.6, where the IOP was obtained by switching  $S_{\text{IOP}}$  (switch 8 in Fig. 3.1) to ground connection from the CAP. Frame a shows a non-cancelled fast capacity current ( $I_{\text{cf}}$ ) response of a CAP to stimulation with 10-mV voltage steps, while amplifier setting was at 10 kHz (low pass). The record shows perfect giga-sealing. In frame b the CAP- $I_{\text{cf}}$  was largely cancelled. Frame c shows the  $I_{\text{cf}}$  record after IOP excision. It is practically the same as the CAP record in frame b. Therefore, this record shows maintenance of giga-seal conditions rather than any electrophysiological change, which is in contrast to the capacity current changes upon OOP formation from the WC (Fig. 3.5). Apparently, the large cell membrane capacity ( $\sim 50\text{pF}$ ) does not contribute to  $I_{\text{cf}}$ , because it cannot be accessed for charging by  $E_{\text{vc}}$  through  $R_{\text{vc}}$ . It is only accessible through  $R_{\text{pip}} + R_{\text{cap}}$ , which is here very much larger ( $\sim 20\text{G}\ \Omega$ ) than  $R_{\text{vc}}$  ( $< 100\text{K}\ \Omega$ ). We would rather expect a tiny, but slower capacity current component for charging  $C_{\text{cap}}$  (a few pF) through  $R_{\text{pip}}$  ( $2.2\text{M}\ \Omega$ ), unaffected by IOP excision because of the large differences between the access resistances  $R_{\text{pip}}$  (for  $C_{\text{cap}}$ ) and  $R_{\text{pip}} + R_{\text{cap}}$  (for  $C_{\text{m}}$ ). This tiny component is not resolved in the records of Fig. 3.6.

However, the **disconnection of the membrane potential** of  $V_{\text{m}} = -60\text{mV}$  from the CAP must have some consequence. It drives a holding current of  $-60\text{mV}/20\text{G}\ \Omega = -3\text{pA}$  through the CAP and it is this current, which must have disappeared in the IOP. The resolution in the records of Fig. 3.6 is too low to observe this change. During high-resolution recording of CAP-channel activity under favorable conditions, one may be able to see such changes. However, **changed channel activity** will probably be a more significant indication of the change from CAP to IOP. This is because the loss of the membrane potential will alter voltage dependent channel activity and the loss of the intracellular chemical environment will cause the disappearance of intracellular ion channel activators or inhibitors (Weidema et al., 1993).

### 3.3.8. Making a permeabilized-patch WC (ppWC)

The formation of ppWC conditions during nystatin or amphotericin (channel forming antibiotics) incorporation in the CAP can elegantly be followed from the **gradual development of an increasing slow capacitor current (Ics)**. This process has already been demonstrated in Fig. 3.4d, where WC conditions improved in steps from  $R_{\text{acc}} = 47\text{M}\ \Omega$  to  $R_{\text{acc}} = 2.2\text{M}\ \Omega$  by applying “successive suction pulses.” The three increasing  $I_{\text{cs}}$  transients may also be seen as three examples

from a gradually growing  $I_{cs}$  during ppWC development. The increase in the  $I_{cs}$  peak would reflect the decrease in  $R_{acc}$  due to permeabilization of the CAP by the antibiotic. The immediate consequence of a decreasing  $R_{ser}$  is a decrease of the decay time constant ( $R_{ser} \cdot C_m$ ) of  $I_{cs}$ . Thus, the better the permeabilization, the faster and closer the WC membrane is charged to the applied potential.

**Current-clamp potential measurements** are again instructive. Long before CAP permeabilization is satisfactory for reliable voltage-clamp recording, conditions may be favorable for zero current-clamp membrane potential measurements if the recording pipette is filled with an intracellular-like solution. For example, at  $R_{ser} \sim R_{acc} = 100M\ \Omega$  (bad ppWC),  $V_{mwc}$  measurements are already acceptable within 10% for  $R_{seal}$  values  $>1G\ \Omega$ , provided input offset-current is well cancelled. In Fig. 3.4d,  $V_{mwc} = -58mV$  at  $R_{acc} = 47M\ \Omega$ , which is practically equal to the  $V_{mwc} = -59mV$  at  $R_{acc} = 2.2M\ \Omega$  (at  $R_{ser} = 4.4M\ \Omega$ , a very good ppWC).

### 3.4. Some instructive model experiments

*The following experiments may be difficult to carry out for a beginning student, because they require a lot of trial and error and may present certain artifacts complicating the interpretation. Nevertheless, we still describe them, because they provide unique illustrations of important experimental problems. You may, however, consider these experiments as optional additions to the more important and easier exercises in the previous section. Reading and studying the results of the experiments below (instead of doing them) can also be rewarding for an experimentalist.*

#### 3.4.1. Checking intracellular voltage clamp during recording of single ion channel currents from cell-attached patches (CAP)

Each successful patch-clamp experiment starts with a cell-attached patch (CAP), as the CAP is the immediate result of the giga-seal procedure. It is, therefore, the oldest measurement configuration and a widely used one. Its great utility lies in its excellent current ( $\sim pA$ ) and time ( $\sim 0.1ms$ ) resolution under maintained intact physiological conditions of the measured cell. Its disadvantages include limited control of the membrane potential and the intracellular conditions of the attached cell. These are often compensated by its advantages and by the use of any of the other measurement configurations. Because of the functional importance of CAP, here we demonstrate the requirements for single-channel recording from CAPs under good intracellular voltage-clamp conditions. We will see that bad intracellular voltage clamp can be easily recognized from the shape of the single channel currents.

We focus first on the conditions for good **stationary voltage-clamp measurements of single channel currents** during spontaneous channel activity, i.e. while holding  $E_{vc}$  at a constant value, hoping that  $V_m$  of the attached cell is also constant. In that case, the cell is half of the voltage-clamp, the other half being the external patch-clamp instrument (cf. the CAP in Fig. 1.2). The patch-clamp may be put on 0 mV holding potential, so that it only becomes an external short-circuit connection containing an ideal (almost zero resistance) current meter. When a CAP channel opens ( $R_{capch}$  inserted in the CAP by closing switch 6 in Fig. 3.1),  $V_m - E_{vc}$  is the driving force sending current through the channel (assuming the CAP does not have its own voltage sources, as in our

model). If  $R_{mcap} \gg R_{capch} \gg R_m$ ,  $V_m$  will not change upon CAP-channel opening and the initial and steady current through the CAP-channel will be

$$I_{capch} = (V_m - E_{vc})G_{capch}$$

Thus, opening of the CAP-channel will cause a sudden, step increase in current (cf. Fig. 3.7a,b) through the patch measured by the patch-clamp. By measuring this step increase in current at different  $E_{vc}$ , one can measure the **single-channel conductance**  $G_{capch}$  as the slope of the **I-V plot** of the channel current, so often done in CAP experiments. At the **reversal potential**, i.e. the  $E_{vc}$  potential where the channel current reverses polarity (crosses the voltage axis),  $E_{vc} = V_m$ . This identity is only true if the CAP-channel has a reversal potential  $E_{capch} = 0$ , which one can realize by filling the patch pipette with a salt solution with a composition close to that of the cytoplasm. Often, that is not the case. The equation for the channel current then is

$$I_{capch} = V_m - (E_{capch} + E_{vc}).G_{capch}$$

In this case uncertainty on  $V_m$  makes it difficult to determine  $E_{capch}$  for establishing the ionic selectivity of the channel. The IOP and OOP configurations are then the preferred configurations.

Fig. 3.7a,b shows simulated single-channel recordings from a CAP in our equivalent circuit model cell. The single-channel conductance of the CAP-channel was chosen rather high (1nS, corresponding to 1G $\Omega$  resistance) to obtain a good signal-to-noise ratio. Intracellular voltage clamp in these recordings was good, since  $R_{capch}(1G\ \Omega) \gg R_m = R_l(90M\ \Omega)$ . This results in perfectly rectangular channel current shapes implying constancy of the membrane potential,  $V_m$ , whether the channels are open or not. The calculated amplitude of the channel currents was  $V_m/R_{capch} = -62mV/1G\ \Omega = -62pA$ , close to the observed amplitudes.

Even though the membrane area of the cell is much larger than that of the CAP, the experimental conditions may be such that a large-conductance channel opens in the CAP, while no large-conductance channels (or many small-conductance channels) are open in the rest of the cell. In this case,  **$R_{capch} \sim R_m$**  (Ravesloot et al., 1994). Then we will have **bad voltage-clamp** conditions. After switching on,  $R_{capch}$  will load  $V_m$  and cause a depolarization with a transient determined by the values of  $R_m$ ,  $R_{capch}$ , and  $C_m + C_{cap}$ . This will be reflected in the channel current. If one views opening of the CAP-channels as the activation of another parallel conductance in the cell, the equations of chapter 2.6 can be used. If one views closing channel switch #6 as a sudden stimulation of the cell by an external source, then ERC-circuit 3 with its equations apply. The equations in both chapters are essentially the same.

Just after channel opening the channel current will be as expected for the original  $V_m$ . Then the current will decline, parallel to the decline in  $V_m$ . Thus, the channel current will not have the familiar **square shape, indicative for good intracellular voltage-clamp** (constant  $V_m$ ), but will overshoot the final, lowered steady-state value (cf. Fig. 3.7c). This means that these declining currents cannot be used for the measurement of single-channel conductance and reversal potential, unless the peak values are taken after a sufficient period for  $V_m$  recovery from the previous channel activation.

Fig.3.7c,d shows simulated single-channel recordings from a CAP under conditions of bad intracellular voltage clamp, because we have chosen here  $R_{capch} = R_m = R_l = 1G$ . The single-channel currents show decay upon channel opening, as predicted. This is due to a depolarization of the membrane caused by the influence of  $R_{capch}$  insertion in the CAP on  $V_m$ . This loading effect is not instantaneous, because it takes time to discharge the membrane to its new steady state in the presence of  $R_{capch}$ . The calculated time constant for this decay is  $R_m/R_{capch}C_m = 0.5G \times 50 pF = 25 ms$ , close to the observed value (see Fig.3.7d) ( $R_m/R_{capch}$  is the symbol for the parallel equivalent resistance of  $R_m$  and  $R_{capch}$ ). The calculated initial (peak) amplitude (after sufficient time for recovery from a previous CAP-channel activation) is again  $E_l/R_{capch} = -62pA$  (as in good intracellular voltage clamp), consistent with the observation in Fig. 3.7d. The calculated steady current value after the decay is  $E_l/(R_l + R_{capch}) = -31pA$ , also close to the observed value (see Fig. 3.7d). Intracellular membrane potential recovery upon CAP-channel closure cannot be seen in the current records, since the recharging current does not flow via the patch-clamp amplifier. That this recovery happens is clear from the fact that CAP-channel openings just after a previous closure show reduced peak amplitudes (see Fig. 3.7c). The calculated time constant for intracellular recovery is  $R_l.C_m = 1G \times 50 pF = 50ms$ .

In conclusion, poor intracellular voltage clamp due to the condition  $R_{capch} \sim R_m$  is easily recognized from decaying single channel currents. Intracellular voltage clamp may be bad for other reasons. If  $R_m$  is very high, random opening and closing of high-conductance single channels in the WC may also cause  $V_m$  changes, affecting the current through open CAP-channels. By studying the present circuit you learn how to recognize these events (rounded-off, non-overshooting currents). Other reasons of unstable  $V_m$  may arise from sealing-induced damage to the attached cell, from spontaneous  $V_m$  changes or from synaptic input when recording from neurons in culture.

The condition of bad intracellular voltage-clamp by the attached cell has been analyzed in detail by Ravesloot et al (1994). It turned out that these bad voltage-clamp CAP conditions are favorable non-invasive conditions for the measurement of  $R_m$  and  $C_m$  of the intact cell, and under certain conditions or assumptions, for the measurement of the membrane potential of the cell. The present equivalent circuit experiment served to make the student **aware of the importance of good intracellular voltage clamp conditions during CAP-channel recordings** and to exercise recognizing intracellular voltage-clamp conditions from the shapes of the CAP-channel currents.

The interested student may now repeat the experiment of Fig.3.7 with the amplifier in current-clamp mode (note, cancel first disturbing amplifier input current offsets!). He may discover that CAP-channel opening and closure can also be followed in the extracellular CAP-potential as changes in the voltage division of the membrane potential over  $R_{cap}$  and  $R_{seal}$ .  $R_{cap} = R_{mcap} = 20G$  when the CAP-channel is closed.  $R_{cap} \sim R_{capch} = 1G$ , when the channel is open. Thus, such CAP-potential recordings added to single-channel current measurements may provide extra information on the electrical properties of the attached cell.

### 3.4.2. Checking whole-cell membrane potential and resistance

One of the first actions of an experimenter after obtaining the WC patch-clamp configuration is measuring the resting  $V_m$  and  $R_m$  in the current-clamp mode. A sufficiently negative  $V_m$  and high  $R_m$  is often a criterion for accepting a cell as a good cell for a continued experiment. Therefore, we

demonstrate these measurements here on our model cell (Fig. 3.1) and show how the conductance properties of a cell determine the membrane potential and resistance properties and, in combination with membrane capacity, also the time constant of the  $V_m$  response of the membrane to current pulses. We apply here the theory explained in chapter 2.6 and 2.3 (parallel conductance equations and exponential transients on current stimulation).

Fig. 3.8 shows observations from such an experiment for experimental conditions further described in the legend of the figure. In Fig. 3.8a  $V_m$  was recorded as a function of time while successively inserting and removing conductance branches with the switches 11 and 12 in Fig. 3.1. In Fig. 3.8b  $V_m(t)$  was recorded upon stimulation by current blocks of 100pA for the cell membrane in 3 different conductance states.

The initial membrane potential was  $V_m = 0\text{mV}$ , since initially  $G_l$  with  $E_l = 0\text{mV}$  was the only conductance present in the membrane. Upon activating  $G_k$ ,  $V_m$  hyperpolarizes towards  $E_k = -86\text{mV}$ . The observed  $V_m = -56.2\text{mV}$ , which is  $E_k$  divided over  $R_k$  and  $R_l$ , is close to the value  $V_{lk} = -57\text{mV}$  calculated from equation 55 in chapter 2.6. Upon additional activation of  $G_{na}$ ,  $V_m$  becomes  $+9.6\text{mV}$ , close to the calculated value  $V_{lkn} = +9.4\text{mV}$  (equation 54, Chapter 2.6). Deactivation of  $G_k$  results in  $V_m = +47.2\text{mV}$ , close to the calculated  $V_{ln} = +48\text{mV}$  (equation 55, Chapter 2.6). The transients between the conductance states are single-exponential with time constant values close to the values calculated from equation 54 in chapter 3.6. The higher the conductance, the faster the time constant. The slowest time constant occurs when the membrane is in the  $G_l$  state and is  $RIC_m = 400\text{M} \times 86\text{pF} = 344\text{ms}$  (cf. last part of record in Fig. 3.8a).

The  $V_m$  responses to the current blocks (panel b) are consistent with these observations. The higher the membrane resistance, the larger and the slower the  $V_m$ -responses. The time constants of the current responses in the various  $G$ -states in panel b are equal to those in the  $V_m$  transients to those states in panel a.

$G_l$  is not the dominant conductance and  $V_m$  is not too depolarized, and this cell would probably be acceptable for the study of  $G_k$  or  $G_{na}$ , though a smaller  $G_l$  would be better. One cannot conclude from the records in Fig. 3.8 whether  $G_l$  is a membrane conductance or a leaky seal. The behavior of the circuit in figure a can serve as a model for effects of opening and closing of single ion channels on  $V_m$  of a cell with only a few channels, but also for effects of abrupt activation of a conductance consisting of a large collection of channels. Usually, activation of a conductance involves successive activation of channels with certain kinetics, but it is good to realize that even in that case sufficient time resolution of such records should, in principle, reveal effects of each channel opening on  $V_m$  as illustrated in Fig. 3.8 for a cell with only 3 channels.

### 3.4.3. Checking the membrane potential change during WC voltage-clamp stimulation using an extra intracellular electrode

The patch-clamp technique in voltage clamp is a **single-electrode voltage-clamp technique**, in which the membrane current is recorded upon voltage steps applied to the patch pipette. Therefore, there is no direct check whether the membrane potential is well clamped by the pipette potential. In two-electrode voltage clamping the actual membrane potential is measured and used as a signal in the clamp circuit to obtain voltage-clamp conditions (Hille, 1992). Thus, here the recorded

membrane potential can be used to evaluate voltage-clamp quality. This is impossible with the conceptually simpler patch-clamp technique, which is based on the assumption that the access resistance through the patch pipette, to the inner side of the membrane, is low enough to obtain well clamped membrane potentials, i.e. close enough to the applied pipette potential.

In order to check this assumption, one needs to make a double WC, with one pipette voltage-clamping the cell and the other zero current-clamping the cell to measure the clamped membrane potential. Such an experiment is more difficult than a single electrode WC experiment, since the manipulations with the second pipette may disrupt the seal of the first pipette. Furthermore, one would need an extra patch-clamp for such a double WC experiment. That is the reason that these double WC-experiments are only rarely done. Instead, one relies on access resistance measurement by slow capacitor transient cancellation, which is in principle good enough for voltage-clamp evaluation. However, the **lack of direct membrane potential observations may tend to make patch-clampers too optimistic on the quality of their patch-clamp voltage-clamp**. Therefore, we demonstrate here a kind of double WC-experiment on our "easier" model cell, where sealing and WC-formation with the second pipette does not spoil the WC made with the first pipette. We can even make a more ideal experiment by directly connecting a good (i.e. high input resistance) voltage amplifier to the inside of the cell without a distorting series (pipette and access) resistance and pipette capacitance. An old-fashioned microelectrode amplifier can be used for this purpose or, with some help, one may be able to build a simple voltage follower.

We have used a micro-electrode amplifier to show that the change in  $V_m$  upon voltage step stimulation runs parallel to the slow capacitor transient, as expected on the basis of the theory of the ERC-circuits in chapter 2, and that slow capacity current ( $I_{cs}$ ) transient cancellation does not affect this change in  $V_m$ .

Fig. 3.9 shows the observations. The cell was stimulated with a 10-mV block pulse in the WC-configuration and the slow capacitor current ( $I_{cs}$ ) transient was recorded while measuring  $V_m(t)$  with an independent electrode directly connected to the  $V_m$ -point of the circuit of the model cell (cf. Fig. 3.1). For simplicity, the resting  $V_m$  was chosen  $V_m = E_l = 0$  mV, with the Na and K branch disconnected and the OOP-segment of the membrane removed. The records show that  $I_{cs}$  and  $V_m(t)$  run perfectly parallel with the same time constant with a value close to the calculated value  $R_{ser}C_m = 4.4 \text{ M} \times 94 \text{ pF} = 0.4 \text{ ms}$ . The peak current is approximately  $dE/R_{ser} = 10 \text{ mV}/4.4 \text{ M} = 2300 \text{ pA}$ . This behavior is as predicted from ERC-circuit I and II in chapter II. The same recordings were made after perfectly canceling  $I_{cs}$  (see flat record in the figure). Maybe to your surprise,  $V_m(t)$  after canceling exactly overlaps with the one before canceling. Thus,  $I_{cs}$  canceling is a cosmetic operation without improving the voltage-clamp conditions. It is merely done to get nicer pictures of current changes occurring already during  $I_{cs}$ . If a current change occurs in this time frame, its initial time course does not reflect a conductance change at a constant potential. This may be a serious problem in measuring fast WC-Na currents (Gaspar et al., 1995).

If the student is interested in measuring  $V_m(t)$  on a voltage-clamp step but does not have an extra current-clamp amplifier at her disposal, she may switch her patch-clamp to current-clamp mode and directly apply the voltage stimulus via an extra pipette sealed to the cell. The stimulus can be obtained from a simple function generator or from the patch-clamp acquisition software and hardware, e.g. pClamp. Make sure that the connection of pipette 2 is identical to that of pipette 1

( $R_{ser2} = R_{ser1}$ ,  $C_{pip2} = C_{pip1}$ ,  $R_{seal2} = R_{seal1}$ ) and that the voltage generator is given an output resistance of  $\sim 100K$  to have similar voltage-clamp conditions as via the patch-clamp. This double-pipette experiment will demonstrate that voltage-clamp is nothing more than providing a potential from a (relatively) ideal voltage source. It is the current measuring (and some extra options) that requires sophisticated technology in a patch-clamp amplifier. The proposed double-pipette experiment is not difficult to carry out, but the  $V_m(t)$  transients will probably not be simple single-exponential transients because of the presence of two WC-pipettes instead of one.

#### 3.4.4. Checking whole-cell current filtering with a sudden conductance change

One might think that, once the membrane potential transient upon voltage step stimulation is over and voltage clamp is established, subsequent conductance changes at that potential will be faithfully recorded as current changes limited only by amplifier filtering. This is not true. The time constant  $R_{ser}C_m$  of  $I_{cs}$  remains a filtering time constant for all subsequent current changes induced by conductance changes. The reason for this is as follows: any conductance change causes even with good voltage clamp a tiny deviation from the applied potential. It is this deviation (or a fraction of it) that is monitored as current through the current measuring resistance ( $R_s$  in Figs. 2.2,3,  $R_{vc}$  in Fig. 3.1). And since this tiny  $V_m$  change requires charge redistribution across  $C_m$  via  $R_{ser}$ , the time constant  $R_{ser}.C_m$  still has a delaying effect on a current change due to a conductance change (explained earlier in chapter 2.5).

We demonstrate this filter effect in the next experiment on our electrical circuit model cell (cf. Fig. 3.1), illustrated in Fig. 3.10. We have chosen favorable conditions (high  $R_{ser}$  and  $C_m$ ) to see this effect, which do occur during real experiments but which would usually not be accepted as good enough to continue an experiment.

An “empty” cell ( $G_m = 0$  nS) with a  $C_m = 94$  pF is stimulated with 50 mV voltage blocks from a holding potential of 0 mV through a series resistance of  $52.2 M$ . The record (Fig. 3.10) shows the typical  $I_{cs}$  transient with an  $I_{cs}$  peak of  $\sim 50mV/52.2M \sim 1nA$  (measured separately at lower gain) and a time constant  $\sim 52.2M \times 94pF \sim 5ms$ . During the test pulses the record shows no current. In one of the records, we abruptly switched on a  $G_k = 1nS$  with  $E_k = -62mV$ , just after the  $I_{cs}$  transient, as if  $G_k$  was activated by the voltage step after a delay. Though the  $G_k$  was switched on instantaneously,  $I_k$  is not instantaneous but follows an (approximately) exponential time course with a time constant  $\sim 5ms$ , equal to that of  $I_{cs}$ . Similarly, switching off  $G_k$  later during the pulse causes a current decline with the same time constant of  $\sim 5ms$ . Thus, **the time constant  $R_{ser}.C_m$  can distort rapid voltage-clamp current changes**, even when the filter settings of the patch-clamp have been chosen favorably. Obviously, short duration ( $<R_{ser}.C_m$ )  $G_k$  activation will not cause full currents, which illustrates that the  $R_{ser}.C_m$  time constant acts as an amplitude filter for short duration (high frequency) currents. This again illustrates the importance of reducing  $R_{ser}$ , not only for good stationary but also for good dynamic voltage clamp. Normal time constants are  $\sim R_{ser}.C_m = 4M \times 50pF = 0.2$  ms. When using  $R_{ser}$ -compensation (not explained here) and choosing small cells, one can obtain even much smaller time constants.

Besides the given “intrinsic” filtering by the cell and the attached pipette, we have adjustable filtering by the amplifier filter setting. This can be used to add extra filtering to the intrinsic filtering, e.g. to remove the higher frequencies of a current record (noise), which passed the intrinsic

filter and spoil the record. Try the various filter settings on your signal and see what happens! The electronic mechanism of signal filtering inside the amplifier may be viewed as similar to intrinsic filtering through the  $R_{ser}C_m$  time constant. Inside the amplifier it is the combination of the equivalent  $R_{vc}$  and  $C_{vc}$  (cf. Fig. 3.1) that causes extra filtering (theory explained in Chapter 2.5). Thus, a perfect current step signal entering the amplifier input will be rounded off to an exponentially rising current with time constant  $R_{vc}C_{vc}$ . One could in principle therefore change a filter setting by changing  $C_{vc}$ . In practice, electronic filtering inside the amplifier is much more complex than simple RC-filtering (see Sigworth, Chapter 4 in Sakmann and Neher, 1995). The approximation of the filtering mechanism by a simple RC-equivalent remains useful as a first attempt to understand amplifier filtering.

### 3.5. Conclusion

After the practical exercises of the present chapter on the electrical equivalent circuit model, you may have experienced that it is not always easy to **recognize the simple theoretical concepts** of the previous chapter in the measurement configuration and the model cell properties. In a real patch-clamp experiment this is even more complex. First, the cell is much more complex, i.e. has many more “hardware” components (ion channel types, ion pumps and exchangers). Second, one cannot see and easily remove or substitute these components. Third, the cell components are usually unknown. Finally, the electrical properties of a cell are often changed during an experiment. Therefore, the experience gained in the present exercises will help to recognize cell properties from artifacts and the new and unusual electrical properties of a cell from its standard properties.

One complication seen in the simulation experiments was the **deformation of the fast capacity current transient by the amplifier**. The filter inside the amplifier reduced the peak and increased the duration of the transient compared to estimated peak and time-constant values for a simple ERC-circuit of the voltage-clamp condition. To understand this we needed to add an extra capacitance,  $C_{vc}$  (Fig. 3.1), to the simple ERC-circuits of voltage-clamp stimulation explained in Chapter 2. This was justified by operational amplifier theory.

The effects of **stray capacitance** were striking. The way they affected the fast capacitor transient (peak increase) could also be understood from an ERC-circuit including  $C_{vc}$ . These observations indicated the importance of minimizing stray capacitance when trying to obtain the best possible time resolution for studying ultra-fast conductance changes upon voltage steps.

The **establishment of the various patch-clamp configurations** could be recognized from electrical changes during the manipulations, except for the IOP. CAP-formation was easily followed from the disappearance of the pipette current during giga-sealing. WC- and ppWC-formation are evident from the sudden and the gradual appearance, respectively, of the slow capacitor current transient. OOP-formation has occurred when the slow capacitor transient suddenly shortens or when a cancelled transient suddenly becomes strongly over-cancelled. IOP-formation cannot be concluded from simple electrical changes, but is signaled by electrophysiological changes, e.g. the disappearance or change of CAP-channel activity or the appearance of new channel activity. The four other configurations are also to be confirmed by electrophysiological changes, e.g. the appearance of typical WC-currents upon voltage stimulation. Analysis of slow capacity transient cancellation resulted in a prescription for a simple and quick cancellation procedure.



The **current-clamp measurements in the CAP and the WC** were instructive, since they showed how important it is to minimize amplifier offset current effects for reliable potential measurements from high-resistance sources. Of special and practical interest were the measurements of the membrane potential,  $V_m$ , of a cell through a cell-attached patch or of fractions of  $V_m$  depending on voltage division over  $R_{cap}$  and  $R_{seal}$ . The WC-current clamp experiments illustrated the standard properties of a membrane with linear ion conductances, consistent with the parallel conductance equation. Simple, single exponential RC-response behavior was seen upon current step stimulation.

**Intracellular voltage clamp** turned out to be very important for the recording of channel activity in the **CAP** configuration. Imperfect intracellular voltage clamp occurs when  $R_m$  of the attached cell has a similar value as the channel resistance. This can easily be recognized from the presence of decaying (rather than flat) channel currents.

A separate experiment proved that **slow capacity current canceling is a cosmetic "editing"** of the record, but does not improve the quality of the dynamic voltage-clamp conditions. Thus, conductance changes upon a voltage step occurring before the  $I_{cs}$  is over, occur at a changing  $V_m$  and do not reflect channel kinetics at a constant  $V_m$ . To go one step further, the same  $R_{ser.Cm}$ -properties which limit voltage clamp speed, cause signal **filtering of WC-current changes** during conductance changes at a clamped, constant membrane potential, e.g. during spontaneous opening of a channel in a WC at a given holding potential. That is why one prefers to study channel activity in patches, CAP, OOP or IOP, where the membrane capacity is much smaller.

We did not touch all practical procedures and problems of importance for patch-clampers. For example, **series resistance compensation** was not discussed, though most patch-clamp amplifiers have this compensation as an option. However, we have seen the importance of minimizing  $R_{ser}$  to improve voltage-clamp quality. One may, for example, use patch pipettes with larger tip diameters to get lower pipette resistances (and therefore lower  $R_{ser}$ ). Nevertheless, minimized  $R_{ser}$  values may still be too large for large and fast currents such as Na currents. Engineers have therefore developed a technique to lower  $R_{ser}$  by electronic means inside the amplifier. This  $R_{ser}$  compensation procedure is not merely cosmetic (as it was for  $I_{cs}$  cancellation!), but it actually improves voltage-clamp as if  $R_{ser}$  has really been reduced. After this ERC-course you may now understand that this point can be verified by checking sharpening up of the  $I_{cs}$  transient!

Another topic not discussed or exercised is various ways of **signal filtering**. We have only explained simple RC-filtering (first order filtering), but we have not paid attention to filters with sharper cutoffs (higher order filters), although many patch-clamp amplifiers have such sharp filters, including the LM-PC used by us. The action of these sharp filters may be recognized from the slight oscillatory ringing (and delay) in the current response to voltage step stimulation, mentioned when analyzing the  $I_{cf}$ -spike of the open amplifier. For an introductory course such as the present one we found it of primary importance to introduce the concept of filtering and explain one simple electronic mechanism to obtain signal filtering, namely RC-filtering. Other signal filtering procedures would be appropriate for more advanced courses.

A last problem to be mentioned is that intracellular voltage clamp may be poor for other reasons than a  $R_{ser.Cm}$  time constant that is too large. If the cell is not a simple sphere but has complex

morphology (e.g. a neuron with axon and dendrites), or if it is coupled to other cells through gap junctions, then the voltage is only clamped in the membrane near the electrode and not more distally. This condition is called “lack of space clamp”. Electrophysiologically, poor **space clamp** can be recognized from the non-single exponential shape of the slow capacity current transient.

Finally, we hope that we have provided the student with two valuable tools to do real patch-clamp experiments. The first is **thinking in terms of simple electrical equivalent circuits of cells**; second is experimenting on cells as if they actually have these electrical equivalent circuits to help you answer your research questions.

Good luck with your experiments!

## REFERENCES

- Buisman HP, DeVos A, Ypey DL (1990). A pipette holder for use in patch-clamp experiments. *J Neurosci. Methods* 31:89-91.
- DeFelice LJ. *Electrical Properties of Cells: Patch Clamp for Biologists* (1997) Plenum Publishing Corporation, New York.
- Gaspar R, Weidema AF, Krasznai Z, Nijweide PJ, Ypey DL. (1995) Tetrodotoxin-sensitive fast Na current in embryonic chicken osteoclasts. *Pflügers Arch. (Eur. J. Physiol.)* 430:596-598.
- Hamill OP, Marty A, Neher E, Sakmann B, Sigworth FJ (1981) Improved patch clamp techniques for high-resolution current recording from cells and cell free membrane patches. *Pflügers Arch. (Eur. J. Physiol.)* 391:85-100
- Hille B. *Ionic Channels of Excitable Membranes* (1992, 2nd edition) Sinauer Associates, Sunderland, MA
- Hirsch MW, Smale S. *Differential equations, dynamical systems, and linear algebra.* (1994) Academic Press, San Diego, New York.
- Horn R, Marty A. (1988) Muscarinic activation of ionic currents measured by a new whole cell recording method. *J. Gen. Physiol.* 92:145-159.
- Horowitz P, Hill W. *The Art of Electronics* (1990, 2nd edition). Cambridge University Press, Cambridge, UK.
- Ince C, VanBavel E, VanDuijn B, Donkersloot K, Coremans A, Ypey DL, Verveen AA. (1986) Intracellular microelectrode measurements in small cells evaluated with the patch-clamp technique. *Biophys. J.* 50:1203-1209.
- Kandel ER, Schwartz JH, Jessell TM. *Essentials of Neural Science and Behavior.* (1995) International Edition, Prentice Hall International, London.
- Läuger P. *Electrogenic Ion Pumps* (1991) Sinauer, Sunderland, Mass., USA.
- Neher E, Sakmann B (1976) Single-channel current recorded from membrane of denervated frog muscle fibers. *Nature* 260, 799-802.
- Neher E, Sakmann B. (1992) The patch-clamp technique. *Sci. Am* 266, 28-33.
- Neher E. Ion channels for communication between and within cells. *Science* 256:498-502.
- Ravesloot JH, Van Putten MJAM, Jalink K, Ypey DL. Analysis of decaying unitary currents in on-cell patches of cells with a high membrane resistance. *Am J Physiol* 266 (Cell Physiol 35), C853-C869, 1994.
- Sakmann B. (1992) Elementary steps in synaptic transmission revealed by currents through single channels. *Science* 256, 503-512.
- Sakmann B, Neher E. *Single-Channel Recording* (1995) Plenum Press, New York and London.
- Sherman-Gold R (ed.). *The Axon Guide for Electrophysiology & Biophysics Laboratory Techniques* (1993) Axon Instruments, Inc., Foster City, CA 94404, USA.

Van Wijk van Brievingh RP, Möller DPF (eds). Biomedical Modeling and Simulation on a PC: A Workbench for Physiology and Biomedical Engineering (1993). Volume 6 of Advances in Simulation, Luker PA, Schmidt B (eds.). Springer-Verlag, Berlin-Heidelberg-New York.

Weidema AF, Ravesloot JH, Panyi G, Nijweide PJ, Ypey DL (1993) A Ca<sup>2+</sup>-dependent K<sup>+</sup>-channel in freshly isolated and cultured chick osteoclasts. *Biochim. Biophys. Acta* 1149:63-72.

Wiltink A, Nijweide PJ, Scheenen WJMM, Ypey DL, VanDuijn B. Cell membrane stretch in osteoclasts triggers a self-reinforcing Ca<sup>2+</sup> entry pathway (1995) *Pflügers Arch. (Eur. J. Physiol.* 429:663-671.

Ypey DL. Practical introduction to patch clamping by simulation experiments with simple electrical circuits (1998) Chapter 7 in: *Signal Transduction - Single Cell Techniques*. B Van Duijn and A Wiltink (eds.). Springer Verlag, Berlin-Heidelberg-New York.

## FIGURES AND TABLE

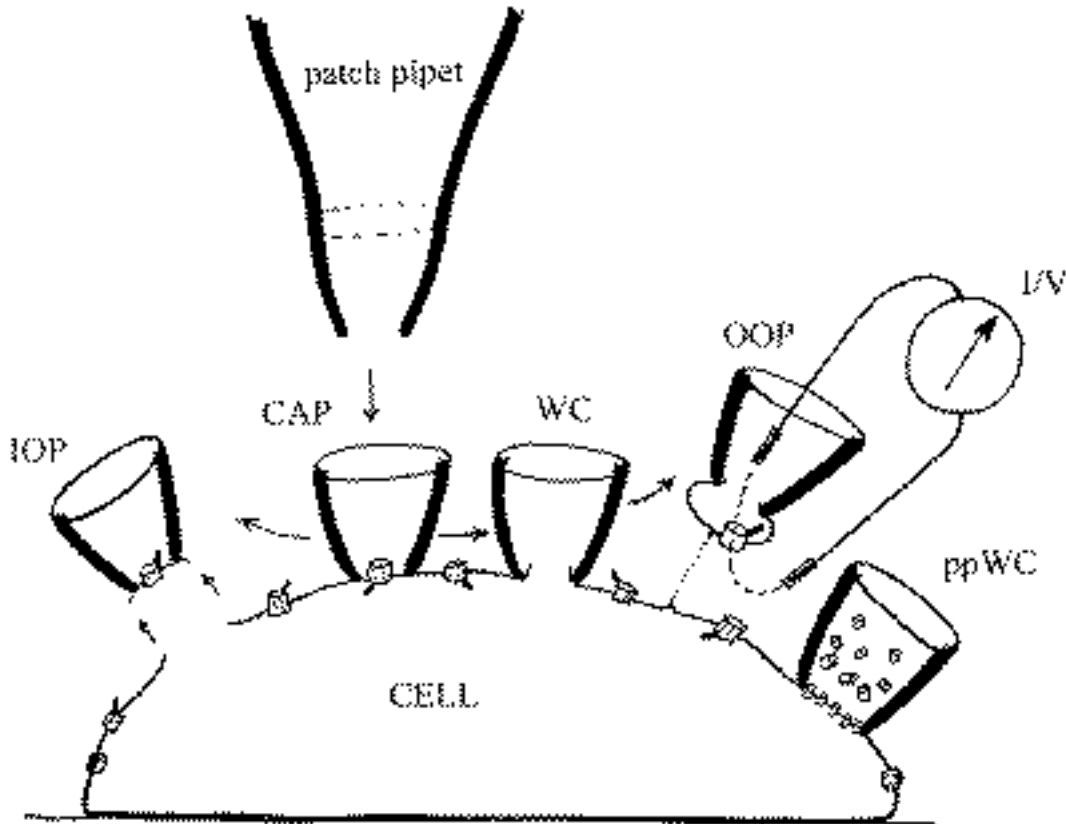


**Figure 1.1. Diagram of the five patch-clamp measurement configurations**

The figure depicts a living cell seen from the side immersed in extracellular solution and adhered to the substrate. The barrel-type pores in the membrane (some with movable lids or gates) represent ion channels. The five “cups” drawn in semi-perspective close to the cell are the tips of fluid-filled glass micro pipettes connecting the cell to the amplifier. The figure is a composite drawing, as if all five pipettes were placed on one cell. Although this is not a practical possibility, it is possible to make simultaneous two-electrode WC/CAP recordings (DeFelice, 1997) and CAP/CAP would not be out of the question. All five tips are in position to illustrate how the various measurement configurations are derived from the initial cell-attached-patch (CAP) configuration, established after the giga-sealing procedure. The inside-out patch (IOP) is a CAP excised from the cell membrane. The whole-cell (WC) configuration is obtained by rupturing the CAP. The outside-out patch (OOP) is a vesicle (a “tiny cell”) pulled from the WC configuration. The permeabilized-patch WC (ppWC) develops from the CAP if the pipette solution contains pore-forming molecules incorporating in the CAP. The measuring patch-clamp amplifier and the connecting electrodes, one inside the pipette and one in the bathing solution, are drawn for the OOP-configuration; however, they apply to the other configurations as well. The amplifier measures current (I) through the membrane or voltage (V) across the membrane.

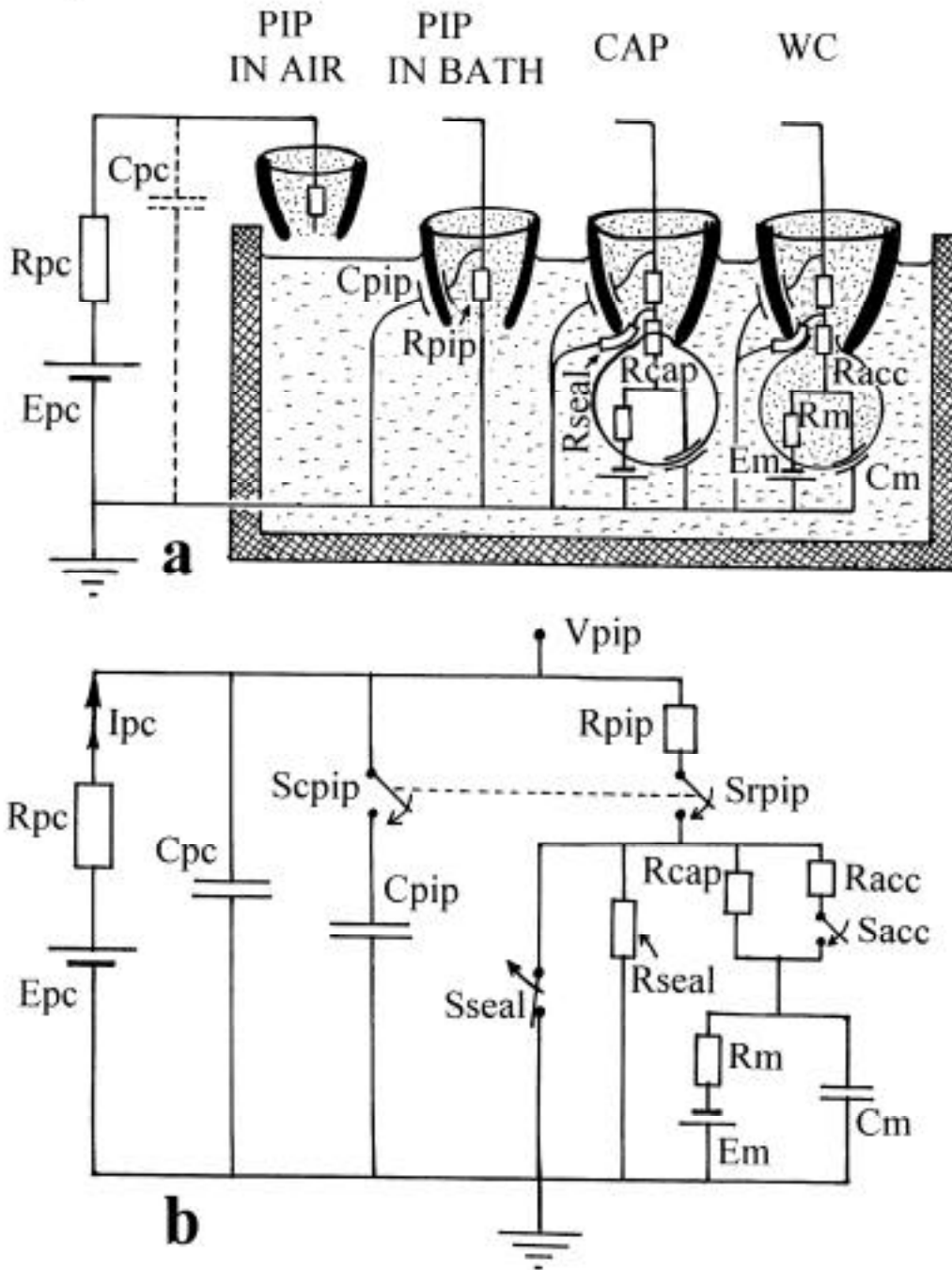


**Figure 1.2. A simple electrical circuit modeling the successive patch-clamp procedures for obtaining the whole-cell configuration**

A pipette (PIP) entering the bath, forming a giga-seal with the cell, and breaking the cell-attached patch. **Part a** shows how the various components of the circuit can be identified with components of the measurement configuration(s). **Part b** shows the circuit abstracted from the drawing in Part a, including the switches (S) for going through the three successive procedures leading to a WC configuration. The procedures and component names are further explained in the text. During the experiment the quality of the pipette, the giga-

seal, and the whole-cell configuration are tested by applying voltage-clamp Epc steps to the pipette and measuring the resulting patch-clamp current Ipc.

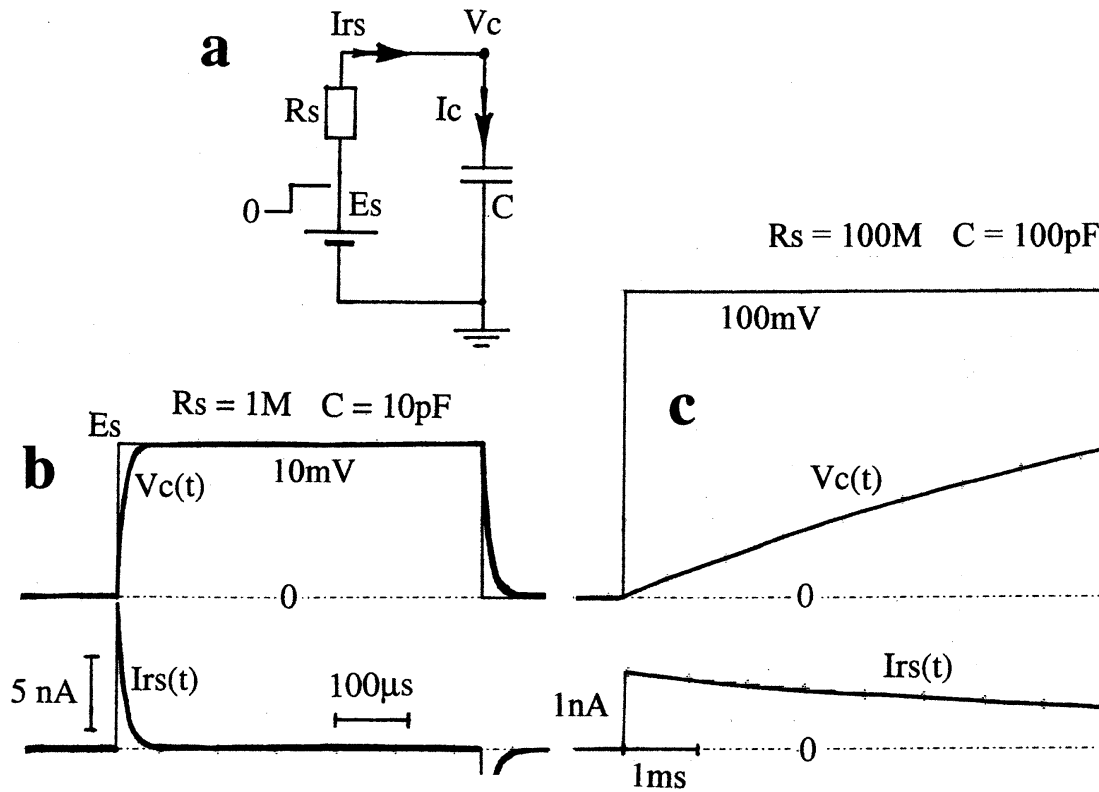


**Figure 2.1. Charging a capacitor: ERC-circuit I.**

Part **a** shows the ERC-circuit studied, **b** the voltage-clamp behavior upon an  $E_s$  voltage step at a given (low) value of  $R_s$  and **c** the current-clamp behavior of the circuit upon a much higher  $E_s$  voltage step at a much higher value of  $R_s$  (notice time calibration difference). The upper records of **b** and **c** show the  $E_s$  voltage steps applied (positive, from zero) and the exponential  $V_c$  responses. The lower records show the exponential current responses. Notice that the  $V_c$  and  $I_{rs}$  transients change with the same time constants and that the current-clamp transients are much slower than the voltage-clamp transients. In both cases there is no stationary current after the transient, since  $V_c$  becomes exactly equal to  $E_s$ .  $E_s$  is the stimulating voltage,  $I_{rs}$  is the current through the source resistance  $R_s$ ,  $V_c$  is the voltage across the capacitor  $C$ , and  $I_c$  is the current flowing into  $C$ . The records in panels **b** and **c** have been calculated with the use of a computer model (PSI, see Note 1.3.1) of the circuit in **a** for the component values given in panels **b** and **c**.



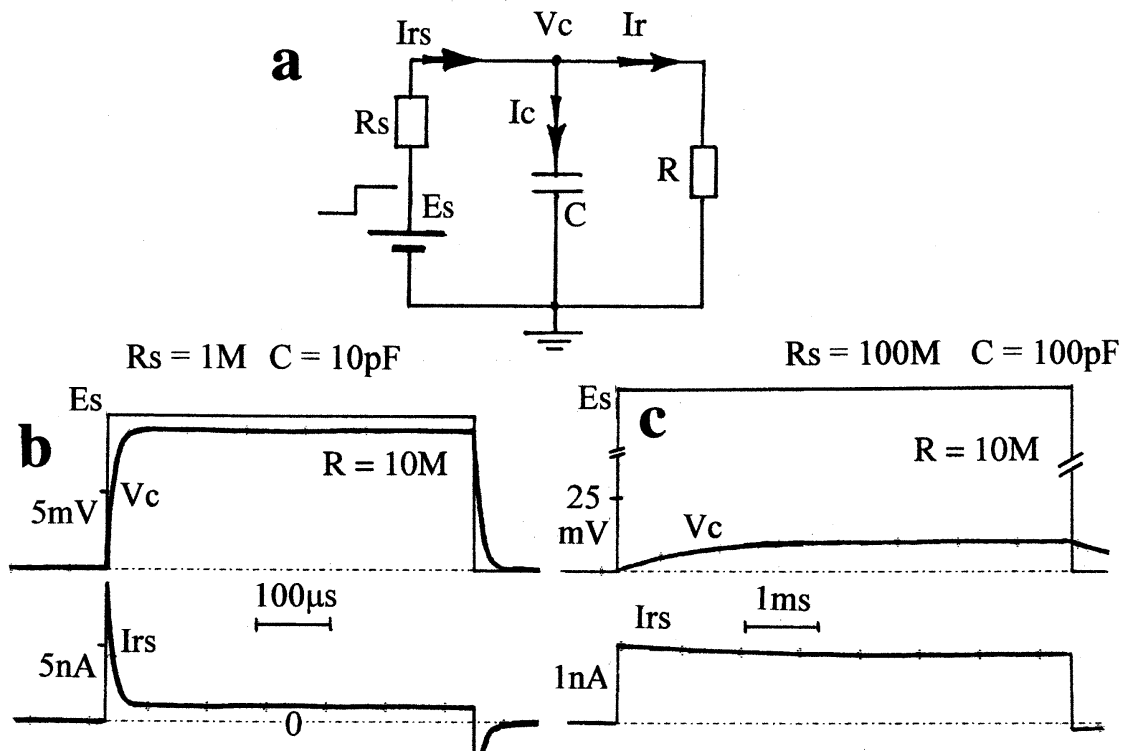


**Figure 2.2. Charging a leaky capacitor: ERC-circuit II.**

Circuit (a), record types (b,c) and symbols are as in Figure 2.1 except for an extra component in the circuit, resistance  $R$  in parallel to  $C$ . It is now the parallel RC-circuit that is voltage-clamped ( $R_s \ll R$ ) (b) or current-clamped ( $R_s \gg R$ ) (c) by the  $E_s/R_s$  source. The records have been calculated for the indicated component values. The  $E_s$  step in c is  $100\text{ mV}$ . The voltage-clamp records at the given resolution do not look very different from those in Fig. 2.1b, but the significant difference is that  $V_c$  never becomes exactly equal to  $E_s$  and that  $I_{rs}$  reaches a stationary value  $\sim E_s/R$ . It is the value after the capacitance transient that is important during a real patch-clamp experiment, because this value reflects the conductance of the membrane if  $R \gg R_s$ . This implies that the capacitance peak current is much larger than the current after the peak transient. The current-clamp records look very different from those in Fig.2.1c.  $I_{rs}$  reaches a stationary value  $E_s/(R_s + R) \sim E_s/R_s$  and  $V_c$  shows a stationary displacement  $\sim I_{rs}R$ . The time constant is now smaller than for ERC-circuit I:  $\sim RC$  in stead of  $R_sC$ .

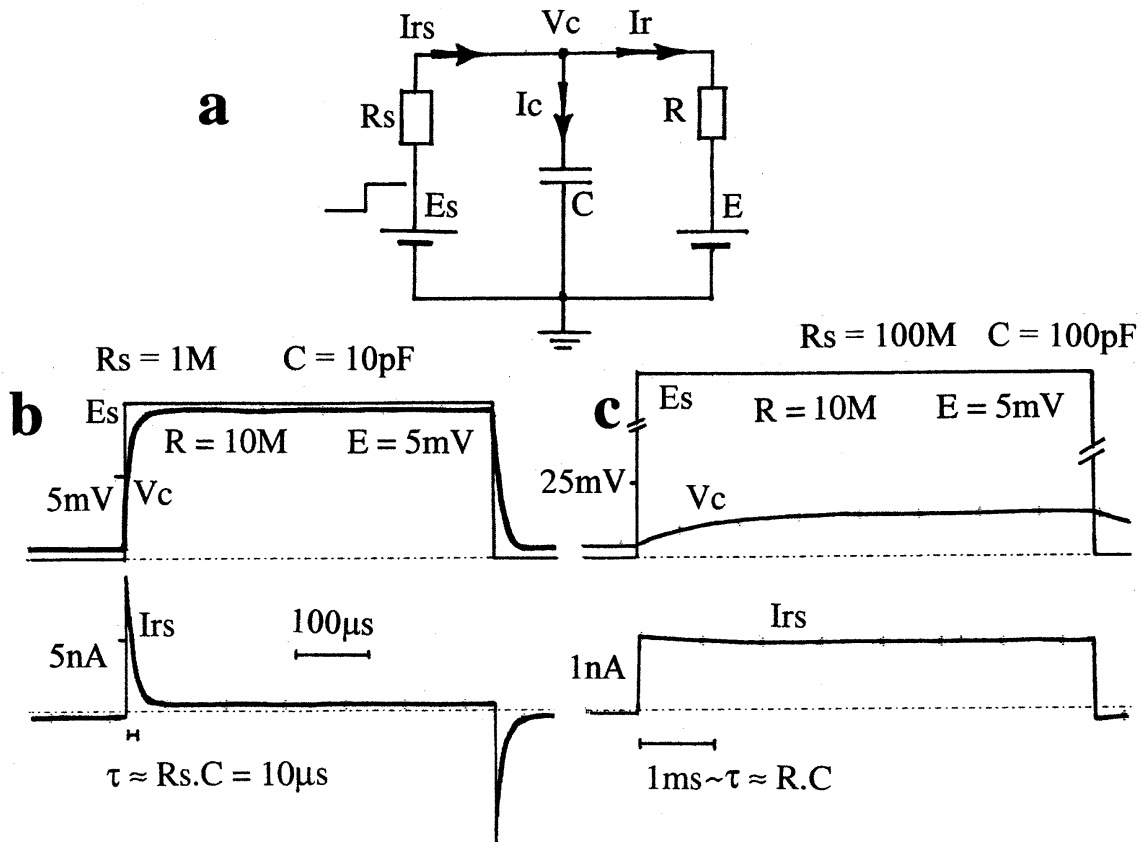


**Figure 2.3. Clamping an ERC-model: ERC-circuit III**

This circuit (a) contains, compared to ERC-circuit II, an extra voltage source E added in series with R. This makes the resulting ERC-circuit resembling a patch pipette with offset voltage or a cell membrane with membrane potential, voltage (b) or current (c) clamped by the  $E_s/R_s$  source. The  $E_s$  step in c is 100 mV. Note the difference in time scale between b and c. The records in b and c have been calculated for the indicated component values and are similar to those in Fig. 2.2b,c, except for the following differences: (1) E causes stationary (inward) current in b when  $E_s = 0$  and the stationary current upon the  $E_s$  step is also different because of the presence of E; (2) the  $V_c$  record in c now starts from E (here chosen positive) instead of from zero.

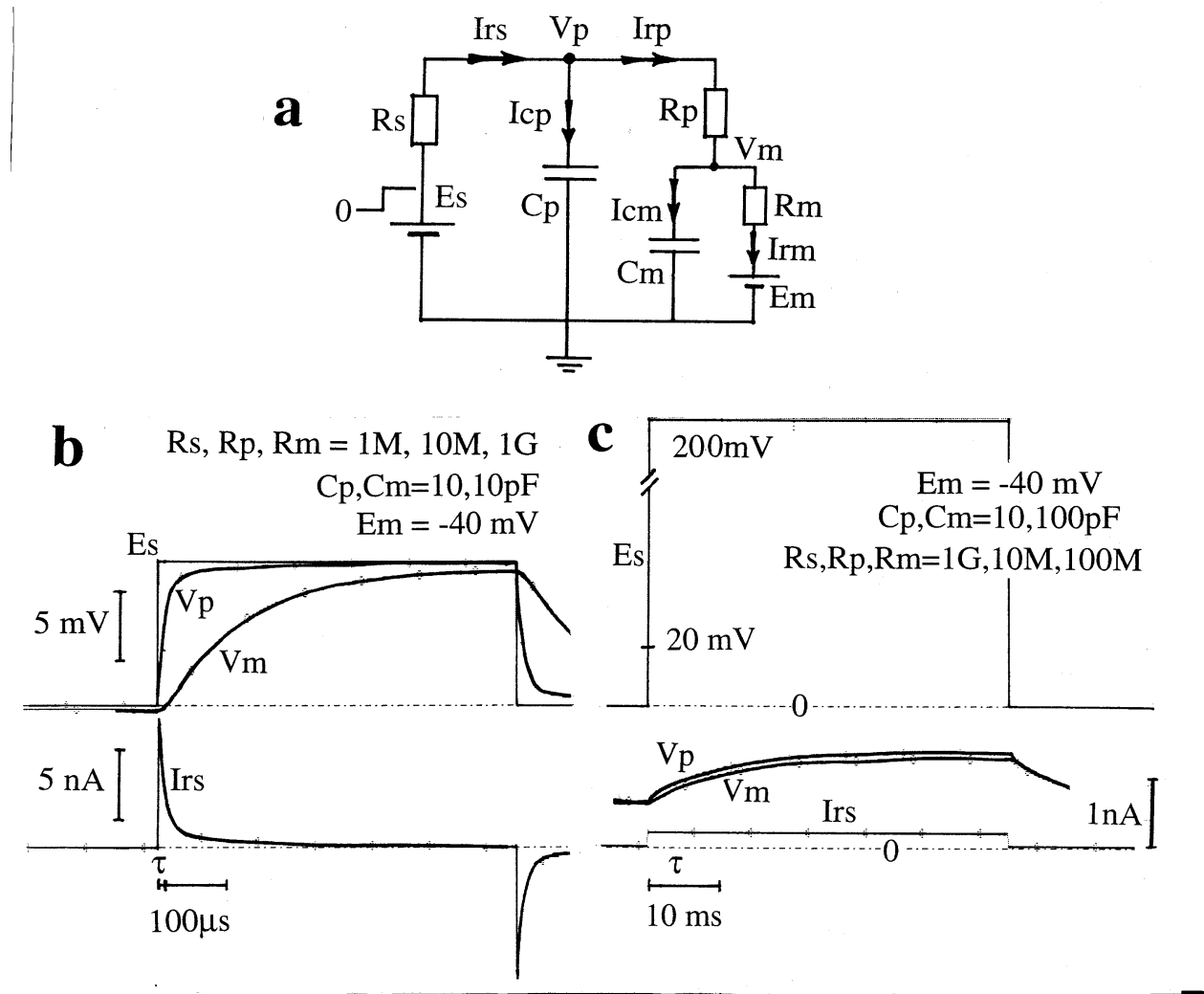


**Figure 2.4. Clamping an ERC cell membrane through a patch pipette: ERC circuit IV**

The circuit in **a** is Fig.2.3a for a whole-cell configuration, extended with components representing the properties of the measuring patch pipette. The pipet resistance  $R_p$  is the access resistance to the  $E_m/R_m/C_m$  membrane circuit, and  $C_p$  shunts the input of the  $E_s/R_s$  source. The presence of two capacitors coupled by a resistor makes the voltage-clamp (**b**) and current-clamp (**c**) responses biphasic (less clearly visible in current-clamp at the given resolution). Records calculated for the indicated component values.

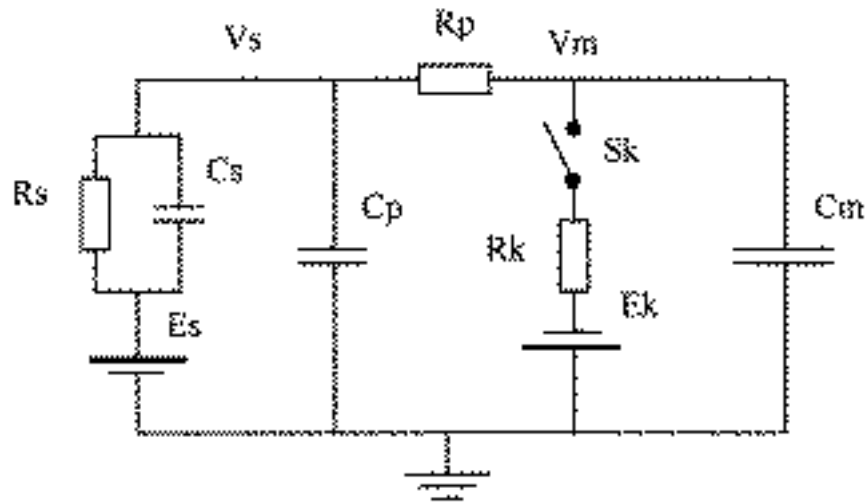


**Figure 2.5. Electrical equivalent circuit (ERC circuit V) of a Whole-Cell (WC) measurement configuration to illustrate filtering of WC-current steps**

The  $E_s/R_s/C_s$  branch at the left is the voltage clamp. The  $E_k/R_k/S_k/C_m$  circuit at the right represents the whole cell. A current step was evoked by closing switch  $S_k$  of the  $G_k$  branch.  $R_p$  and  $C_p$  represent the pipet, connecting the WC with the voltage clamp. The only difference with Fig. 2.4a is the presence of  $C_s$ . In the example in the text,  $V_m$  is clamped at  $E_s = 0\text{mV}$ , which makes  $C_p$  and  $C_s$  parallel capacities. Note that  $R_k \gg R_p \gg R_s$  and  $C_m \gg C_p$  and  $C_s \gg C_p$ . The first filter acting on  $I_k$  upon activation of  $G_k$  is the  $R_p C_m$ -filter. The second filter acting on  $I_k$  is the  $R_s C_s$  filter. If  $R_s C_s > R_p C_m$ , then the  $R_s C_s$ -filter removes a fraction of the high signal frequencies, which passed the  $R_p C_m$ -filter.

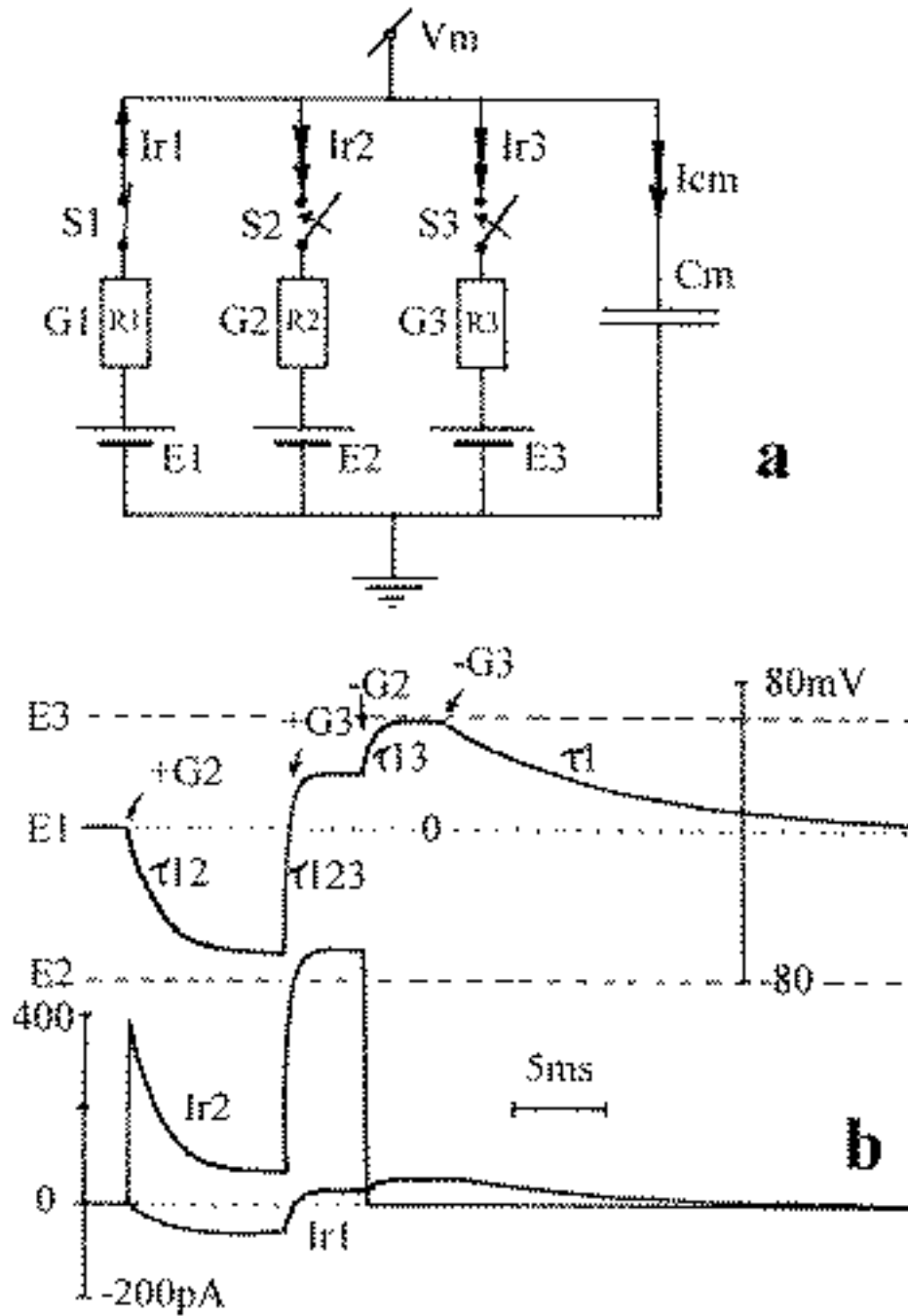


**Figure 2.6. Membrane potential and current changes during conductor switching in an ERC-membrane model in current clamp: ERC-circuit VI**

The circuit in **a** is a parallel conductance model of three conductances  $G_1$ ,  $G_2$  and  $G_3$ , which can be switched on or off with the three switches  $S_1$ ,  $S_2$  and  $S_3$ . Each of the three conductance branches contains a voltage source  $E$  ( $E_1$ ,  $E_2$ , and  $E_3$ , respectively). The membrane capacity  $C_m$  is parallel to the conductances. The membrane is under zero-current clamp conditions by assuming that the external current  $I_{rs} = 0$ .  $V_m$  is the

membrane potential, and  $I_{cm}$  the capacitance current.  $I_1$ ,  $I_2$  and  $I_3$  are the currents through the conductance branches 1, 2 and 3. The upper record of part **b** shows  $V_m$  changes upon switching the conductors for the condition that  $E_1 = 0$ ,  $E_2$  is negative and  $E_3$  is positive (as indicated) and that  $G_3 > G_2 > G_1$ .  $G_1$  is switched-on all the time. First  $G_2$  turns on, then  $G_3$  (first turning off  $G_2$ ). The various time constants are indicated. The currents  $I_2$  and  $I_3$  are monitored in the lower record. The records were calculated with a computer model (see Note 1.3.1) based on Eq. 53a.

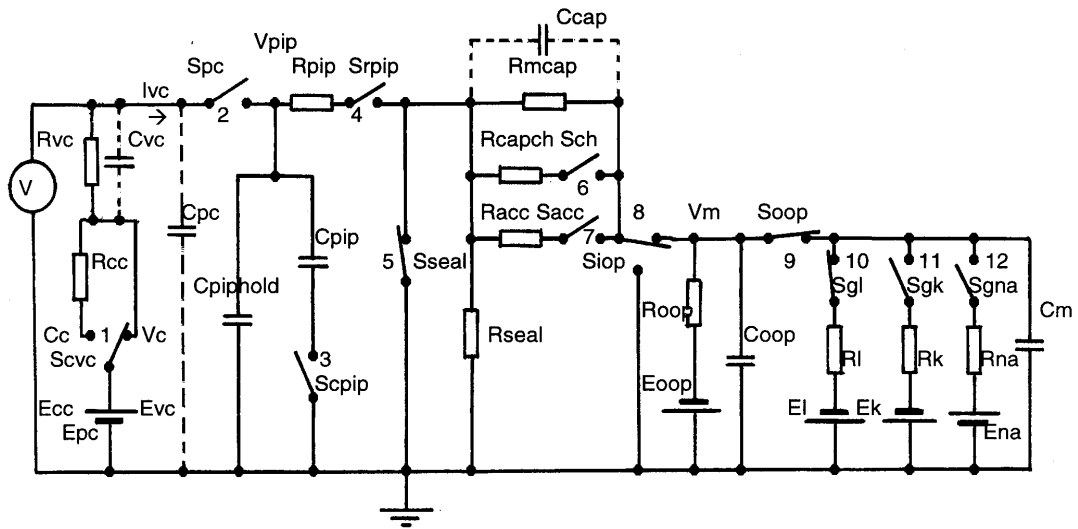


**Figure 3.1. Diagram of the electrical equivalent circuit of the model used to exercise patch-clamp procedures and measurements**

The dashed capacitors are stray capacitances, not added to the circuit as components. For further explanations, see text and Table 3.1.

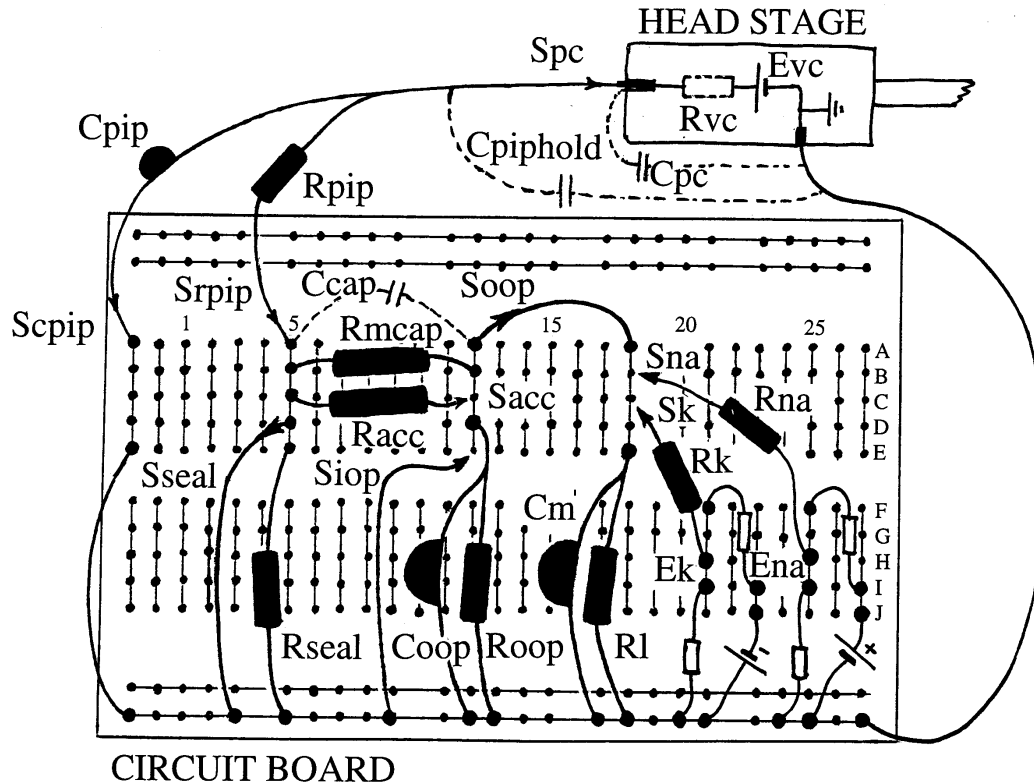


**Figure 3.2. Example of equivalent circuit wiring on the breadboard (or circuit board)**

The figure shows a 8x6cm breadboard seen from above. The dots are wire insertion holes for easily making electrical connections without soldering. The straight lines between the dots are the connecting wires between the insertion holes, under the surface of the board. These connections cannot be seen but can be checked with an Ohmmeter. By inserting the leads of the components (resistors, capacitors, batteries) in the holes, one can easily build circuits to study the electrical properties of the various patch-clamp configurations and to exercise the experimental procedures. Resistors (cylinders) and capacities (half-drops) added as components to obtain the equivalent circuit of Fig. 3.1 are black. The switches of the circuit diagram in Fig. 3.1 are just the leads with the arrow points, pointing to or from a connection hole. The enlarged dots show the established contacts. Arrows pointing to close-by holes indicate switch contacts to be made during the proposed series of model experiments. Arrows pointing away from holes indicate contacts to break during the experiments. By comparing this practical breadboard circuit with the circuit diagram in Fig. 3.1, one can identify the various components. In the present circuit wiring, the probe (pre-amplifier) of the patch-clamp amplifier has been connected to the pipette-holder with pipet (switch S<sub>pc</sub> on), the “pipet has entered the bathing solution around the cell” (S<sub>cpip</sub> and S<sub>rpip</sub> on) and the pipet is “touching the cell, ready for giga-sealing”. Giga-sealing is established by opening the seal switch, S<sub>seal</sub>. This results in the CAP measurement configuration. By connecting R<sub>acc</sub> to hole 12C (switch S<sub>acc</sub> on), one can make a WC from the CAP. By opening S<sub>oop</sub> one obtains an OOP from the WC. In stead, connecting S<sub>iop</sub> under CAP conditions results in an IOP. With switches S<sub>k</sub> and S<sub>na</sub> one can introduce into the WC a G<sub>k</sub> and a G<sub>na</sub>, respectively. The Nernst potentials have been established with a simple voltage-divider circuit (the small white resistors). The leak conductance has been given a reversal potential E<sub>l</sub>=0mV. The interrupted-line wires are non-existing wires, but indicate the presence of stray capacities (C<sub>pc</sub>, C<sub>piphold</sub>, C<sub>cap</sub>). Resistor R<sub>capch</sub> with switch S<sub>capch</sub> (Fig. 3.1) is not shown on the circuit board.



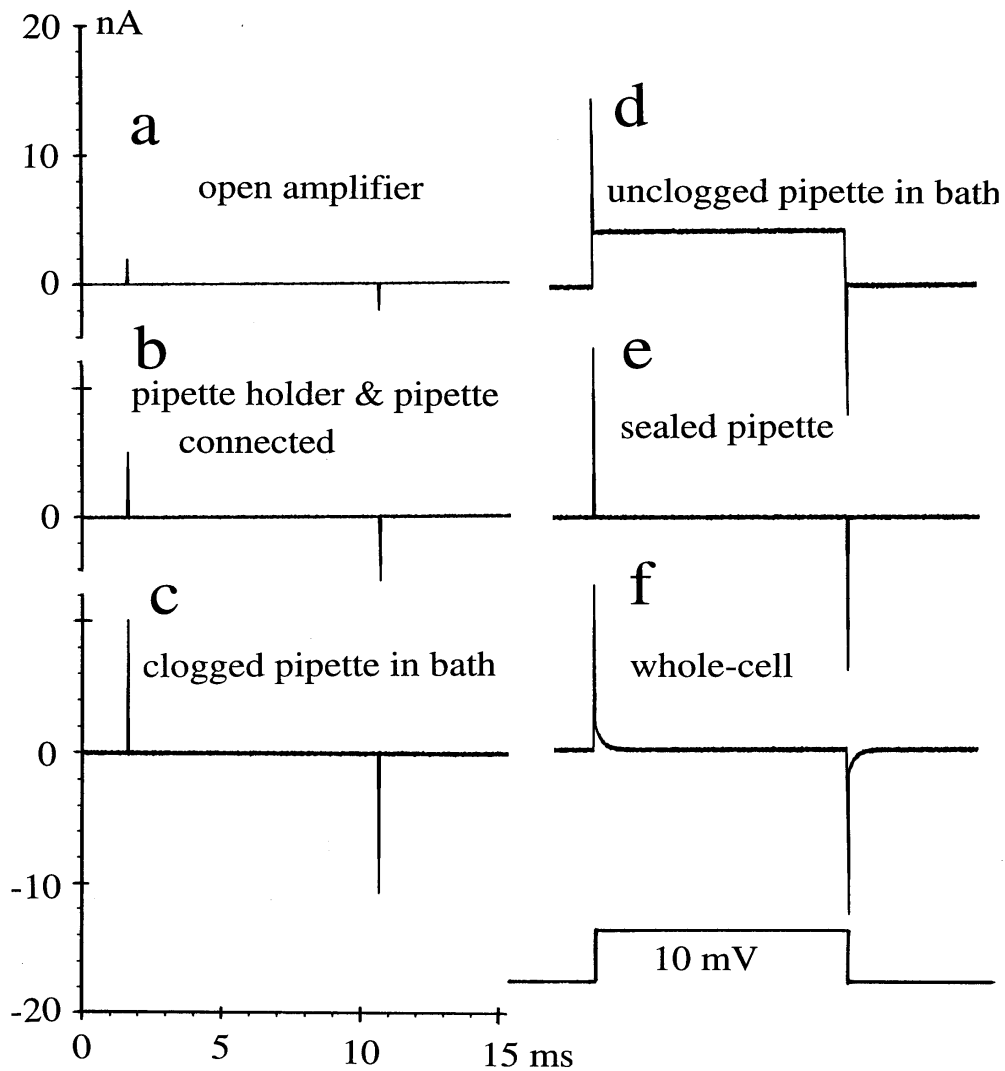


**Figure 3.3. Voltage-clamp records obtained during patch-clamp procedures leading to the whole-cell (WC) configuration, all on one scale (lowest gain recording)**

The various procedures, described in the text, were carried out while applying voltage-clamp steps of 10mV. The initial model settings were as illustrated in Fig.3.1. Record a applies to these initial settings. Record b is taken after closure of switch  $S_{pc}$ , c after closing  $S_{cpip}$ , d after closing  $S_{rpip}$ , e after opening  $S_{seal}$  and f after closing  $S_{acc}$ . The model components were as in Table 3.1, with  $R_{acc}=2.2M$ ,  $E_l=E_{oop}=\sim -60mV$ . The  $G_k$  and  $G_{na}$  branches were not connected (switches 10-12 open). Amplifier settings: 80KHz filtering and no capacitive transient cancellation.

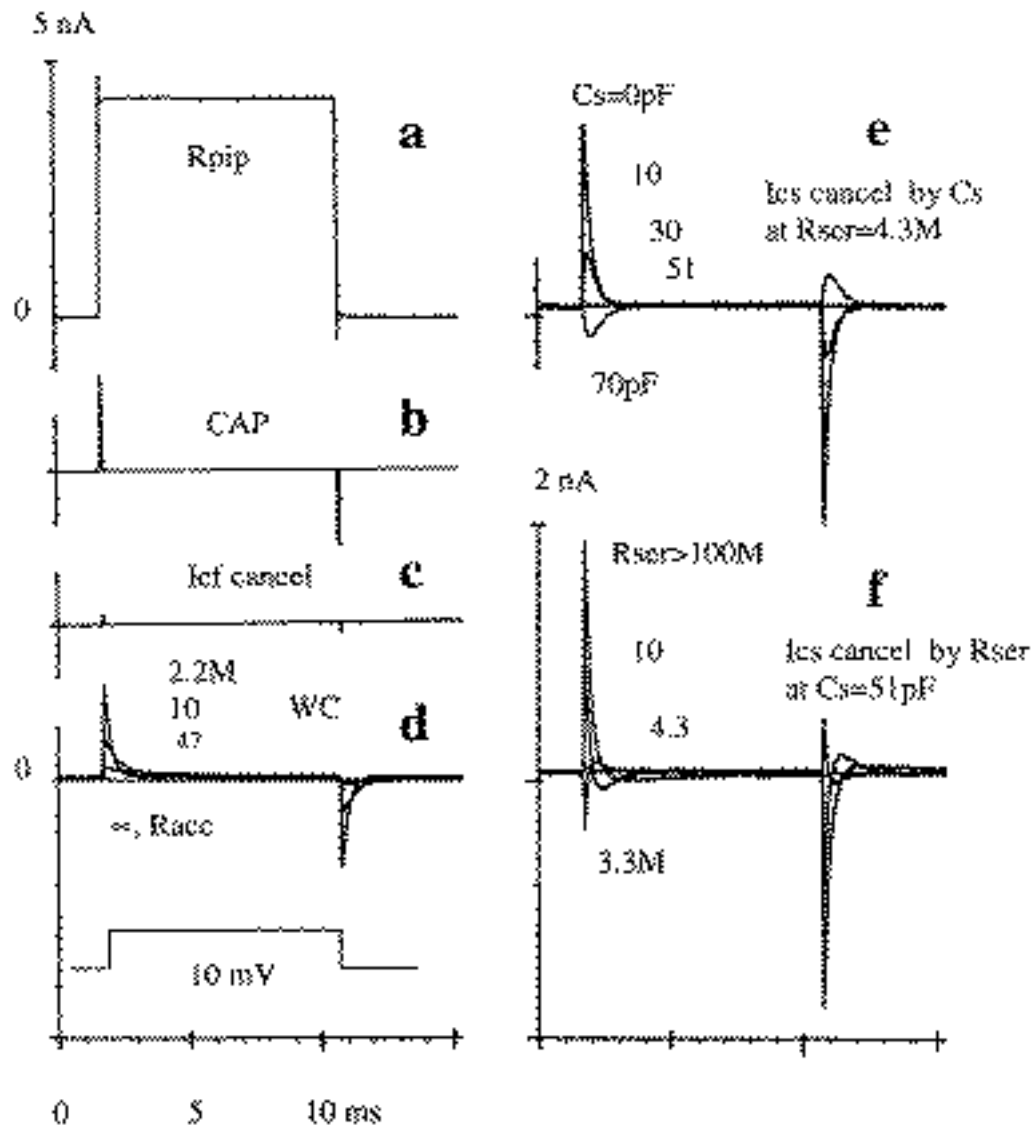


**Figure 3.4. Experimental procedures for preparing a conventional whole-cell experiment, including fast capacity current ( $I_{cf}$ ) and slow capacity current ( $I_{cs}$ ) cancellation during 10mV voltage step application**

Record **a** serves to calculate  $R_{pip}$  (here 2.2M), record **b** shows  $I_{cf}$  after giga-sealing, thus in the cell-attached-patch (CAP) configuration. Record **c** shows  $I_{cf}$  after almost complete cancelling. The records in frame **d** show the sudden appearance of  $I_{cs}$  upon establishing a WC from the CAP. The better the access to the WC (the lower  $R_{acc}$ ), the higher and faster  $I_{cs}$  (examples  $R_{acc} = \infty, 47, 10$  and 2.2M). Frames **e** and **f** illustrate the changes in  $I_{cs}$  during  $I_{cs}$  cancellation, in frame **e** for  $C_s$  adjustments (0-70pF) at the right  $R_{ser}$  value (4.3M) and in frame **f** for  $R_{ser}$  adjustments (>100M-3.3M) at the right  $C_s$  value (51pF). Low-pass frequency filter setting is at 10KHz. Other general conditions are as in Fig. 3.3.

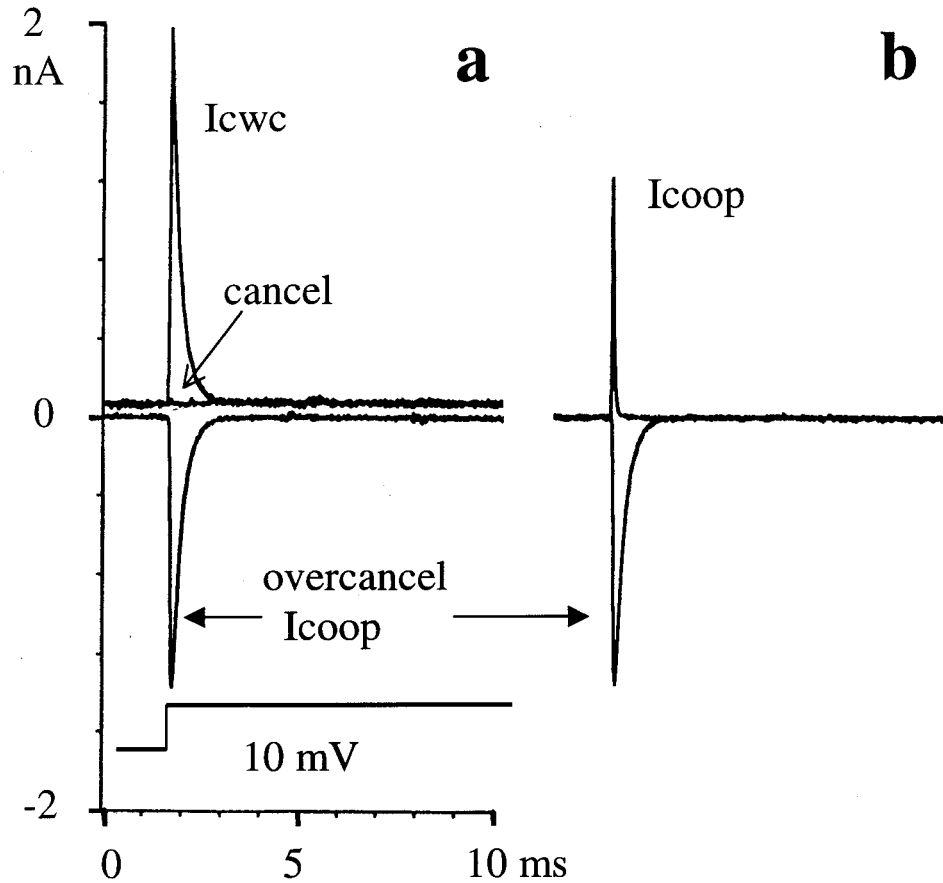


**Figure 3.5. Slow capacity current ( $I_{cs}$ ) changes upon establishment of the outside-out-patch (OOP) measurement configuration**

The model cell and the test pulse are the same as those in Fig. 3.4.  $I_{cwc}$  is the uncanceled  $I_{cs}$  of the WC (frame **a**) and  $I_{coop}$  is the uncanceled  $I_{cs}$  of the OOP (frame **b**). The flat record in frame **a** is the perfectly cancelled  $I_{cwc}$ , while the negative records in frames **a** and **b**, labeled overcancel  $I_{coop}$ , are the records obtained just after OOP formation from the condition of perfect  $I_{cwc}$  cancellation (flat record in frame **a**). The sudden appearance of the large inverse  $I_{cwc}$ -like current transient is indicative for the formation of an OOP.

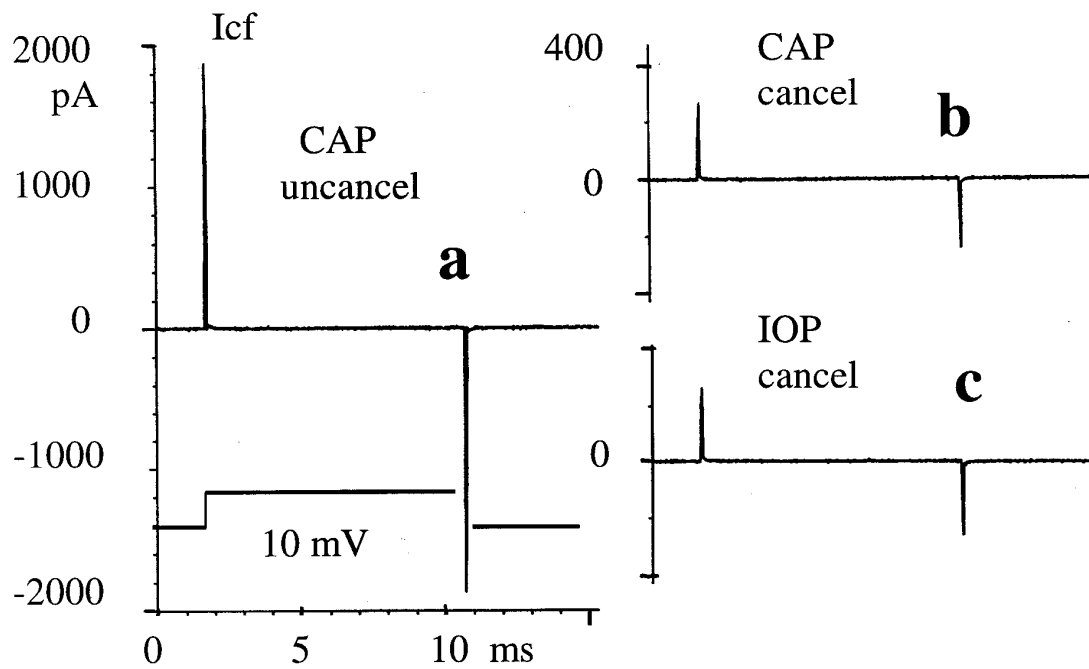


**Fig. 3.6. Fast capacitive current ( $I_{cf}$ ) transients of the cell-attached-patch (CAP) and inside-out-patch (IOP) compared.**

The uncanceled CAP- $I_{cf}$  transients in frame **a** are the same as those in Fig. 3.4b for the same experimental conditions. Largely canceled CAP- $I_{cf}$  transients are shown in frame **b**. Essentially the same  $I_{cf}$  transients are seen in frame **c** after excision of the CAP to obtain an IOP (by switching  $S_{iop}$ , switch 7 in Fig.3.1, to ground connection).  $I_{cf}$  was largely canceled in frames **b** and **c**, in order to be able to better observe changes in  $I_{cf}$  upon uncoupling the cell from the CAP.

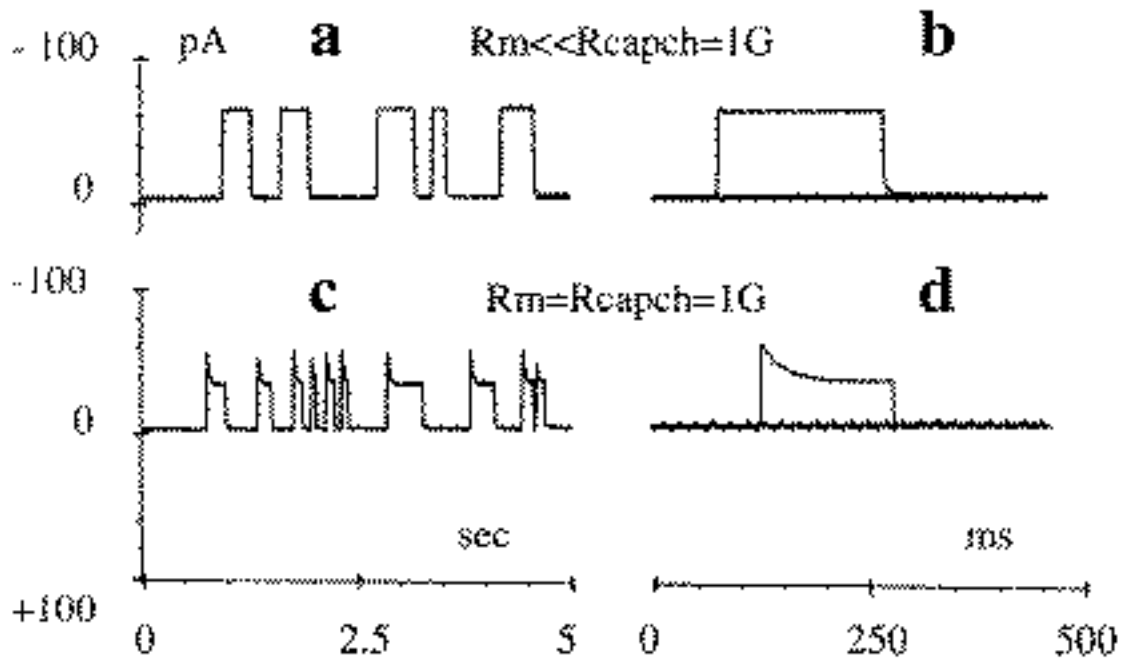


**Figure 3.7. Single-channel current recordings from a cell-attached patch under perfect intracellular voltage clamp (square currents in frames a and b) and imperfect intracellular voltage clamp (decaying currents in frames c and d)**

The records of a and c are single sweeps on a slow time scale to show repeated channel opening. The records of b and d are 4 superimposed sweeps on a 10x faster time scale for a better resolution of the single channel current shape. In only 1 of the superimposed sweeps of frames b and d a channel current was captured. According to conventions in electrophysiology, inward current through channels is negative. Thus, the current into the CAP-channel from the pipet is negative, but the amplifier shows current flowing out of the pipet as positive, consistent with positive current flow during outward WC-currents. Therefore, the currents have been plotted upward, as produced by the amplifier, but the indicated current polarity is conventional. Conditions:  $R_m = R_l = 90M$  ( $\ll R_{capch}$ ) in frames a and b,  $R_m = 1G$  ( $= R_{capch}$ ) in frames c and d. General conditions:  $R_{capch} = 1G$ , ( $E_{capch} = 0mV$ ),  $R_{mcap} = 20G$ ,  $R_{seal} = 20G$ ,  $V_m = E_l = -62mV$  (measured in current-clamp whole-cell with  $R_{ser} = 4.4M$ ),  $C_m \sim 50pF$ , OOP-components removed and sodium and potassium branches disconnected,  $R_{pip} = 2.2M$ ,  $C_{pip} \sim 5pF$ , low-pass filter setting at 1 KHz. The CAP-channel was opened and closed by opening and closing a magnetically operated switch (reed contact) in series with the channel by moving a small magnet to and from the switching contact. The small ripples in records b and d are due to 50Hz noise, induced by exposure of the set-up to the experimenter. The movements of the magnet sometimes caused small artifacts in the records, e.g. small waves in the baseline, not significant in these records, except maybe in the tail of the off-current in figure b.

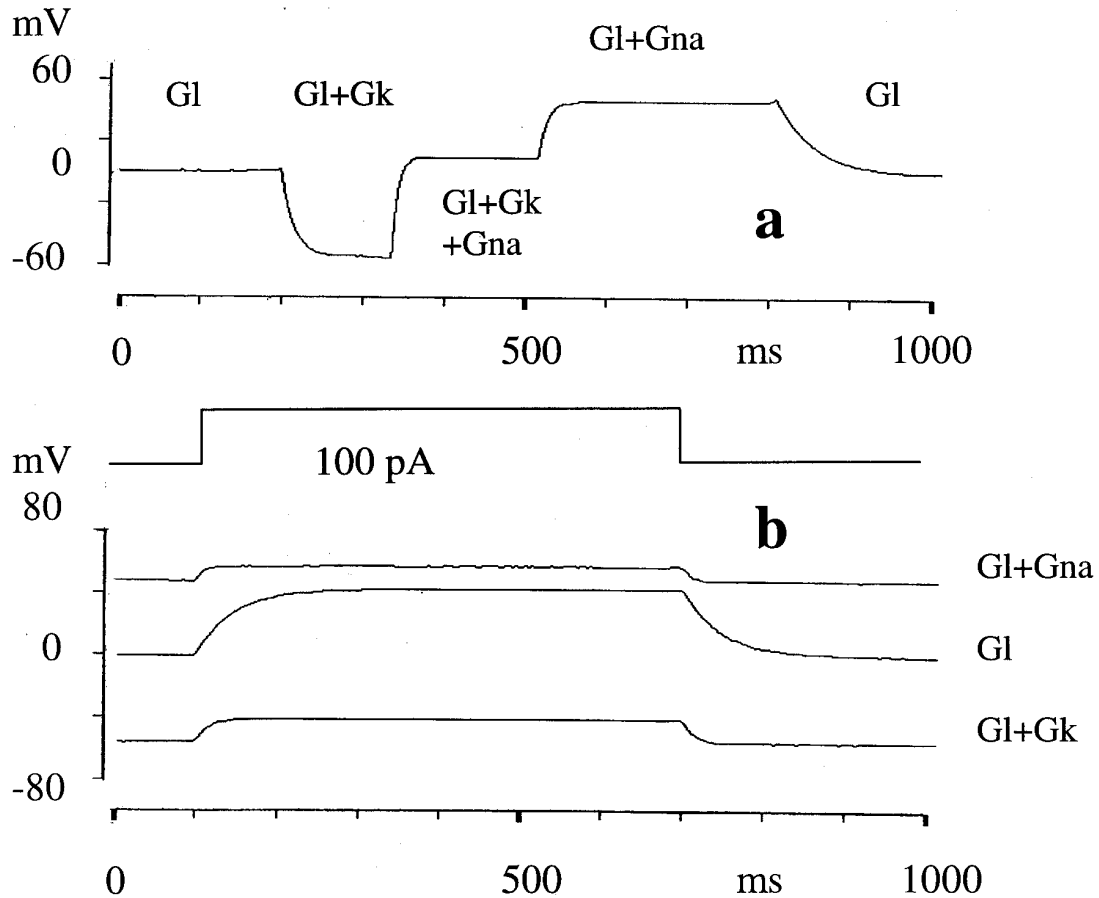


**Figure 3.8. Whole-Cell membrane potential changes upon sudden conductance changes (a) and upon current-step stimulation (b)**

Gk and Gna were switched on and off with the use of a reed contact in series with Gk and Gna, which can be operated by approaching it with a small magnet. In the initial condition of the experiment of figure a only the Gl branch of the 3 conductance branches Gl, Gk and Gna was switched on ( $S_{gl}$  on and  $S_{gk}$  and  $S_{gna}$  off, see Fig. 3.1), which caused the initial  $V_m = E_l = 0$  mV. At ~200 ms  $S_{gk}$  was also switched on, which resulted in a hyperpolarization towards  $E_k = -86$  mV. At ~340 ms  $S_{gna}$  was added, causing a depolarization towards  $E_{na} = +60$  mV. At ~500 ms  $S_{gk}$  was switched off, causing a further depolarization towards  $E_{na}$ . When finally  $S_{gna}$  was switched off at ~800 ms,  $V_m$  returned to the initial  $V_m = E_l = 0$  mV. In figure b the cell was stimulated by a 100 pA block-pulse current in the 3 conductance states of figure a indicated. The responses reflect the RC-properties of the membrane in the 3 conductance states. Other circuit model properties:  $R_{pip} = R_{acc} = 2$  M,  $R_l = 400$  M,  $R_k = 200$  M,  $R_{na} = 100$  M,  $R_{seal} = 20$  G,  $R_{cap} = 20$  G,  $C_m \sim 86$  pF and  $C_{pip} \sim 5$  pF (measured by cancellation).

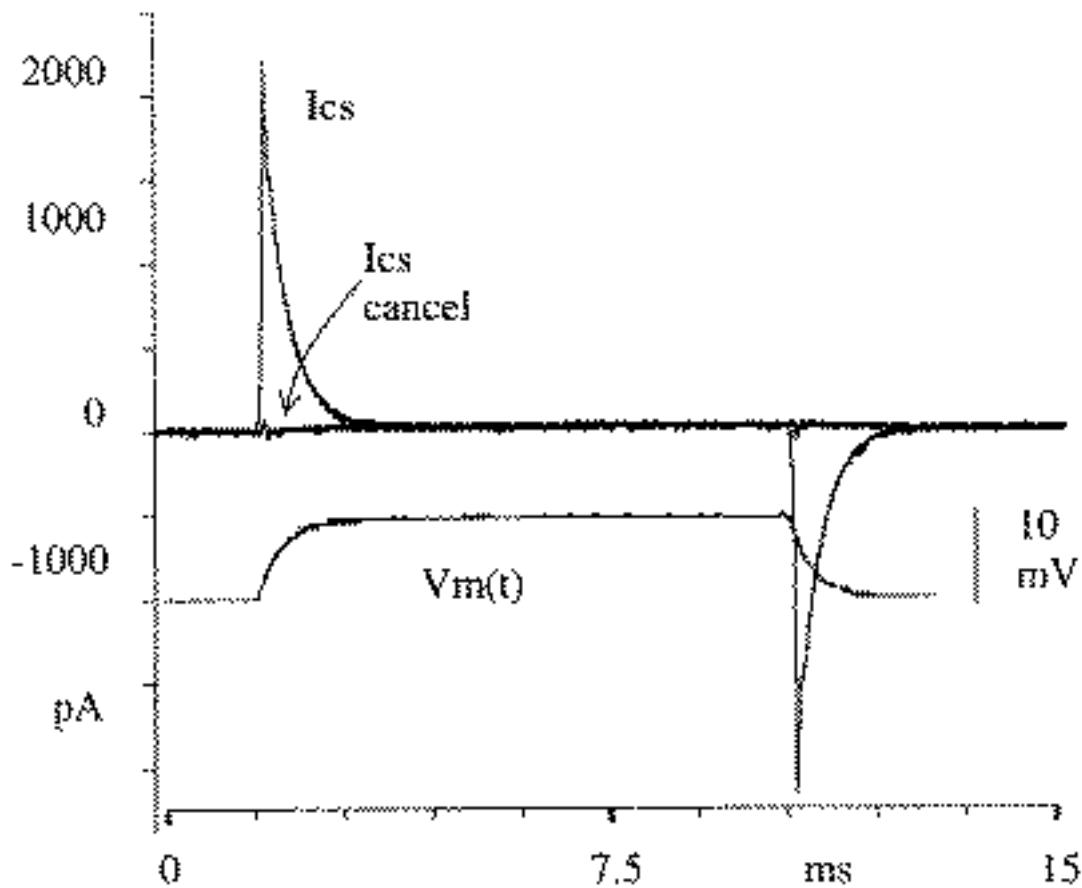


**Fig. 3.9. The membrane potential transient,  $V_m(t)$ , during the slow capacitive current ( $I_{cs}$ ) transient upon voltage-clamp WC-stimulation and the lack of an effect of  $I_{cs}$  transient cancellation on  $V_m(t)$**

The records shown are ~30 superimposed sweeps. Experimental conditions (see circuit of Fig. 3.1):  $R_{pip}=2.2M$ ,  $C_{pip}\sim 5pF$ ,  $R_{seal}=20G$ ,  $R_{mcap}=20G$ ,  $R_{acc}=2.2M$ ,  $R_m=R_l=1G$ ,  $C_m\sim 94pF$  (nominal value), resting  $V_m=E_l=0mV$ ,  $S_{gk}$  and  $S_{gna}$  are off, the OOP-segment of the membrane is removed, patch-clamp amplifier filter setting on 10KHz. An intracellular microelectrode (current-clamp) amplifier was directly coupled to  $V_m$  in the circuit to measure  $V_m(t)$  and  $I_{cf}$  was completely cancelled at a  $C_f=4.5pF$  (at the best fitting  $f$  dial position). Complete  $I_{cs}$  cancelling occurred at  $C_s=84pF$  and  $R_{ser}=4.3M$  (see flat record indicated by arrow), close to the nominal values of the used components ( $C_m=94pF$ ,  $R_{ser}=4.4M$ ). The basic observation is that the  $V_m(t)$  record did not change upon  $I_{cs}$  cancellation.

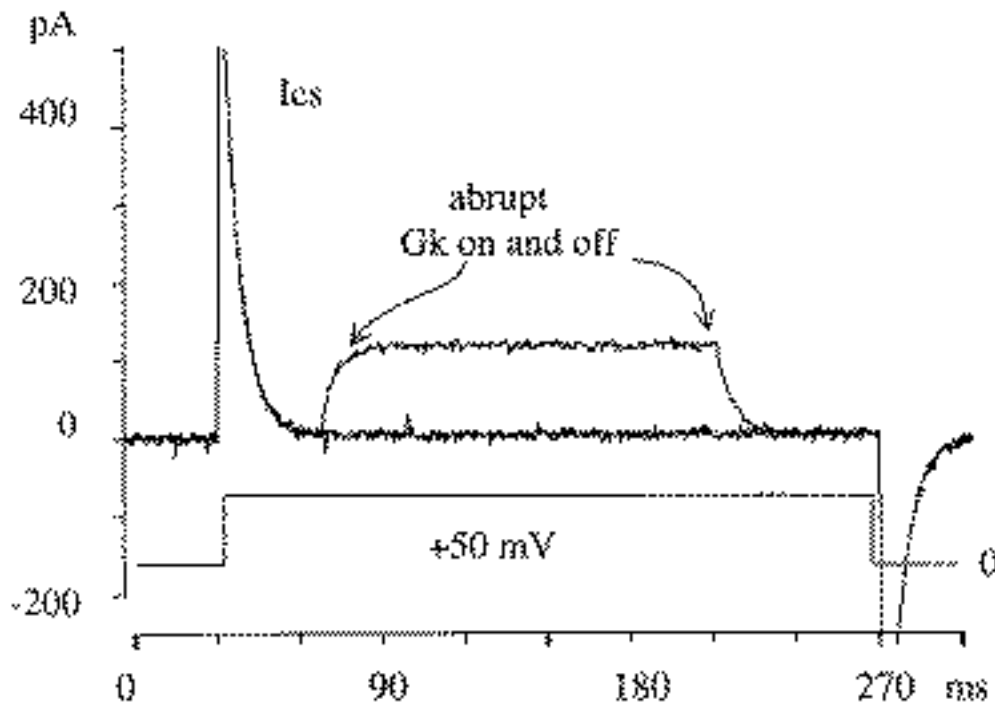


**Figure 3.10. Whole-cell current filtering by the  $R_{ser} \cdot C_m$  time constant**

A  $G_k = 1 \text{ nS}$  ( $R_k = 1 \text{ G}$ ) is abruptly activated (on) and deactivated (off) by closing and opening, respectively, a series reed contact by a magnet movement upon a depolarization step from 0 to +50 mV. Three superimposed records, 2 controls and 1 with  $G_k$  activation. Timing of  $G_k$  switching was obtained by trial and error. The on and off time constants of  $I_k$  are approximately the same as the time constant of the  $I_{cs}$  decay ( $\sim 5 \text{ ms}$ ). Experimental conditions (cf. Fig. 3.1): no other membrane conductances than  $G_k$  ( $G_l$  and  $G_{na}$  off, OOP uncoupled),  $E_k = -62 \text{ mV}$ ,  $R_{pip} = 2.2 \text{ M}$ ,  $R_{acc} = 50 \text{ M}$ ,  $C_m = 94 \text{ pF}$ ,  $R_{seal} = R_{mcap} = 20 \text{ G}$ , filter setting at 10 kHz. The  $I_k$  on and off response are not perfectly exponential (too steep initial slopes) probably due to non-ideal switching, but at these time constant values ( $\sim 5 \text{ ms}$ ) these irregularities are not too disturbing.

**Table 3.1. Component abbreviations, used or recommended component values (nominal or estimated) in the model cell experiments and full names of the components**

The components are listed in groups and, within the groups, from left to right and clock-wise in the circuit. The abbreviations CAP, WC, OOP and IOP are explained in Fig. 1.1. In some experiments magnet operated reed contacts were used for the switches S6, S11 and S12.



COMPONENT	VALUE(S)	NAME
Rcc	>> 100G (amplif. specif.)	current-clamp Resistance
Rvc	<< 1 M (amplif. specif)	voltage-clamp Resistance
Rpip	2 or 2.2 M	pipette Resistance
Rseal	10 or 20 G	seal Resistance
Rcapch	1 or 2 G	CAP channel Resistance
Rmcap	10 or 20 G	CAP membrane Resistance
Racc	2, 2.2, 5, 10 M	access Resistance
Roop	10 or 20 G	OOP Resistance
Rl	400M, 1 G	leak Resistance
Rk	200 M	potassium Resistance
Rna	100 M	sodium Resistance
Rser	Rpip+Racc	series Resistance
Gl	1/Rl	leak Conductance
Gk	1/Rk	potassium Conductance
Gna	1/Rna	sodium Conductance
Cpc	~1 pF	patch-clamp Capacitance
Cpiphold	~1 pF	pipette-holder Capacitance
Cpip	4.7 pF	pipette Capacitance
Ccap	~ 1 pF	CAP (stray) Capacitance
Coop	3.3 pF	OOP Capacitance
Cm'	47 or 94 pF	membrane' Capacitance
Cm (=Cwc=Cm'+Coop)	~ 50 or ~100pF (excl. Ccap)	WC membrane Capacitance
Cvc		Internal vc Capacitance
Epc		patch-clamp Voltage source
Evc	-100 to +100 mV	voltage-clamp Potential
Ecc		current-clamp Potential
Eoop	0 or ~-60 mV	OOP membrane Potential
El	0 or ~-60 mV	leak reversal Potential
Ek	-60 to -90 mV	potassium Nernst Potential
Ena	~ +60 mV	sodium Nernst Potential
Scvc (S1)		cc-to-vc Switch
Spc (S2)		patch-clamp Switch
Scpip (S3)		pipette capacitance Switch
Srpip (S4)		pipette resistance Switch
Sseal (S5)		seal Switch
Scapch (S6)		CAP channel Switch
Sacc (S7)		access resistance Switch
Siop (S8)		IOP Switch
Soop (S9)		OOP Switch
Sgl (S10)		Gl Switch
Sgk (S11)		Gk Switch
Sgna (S12)		Gna Switch